

Accident Reconstruction Guidelines

Part of Deliverable D4



CONTRACT N° : G3RD-CT-2002-00802

ACRONYM : PENDANT

TITLE : Pan-European Co-ordinated Accident and Injury Databases

PROJECT CO-ORDINATOR: VSRC, Loughborough University

PARTNERS :

1. VSRC	UK
2. INRETS	F
3. ARVAC	F.
4. ARU-MUH	D
5. TNO	NL
7. TUG	A
8. C.E.T.E. S-O	F
10. Chalmers	S
11. UPM - INSIA	E
12. U-Turku/VALT	Fin
13. SWOV	NL

PROJECT START DATE : 2003/01

DURATION : 36 months

Prepared by: Ernst Tomasch
Graz University of Technology, AT
October 2004



Project funded by the European
Community under the 'Competitive and
Sustainable Growth' Programme (1998-
2002)

Table of Contents

1. Introduction.....	5
1.1 Impact Theories overview.....	8
1.2 Backward Simulation.....	11
1.3 Forward Simulation.....	12
2. Measurement of the accident.....	13
2.1 Measuring procedures.....	13
2.1.1 Triangle measuring procedure.....	13
2.1.2 Right angle coordinate procedure.....	14
2.1.3 Measure curves.....	15
2.2 Photogrammetry.....	17
2.2.1 Sources of error and accuracy.....	18
2.2.2 PC-Rect.....	20
2.2.3 PHIDIAS.....	21
2.2.4 PhotoModeler.....	22
2.3 Aerial photography.....	23
2.4 Measurement equipment.....	24
2.4.1 Tape measure.....	24
2.4.2 Yardstick.....	24
2.4.3 Measuring wheel.....	25
2.4.4 Laser rangefinder.....	25
2.4.5 Camera.....	26
3. Accident evidence.....	28
3.1 Damage marks.....	28
3.2 Material marks.....	28
3.3 Wiping marks.....	29
3.4 Casting marks.....	30
3.5 Abrasion, melting marks.....	30
3.6 Biological traces.....	31
3.7 Webbing marks.....	31
3.8 Airbag control unit.....	35
3.9 Throwing range of broken glass.....	36
4. Tyres and pavement.....	39
4.1 Tire-Roadway friction values.....	39
4.1.1 Influence of the vehicle speed.....	40
4.1.2 Interaction between tires and pavement.....	40
4.2 Skid marks.....	41
4.2.1 Skid mark interferences.....	44
4.2.2 Influence parameter for skid marks.....	45
5. CRASH3 measurements.....	49
5.1 Damage width.....	49
5.2 Damage measurement.....	50
5.3 Setting a datum.....	53
5.3.1 Front and Rear impacts.....	53
5.3.2 Side impacts.....	54

5.3.3	Bowed vehicles in side impacts	54
5.4	Spacing C ₁ to C ₆ measures	55
5.4.1	Spacing narrow penetrating profile	57
5.5	Offset of the crush location	58
6.	Reconstruction methods	60
6.1	Reconstruction by hand / empirical method	61
6.2	Computer methods	62
6.2.1	CARAT	63
6.2.2	MADYMO	64
6.2.3	PC-Crash	67
6.2.4	CRASH	73
6.2.5	SMAC / EDSMAC	76
6.2.6	HVOSM / EDVSM	78
6.2.7	PHASE / EDVDS	80
6.3	Conclusions	81
7.	Collision Classification	84
7.1	CDC – Collision Deformation Code	84
7.1.1	CDC 1&2 - DoF – Direction of Force	85
7.1.2	CDC 3 - General Location	90
7.1.3	CDC 4&5 - Horizontal Location	91
7.1.4	CDC 6 - Vertical Location	92
7.1.5	CDC 7 - Damage Pattern	93
7.1.6	CDC 8 – Crush Extent	94
8.	Reconstruction Parameters	95
8.1	Energy Equivalent Speed (EES)	95
8.2	DELTA-V - Δv	98
8.3	Closing Speed	101
8.4	Equivalent Test Speed (ETS), Equivalent Barrier Speed (EBS), Barrier Equivalent Velocity (BEV)	102
8.5	Difference between EES and Delta-v	103
8.6	Difference between BEV and Delta-v	104
8.7	Coefficient of Restitution	104
9.	Pedestrian accidents	106
10.	References	108
11.	Appendix	115

Figueres

Fig. 1: Impact-crash phases.....	7
Fig. 2: Global phases.....	7
Fig. 3: Obtuse or acute angle	13
Fig. 4: Triangle measuring procedure.....	14
Fig. 5: Right angle coordinate procedure.....	14
Fig. 6: Chord measuring method	15
Fig. 7: Triangulation of curves.....	16
Fig. 8: Right angle coordinate measurement of curves.....	17
Fig. 9: Non-planarity error	19
Fig. 10: Tape measure.....	24
Fig. 11: Yardstick.....	24
Fig. 12: S-shaped characteristic	25
Fig. 13: Measuring wheel with counter	25
Fig. 14: Laser rangefinder.....	26
Fig. 15: Reference length equipment	27
Fig. 16: Damage marks	28
Fig. 17: Material marks.....	29
Fig. 18: Wiping marks	29
Fig. 19: Casting marks	30
Fig. 20: Abrasion marks.....	30
Fig. 21: Biological traces	31
Fig. 22: Swivel/D-ring, tongue	33
Fig. 23: Webbing marks.....	34
Fig. 24: Seating positions.....	35
Fig. 25: Throwing range of broken glass from headlights - Schneider	37
Fig. 26: Throwing range of broken glass from headlights - Kühnel.....	37
Fig. 27: Throwing range of broken glass from windscreen and headlights - Braun....	38
Fig. 28: Modified length of throwing range of broken glass - DEKRA	38
Fig. 29: Friction and normal forces in sliding and rolling	39
Fig. 30: Available and demand friction on wet pavements	41
Fig. 31: Axis of possible movement of a vehicle.....	42
Fig. 32: Skid mark appearance – intensity degree	45
Fig. 33: Skid marks	46
Fig. 34: Crash measurement	49
Fig. 35: Crush of stiff frontal structures.....	51
Fig. 36: Damage measure	51
Fig. 37: Bowed vehicle due to side impacts	55
Fig. 38: Spacing of bowed vehicles	55
Fig. 39: Offset measurement location.....	58
Fig. 40: Balance point for side and frontal impacts.....	59
Fig. 41: Crash phase of Ford Explorer Multi-Body (left) and Finite Element (right) model at t=0, 20, 40 and 60 ms (top-down).....	65
Fig. 42: Comparison of head acceleration	66
Fig. 43: Geometrical front shape classifications (DIN 75204).....	72
Fig. 44: Comparison between CRASH3 results and crash-test measurements	75
Fig. 45: CDC 1&2 – Direction of Force	85
Fig. 46: Direction of Force – clock face	86
Fig. 47: DoF – Direction of Force	86
Fig. 48: Relationship between Vehicle Orientation and DoF	87
Fig. 49: Vehicle sections.....	89

Fig. 50: CDC 3 – General Location	90
Fig. 51: Deformation Location	90
Fig. 52: CDC 4&5 – Horizontal Location	91
Fig. 53: Impact references – frontal and side.....	92
Fig. 54: CDC 6 – Vertical Location.....	92
Fig. 55: CDC 7 – Damage Pattern	93
Fig. 56: CDC 8 – Crush Extent.....	94
Fig. 57: EES Database pictures.....	97
Fig. 58: Straight line centric impact.....	98
Fig. 59: Change of Velocity as Vector Quantity.....	100
Fig. 60: Closing speed.....	102
Fig. 61 Geometrical front shape classifications (DIN 75204) and enhanced by DEKRA.....	107
Fig. 62: Throwing range approach of Stcherbatcheff/Kühnel/Rau.....	107

Tables

Tab. 1: Digital photography comparing with photography on negative films.....	22
Tab. 2: Skid mark interferences	45
Tab. 3: Accident evidence.....	48
Tab. 4: D/C.....	50
Tab. 5: Examples of damage width.....	52
Tab. 6: Setting a datum for front and rear impacts	53
Tab. 7: Setting a datum for side impacts.....	54
Tab. 8: Spacing C ₁ to C ₆ measures	56
Tab. 9: Spacing narrow penetrating profile	57
Tab. 10: Input data and CARAT-4 reported crush	64
Tab. 11: Comparison between the CARAT-4/ SMAC results and the RISCAC data.....	64
Tab. 12: Comparison of CRASH3 Delta-V estimates with test results	74
Tab. 13: Comparison of simulation results and test results	77
Tab. 14: Side of vehicle most damaged by DoF	90
Tab. 15: Horizontal location of the direct contact	91
Tab. 16: Vertical location of the direct contact damage	93
Tab. 17: Nature of the impact type	94
Tab. 18: Special cases for straight line centric impacts.....	99
Tab. 19: Calculation of Δv	100
Tab. 20: Examples for EES and Δv	103
Tab. 21: Speed Rating of tyres.....	131

1. Introduction

The *MAIN* purpose of Work Package 1 is to ensure that accident data which are collected by several teams is directly comparable. To collect accident data of all teams in a similar way is essential for comparing data as well as injury data of involved persons in an accident. This shouldn't be only for this project; this should be for subsequent projects too. Topic of task 1 in this Work Package: "*Accident reconstruction and collision severity assessment guidelines*". Therefore task 1 was divided into three subtasks: objective is firstly to develop methods and guidelines for the reconstruction of road traffic accidents, secondly to develop a database which includes the main information about available public domain crash tests and thirdly develop methods for determining the comparability and accuracy of reconstruction methods.

A definition of an accident could be: "*An accident is an unexpected or surprised incident which changes the situation of vehicles involved as well as situations of passengers or pedestrians*".

Accident reconstruction is a field of practice that requires specialized study, training and experience.

Which things are useful now for accident reconstruction? For reconstruction of accidents the evidence taken from scene and vehicles is very important. Normally police is present on scene and they take pictures and measure skid marks, highlight rest positions, collect personal data etc. Skid mark lengths, car rest positions, obstacle locations, crush damage and other parameters are useful for reconstruction. Biological traces are helpful to find out the seating position of participated occupants. In cases where no police is present (only damaged vehicles) no information will be available to investigation teams anyway these accidents are not of interest. Depending on the method used for reconstruction pictures are necessary from damaged profile or on-scene photos. For teams which can't be directly on scene the pictures taken from the police need to fulfill our requirements to reconstruct accidents.

Unfortunately, the skid marks at the scene may have long since vanished, or significant scene changes may have occurred. However, all is not necessarily lost if photographs of the accident are available.

This booklet provides a brief description of accident reconstruction methods which exists their validation techniques as well as measure deformation of vehicles and the accident scene. Furthermore a description of reconstruction parameters exists and how to deal with evidence. Some different software tools are described within this booklet, but there is no recommendation which one should be used. This is just the decision of the person itself.

Accident reconstruction requires estimating the change of velocity (Delta-V) imparted to vehicles during collision. Estimating Delta-V commonly involves measuring or estimating the deformation of the vehicles involved in a collision. Material coefficients, which relate barrier equivalent velocity (BEV) to deformation for the two vehicles, are then interpolated or if it is sensibly possible to extrapolated from barrier crash test data.

Why do we need accident reconstruction? Well, there are many different topics in which accident reconstruction can be used. Car manufacturer may use it for their research activities – make cars safer - as well as the government can use it for new regulations. Which kind of problems occur on special roads? In which way is it possible to avoid accidents? How to design road furniture? Many questions and many answers can be given, but for this document they are not that relevant. For our purpose it is just necessary to collect data in a similar way.

If occupants are injured in accidents the crown prosecutor scrutinise the guiltiness of the involved accident participants. For the adjustment of claim the accident course of events must be reconstructed if there is no amicable arrangement of the involved accident participants.

On the next page two descriptions of the accident phases have been made. One is “*impact*” based and the other one is “*global*” based.

Impact-crash phases:

The first is the pre-crash phase which is the period in between the accident critical situation and the first contact with the other vehicle. This phase is the accident initial phase. During this phase an imminent accident can be indicated by critical driving manoeuvres such as hard braking, skidding or rapid steering inputs.

The second phase is the running-in period which includes the reaction of the driver from realising the situation until the first contact.

Thirdly the phase is characterised through the run-out after an impact until the vehicle(s) stop(s) or hit another vehicle.

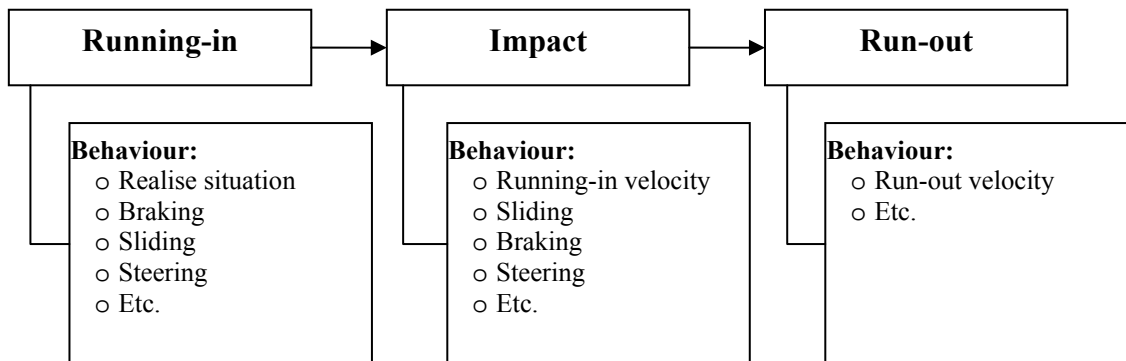


Fig. 1: Impact-crash phases

Global phases:

Anyways, there could be another definition of the pre-crash phase. This would be the behaviour of the driver. Was he excited; what did he do before the accident happened; did he feel well; etc.

The second phase is the crash phase which is the period during the collision from first contact until the vehicle(s) stop.

After all relevant parties stopped the third phase starts. This phase includes all the actions taken to secure the accident scene, calling rescue, etc.

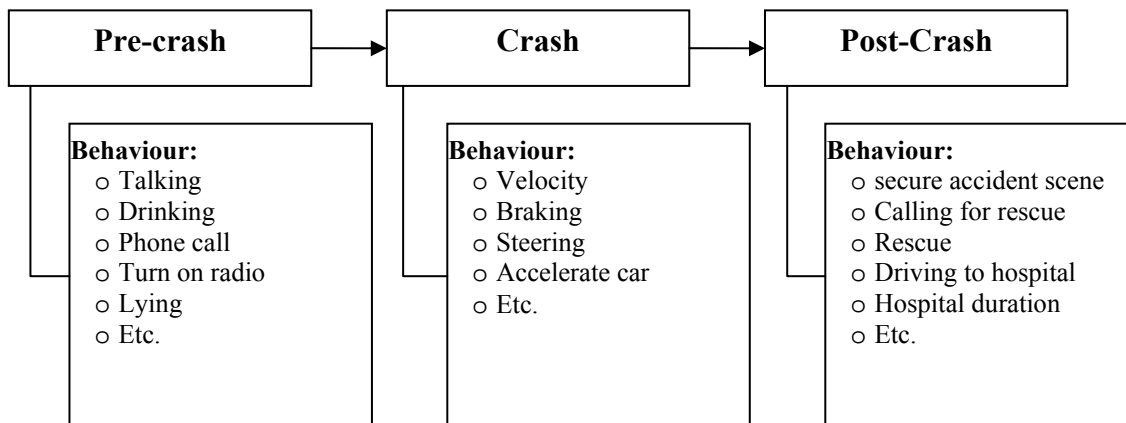


Fig. 2: Global phases

1.1 Impact Theories overview

Impact Theory of Hertz and Saint Venant

The goal of the theory of elastic bodies is the calculation of the maximum forces of the impact and the duration during the impact with the help of Hook's laws of deformation. The presumption of this theory is that based on the "theory of hardness" the determined static flattening is applying for the impact procedure. That means that the duration of the impact is large compared to the "shock wave time".

Impact Theory of Galilei, Huygens and Newton

The goal of this theory is rather the velocity at the end of the impact calculated from the velocity at the beginning than the determination of the force of impact and the chronological process.

Following assumptions are made:

1. Duration of the impact is short and the forces are huge
2. All external forces are small comparing to the momentum and negligible
3. Time integral of momentum is finite $\int \vec{F} dt = \vec{P}$
4. Conservation of kinematics configuration during impact
5. Deformation of the bodies during the impact are not counted in the calculation

Basis for accident reconstruction and mechanics are the Newton's theory of impact – *the Newton's classical laws*.

The three fundamental Newton's classical laws:

Isaac Newton, born in Woolsthorpe, England (A.D. 1642-1727), was a mathematician and physicist. Newton first stated these laws in his Principia published in 1687.

Newton's *First Law* of Motion:

Every object in a state of uniform motion tends to remain in that state of motion unless an external force is applied to it.

Newton's *Second Law* of Motion:

The relationship between an object's mass m , its acceleration a , and the applied force F is $F = m \cdot a$. Acceleration and force are vectors (as indicated by their symbols being displayed in slant bold font); in this law the direction of the force vector is the same as the direction of the acceleration vector. F is the acting force, m the mass of the body and a the acceleration of the body due to the acting force.

Newton's *Third Law* of Motion:

Action and reaction are equal and opposite, i.e. when two bodies interact the force exerted by the first body to the second body is equal and opposite to the force exerted by the second body on the first.

Newton defined the collision into two phases: the *compression* and the *restitution* phase. In case of a full impact, at the end of the compression phase the velocities of both vehicles at the impulse point are identical. Due to elasticity of the vehicle structures, the two vehicles will separate again.

An accident reconstruction is based on three laws of physics, which have to be used by the investigator in order to define parameters such as initial speeds and post crash speeds. These laws can be used separately (if only one variable is unknown) or combined (if more variables are unknown).

These three laws are:

Conservation of energy

Conservation of linear momentum

Newton's second law

Conservation of energy

The principle which states that the amount of energy in a closed system is constant, regardless of the changes in form of that energy. Energy can neither be created nor destroyed. Therefore the kinetic energy before the impact equals the kinetic energy after the impact plus the energy loss:

$$\sum_{i=1}^n \frac{1}{2} \cdot m_i \cdot v_i^2 = \sum_{j=1}^n \frac{1}{2} \cdot m_j \cdot v_j'^2 + \text{EnergyLoss} \quad 1-1$$

where:

m the total mass of the bodies

v the body velocities before and v' after the impact

i and j the bodies involved in the crash

Energy can be lost during the impact due to:

- Deformation of vehicles
- Rotation of vehicle
- Friction between tires and pavement
- Sound due to impact

The energy loss due to deformation is the most important value, because its amount is much greater than the other losses. The other losses are difficult to be defined, because of the unknown parameters that are depending on (e.g. duration of impact, moments of inertia of vehicle, centre of gravity of vehicle). Since they are typically one order of magnitude smaller, they are most often neglected. A parameter, which is commonly used to define the deformation energy loss, is the Energy Equivalent Speed (EES). The reconstruction parameter EES will be described later on. There are crash test databases (the NCAP database for example) from which the EES can be obtained

Principle of linear momentum:

Momentum is the product of inertia and velocity. During any collision, momentum is conserved as a consequence of Newton's 3rd Law - the Law of Action-Reaction. So momentum means the tendency of an object in motion not to slow down. What this means is that the total momentum before a collision is always equal to the total momentum after a collision.

$$\vec{S}_{1,2} = \int_{v_1}^{v_2} d(m \cdot \vec{v}) = \int_{t_1}^{t_2} \vec{F} \cdot dt = m \cdot \vec{v}_2 - m \cdot \vec{v}_1 \quad 1-2$$

A useful way of increasing the applicability of the above mentioned equation is by using the concept of elasticity (ϵ). Elasticity is a measure of the ratio between the separation and the closing velocity. “ ϵ ” can vary between 0 (fully elastic impact) and 1 (plastic impact, no separation).

Principle of conservation of angular momentum:

Angular momentum is the tendency of a rotating object to keep rotating at the same speed about the same axis of rotation.

$$\int_{t_1}^{t_2} \vec{M}_{Res} \cdot dt = \int_{t_1}^{t_2} d(\vec{r} \times m\vec{v}) = \int_{t_1}^{t_2} d\vec{L} \quad 1-3$$

Amendment hypothesis

Hypothesis of coefficient of restitution (Newton):

Coefficient of restitution $\epsilon = \frac{S_R}{S_C}$ describes the elastically and plastically behaviour of the bodies. The coefficient of the restitution is defined as ratio between restitution S_R and compression S_C impulse. Border case of elastic impact is identified with $\epsilon = 1$, plastic impact $\epsilon = 0$.

Hypothesis of direction (Marquard 1962):

The actuation of impulse is in the direction of the relative velocity of the centre of gravity at the point of the first contact and is independent of shape of the bodies at the point of impact.

Classical impact model of Kudlich-Slibar (1966):

The tangential relative velocity between the bodies is zero if the actuation of impulse is within the friction cone $T \leq \mu \cdot N$.

Two different kinds of impacts:

- Full impact
- Sliding impact

Full impact:

1. no relative movement between both vehicles can be found in the impulse point at the end of the compression phase.
2. the average between compression and restitution momentum is defined by the coefficient of restitution

Sliding impact:

In certain collisions the two vehicles will never reach identical velocities in the impulse point during the impact. In such a case a contact plane has to be defined, along which the two vehicles slide. The impulse point must coincide with this plane. For such a situation the following assumptions has to be made:

1. no relative movement between both vehicles can be found in the impulse point at the end of the compression phase in direction normal to the contact plane.
2. the direction of the momentum is limited by friction μ . This value defines the friction between the two impacting vehicles.
3. the average between compression and restitution momentum is defined by the “*coefficient of restitution*”.

Out of this relation the post impact velocity conditions for both involved vehicles can be calculated.

It is important for a good prediction of the collision phase to define the correct overlapping of the vehicle bodies when the forces are exchanged.

Sliding collision (Böhm, Hörz 1968):

In a sliding impact, the two vehicles do not reach a common velocity at the impulse point during the impact. In such as case a contact plane has to be defined, along which the two vehicles slide. The impulse point must lie in this plane. For this case, the following assumptions are made:

- No relative movement between the vehicles occurs at the impulse point at the end of the compression phase in the direction normal to the contact plane.
- The direction of the momentum transfer is limited by an inter-vehicle friction coefficient (μ)
- The ratio between compression and restitution impulse is again defined by the coefficient of restitution.

1.2 Backward Simulation

This is the classical method for accident reconstruction. The final positions of the vehicles involved are the initial points for the calculation. From this position the point of collision will be calculated. At first the calculation of the collision, which is based on conservation of mass, impulse, angular momentum and energy has to be done. Finally the calculation of the running-in movement of the vehicles is taken place. For this method only elementary, kinematics approaches are possible. For this method the position of the collision and the way how those locations were reached have to be known. The traces at the accident scene have to be measured very carefully and a sketch would be as useful as well.

1.3 Forward Simulation

Basic principle for this method is to establish a complete mathematical vehicle model. Due to developing of powerful computers this method becomes more important. 2D and 3D models are available. Sliding collisions could be calculated as well as driving behaviour. For this method, the running-in of the vehicles into the first collision is the initial point for the calculation. From this point of position the run-out to the final position could be analysed as well as the process of impact. Due to variation of parameters the final positions of the vehicles, investigated at the accident location, could be harmonised. If a sliding collision was occurred the calculation starts at the beginning of the sliding movement.

2. Measurement of the accident

Other important points for the reconstruction of accidents are the pictures taken from the scene (photogrammetry). Without good-quality measurements taken at the time of an accident the analyst is faced with the need to extract measurement data from incident scene photographs.

2.1 Measuring procedures

2.1.1 Triangle measuring procedure

With this procedure two points of reference are selected, where the distance between these points is known. Each distance to any point can be measured. To reduce the errors during measurement, the distances must be determined as exactly as possible. The angle between the lines shouldn't be obtuse nor too acute. If the distance between point A and point B is too long and point C is too close to the connecting line \overline{AB} then there won't be an intersection and point C can't be found with this method. An acute angle and inaccurate measurement causes an offset of point C (right picture).

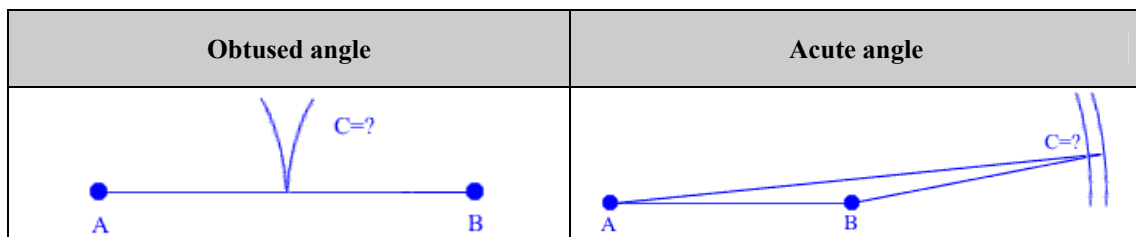


Fig. 3: Obtuse or acute angle

The points A and B in the next picture form the fixed points. Such points should be points which can't be razed easily, e.g. street lights, quoin of a house etc.

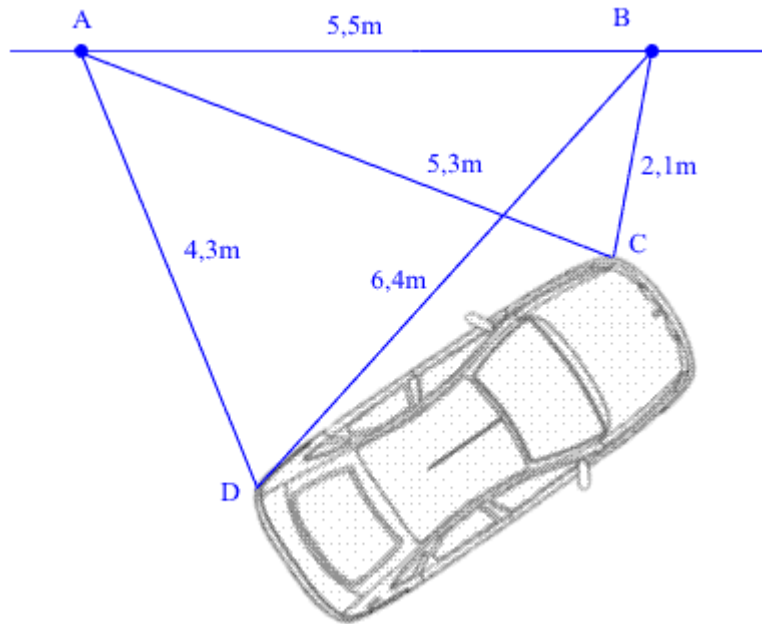


Fig. 4: Triangle measuring procedure

2.1.2 Right angle coordinate procedure

To a suitable place the point of origin will be put. Such points could be street lights, gully, etc. From this point all substantial local conditions under a respective right angle are measured. The problem with this procedure is the construction of the right angles. It is more difficult if points of interest which should be measured do not lie in the right angle to the coordinate system. This procedure is very fast if straight roads should be measured.

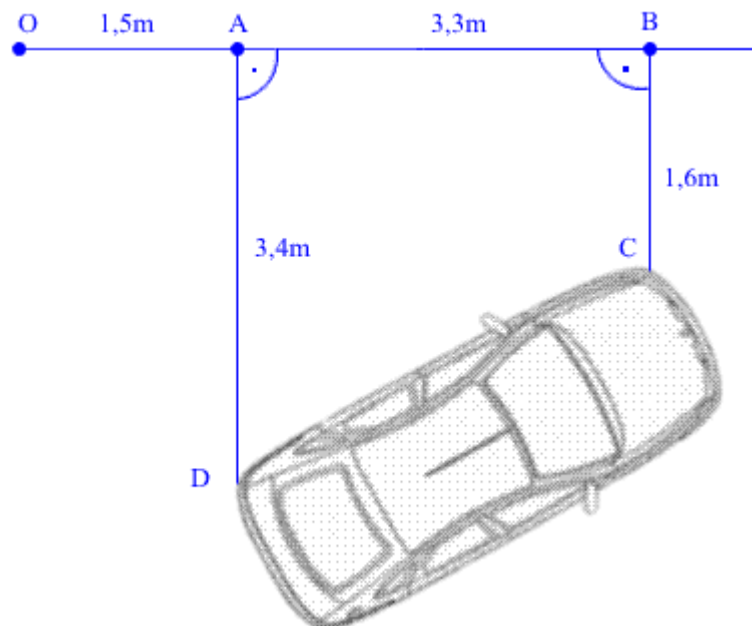


Fig. 5: Right angle coordinate procedure

2.1.3 Measure curves

Chord measuring procedure

With this method curves will be measured. At first a fixed point will be chosen from which the curve will be divided into chords. In each case from the centre of the chord in the right angle the height is determined to the trajectory. To determine the radius of each part of the curve following formula is used:

$$R = \frac{S^2}{8 \cdot H} \quad 2-1$$

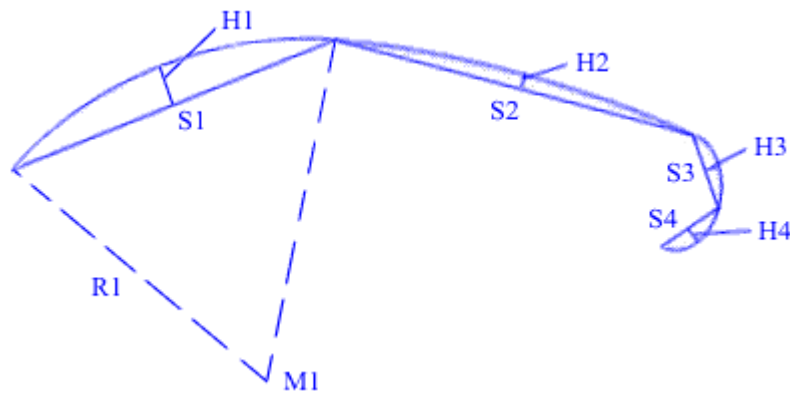


Fig. 6: Chord measuring method

Triangulation of curves

The location will be divided into a connected network of triangles, which can be measured. The basic principle is the triangle measuring procedure which was already described above. To divide an area into a connected network of triangles is called triangulation. To measure the curve the roadside should be split up into equal lengths of approximately 5 to 10 meters. Point A and B should be lying at fixed point like a milestone or something else. Afterwards only the distances to the other points are measured: B to C, C to D, etc.

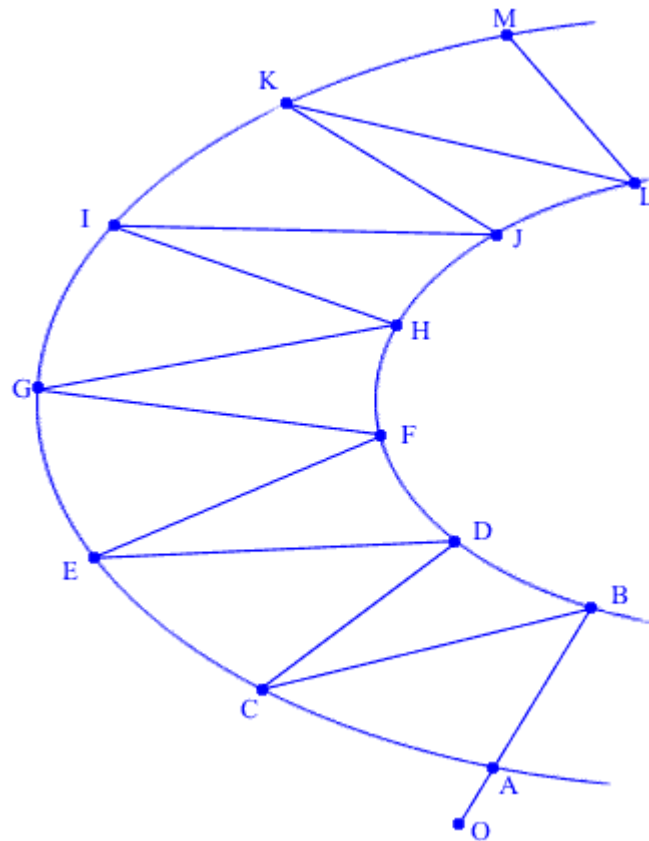


Fig. 7: Triangulation of curves

Right angle coordinate measurement of curves

With this method a straight line – the baseline, which starts from point B (at the outside of the road) to point B6 will be marked. In a right angle to this baseline the distances from C1 to A1 and from C1 to B1 will be measured. The distances between B to C1, C1 to C6 and C6 to B6 must not be equal.

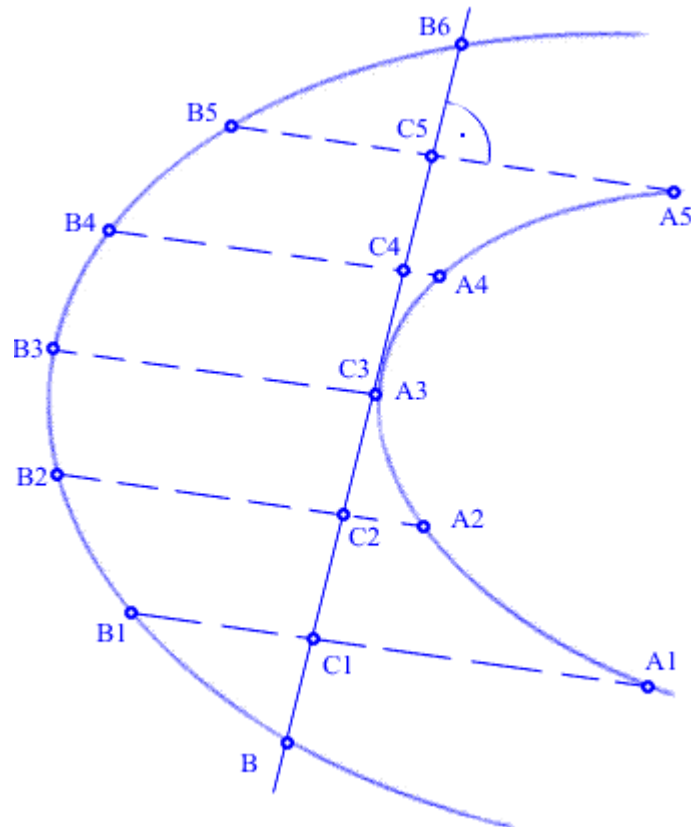


Fig. 8: Right angle coordinate measurement of curves

2.2 Photogrammetry

Photogrammetry is the science of producing real world measurements from photographs. There are several photogrammetric techniques available to the reconstructionist. 3D photogrammetry requires at least two photographs, both containing all points of interest and will yield measurements in three dimensions. 3D photogrammetry and do not require planar surfaces. Relatively simpler is 2D photogrammetry. 2-D methods require only one photograph and can provide adequate accuracy for nominally flat surfaces.

Even when no measurements have been taken at the time of an accident the reconstructionist can obtain enough dimensional data to rectify photographs by going to the scene and taking measurements of painted lines or other long-lasting roadway features that appear in the original photographs.

Police is taken photographs of the roadway and incident artefacts. The film plane or image plane is nearly vertical in respect to the roadway or object plane. The

photograph is simply a projection of the object plane onto the image plane. The process of reversing this projection is known as rectification.

Accuracies of 0,3m for the scene information may be adequate to reconstruct collisions where speed from skid marks is the task.

The cameras used for photogrammetry are defined as metric or non-metric. Metric cameras have stable internal geometry, are calibrated to account for distortion, and are used primarily for photogrammetric purposes. Non-metric cameras have less stable internal geometry and can also be calibrated, but generally yield results of lower accuracy than metric cameras.

Photogrammetry could be divided into following methods:

- Four point method
 - Paper-point method
- Projective reference net
 - Möbius net method
 - Random raster method
 - Reference raster method
 - Template raster method
- Upright and horizontal projection
 - Point wise rectify method

In-depth descriptions of those methods are in literature available.

2.2.1 Sources of error and accuracy

Camera:

There is no perfect camera. The “metric” camera traditionally used in photogrammetry has a fixed focal length, and the variations from the ideal optical axis and principal point are known. The distortion of the lens has been determined and can be accommodated in the analysis. “Non-metric” cameras produce adequate accuracy for accident reconstruction purposes as well.

Bitmap:

To produce a bitmap from a negative several methods are available. One option is scanning a print made from the negative, which involves the accuracy of the printing process as well as the accuracy of the scanner. To avoid inaccuracy of this equipment it's better to use digital cameras which can be directly connected with a computer.

Road surface:

The greatest potential source of error in 2D rectification of photographs taken from oblique angles is any vertical variance of the ground points with respect to the plane defined by the control points. When rectified point on the road surface which lie above the object plane will appear farther away from the camera than they actually

are. Similarly, points on the road surface which lie below the object plane would appear closer to the camera when rectified. The non planarity error increases linearly by the horizontal distance from the camera, although the error also depends on the camera height and the point height. The error increases as the height of the point above the object plane increases, and decreases as the camera height increases. This problem can, however, be overcome with a piecewise analysis in which each side of the road is rectified separately. In this case the maximum error can be reduced.

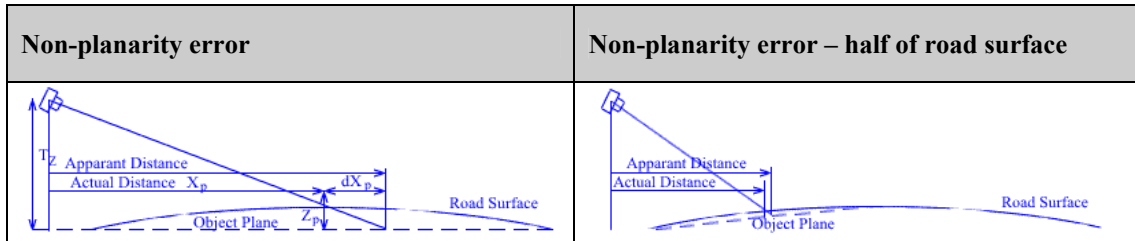


Fig. 9: Non-planarity error

The amount of error in the rectification of a point at some height above or below the object plane can be derived similar triangles as follows:

$$\delta X_p = \frac{Z_p \cdot X_p}{T_z - Z_p} \quad 2-2$$

- T_z camera height
- Z_p height of point p
- X_p distance to road plane from camera
- δX_p apparent distance – actual distance

Control point accuracy and location:

The accuracy in the measurement of the control points will also influence the accuracy of the rectification process. For nominally flat surfaces, control points with long distances between them will result in greater accuracy than for control points with short distances between them, since any uncertainty in the position of the points will be averaged over the longer distance. It is also important to choose control points which surround the area of interest.

Bitmap resolution:

The resolution of the bitmap will influence the accuracy of the rectification, especially at increasing distances from the camera. In a typical scene photograph, moving from the bottom of the photograph upwards, the road surface occupies less and less of the photograph width. In the upper portion of the photograph, each pixel represents a greater length and width of the road surface. Therefore, when a bitmap is rectified the resolution will diminish as the distance from the camera increases. The final resolution of the rectified bitmap and the distance from the camera to the area of interest, but will also depend on factors such as camera height, focal length and photograph print size.

2.2.2 PC-Rect

PC-Rect is a program for the rectification of photographs. The program allows the user to rectify photographs of surfaces which are close to being planar, such as roadway surfaces at accident scenes. As a result of the rectification, an image view normal to the surface (a plan view for horizontal surfaces) is created. This makes it possible to view all distances in the planar surface true to scale and angle. This image contains all the skid marks, road lines and other road markings that appear in the original oblique photograph, as well as discrete points of interest. Even when no measurements have been taken at the time of an accident, the reconstructionist can obtain enough dimensional data to rectify photographs by going to the scene and taking measurements of painted lines or other long-lasting roadway features that appear in the original photographs.

PC-Rect allows the connection of several pictures using two common points in each picture. Always use long reference distances. The greater the reference distance the more accurate the overall result will be. In addition both orthogonal and diagonal reference distances should be used. Try to locate the reference distances in the area of the picture that is of interest for the rectification. Optimally, the area of interest should be within an area defined by the reference points.

After the picture is straightened a plan view is available and the lengths of the skid marks or other special points could be taken from the straightened image. Conclusions of Cliff et al:

1. PC-Rect can be used to rectify photographs of flat accident scenes, resulting in a high degree of accuracy.
2. PC-Rect can be used to determine the approximate height and lens focal length of the camera used to take a photograph.
3. It is desirable to have diagonal reference lengths in the photograph as well as lateral and longitudinal ones to avoid skewing of the rectified image. However, when no diagonal reference lengths are used the resulting small amount of skewing doesn't cause a significant increase in error.
4. PC-Rect can be used to rectify photographs of non-flat scenes, although lower accuracies can be expected for flat scenes. For better accuracy, non-flat scenes can be divided into smaller areas of relatively small unevenness, which are rectified into a separate image. These can then be joined together into one image which has the same absolute accuracy as each individual image.

PC-Rect 3D

The 3D version of PC-Rect can be used to generate a 3-dimensional drawing from two or more photographs. The general proceeding is very similar to the way you have to work in the 2D version. In addition you have to have two or more photographs of the object from which you want to get 3-dimensional information.

It is important to specify reference distances on the same plane in all pictures, in this case reference distances on the ground are used. The first reference distance has to be the same in all pictures to get a reference for the camera position in the global coordinate system.

PC Video Rect

PC-Rect 3.0 also enables to handle videos. The investigator has to make a video of the accident scene and after this the video must be divided into individual pictures, which are continuous numbered. A cut-out has to be selected and reference distances have to be defined. The process is in principle the same as in the preceding versions.

Not many facilities are necessary to use PC-Video Rect. At first you need a digital camera and second a tripod on which the camera can be fixed. Camera and tripod will be fixed on the outside of the windscreen of a car. The investigator has to drive along the accident scene. After the movie has been made the person has to split up the movie into several pictures the movie consists of.

2.2.3 PHIDIAS

PHIDIAS is the latest development in the field of digital photogrammetric workstations and is an MDL-application for MicroStation (Bentley Systems). The data generated by PHIDIAS will be directly stored in MicroStation design files and processed there. PHIDIAS can be used in conjunction with Bentley Engineering configurations like TriForma, GeoGraphics and PlantSpace.

Use of PHIDIAS:

- Industrial plant documentation
- Deformation measurement
- Archaeology
- Stereo aerial photogrammetry
- Data acquisition for geo information systems
- Accident and site of crime sketches
- Digital picture rectifying
- Visualisation

PHIDIAS runs in MicroStation 95 / SE, MicroStation /J and MicroStation V8 with Windows 95 / 98 / NT / 2000 / XP. There are no special requirements to the hardware. You only need enough RAM to store the digital images. The image size is not limited; nevertheless enough RAM will reduce hard disk access and speed up image display.

PHIDIAS works with digitized measurement photographs. There are several possibilities to collect digital image data:

A digital camera with a CCD-sensor (i.e. Kodak DCS) is used for the photographs. The negatives are transferred to a Photo-CD (Kodak). The negatives or enlarged positives are digitized with a scanner. Images are captured from a video source.

Depending on the measuring task either a digital camera or negative film should be preferred. The following summary shows the main differences between digital photography and photography on negative or reversal films:

Digital Photography	
Advantages	Disadvantages
<ul style="list-style-type: none"> • Easy image capturing • High geometric stability • Instant control of image quality 	<ul style="list-style-type: none"> • Costs for camera systems • Compact cameras with built in lenses have very high distortion and the calibration is not stable • Limited image memory and high consumption of power
Photography on negative film	
Advantages	Disadvantages
<ul style="list-style-type: none"> • High resolution • Better reproduction of colours • Larger density range • Nearly unlimited image storage 	<ul style="list-style-type: none"> • Film deformation reduces geometric accuracy • Control of exposure and image quality after film development • Images need to be scanned

Tab. 1: Digital photography comparing with photography on negative films

Accuracy of PHIDIAS

General information on accuracy usually does not make sense for photogrammetric close-range applications for which PHIDIAS is designed for, because the obtained accuracy of measurement depends on many factors which differ from project to project. The most important factors are the geometrical resolution during the digitizing process and the scale of the images. Especially the camera positions have a great influence on the attainable accuracy. For a precise estimation of the evaluation accuracy PHIDIAS can carry out corresponding simulation calculations, which also take the image configuration into account.

2.2.4 PhotoModeler

PhotoModeler Pro is a Windows based software program from Eos Systems, allows creating accurate, high quality 3D models and measurements from photographs. The product is in the fields of accident reconstruction, architecture, archaeology, engineering, forensics, web page design, and 3D graphics.

PhotoModeler Pro 5 offers fully automated camera calibration, NURBS Curve and NURBS Surface modelling. Camera calibration is the process of finding the true parameters of the camera. Some of these parameters are focal length, format size, principal point, and lens distortion. NURBS (= Non-Uniform Rational Bezier Spline) are 2D or 3D curves in space.

The differences in accuracy are due to many factors such as the camera proximity, the positioning and number of photographs used, the equipment used, the procedures followed. Normally the reconstructionist will have knowledge of the camera and lens,

control over the positions from which the photos were taken, many distinct points in the photos with precisely known coordinates, and access to the negatives or equivalent primary image. On the other hand it's possible that the photographs are taken from an unknown camera and lens, from unknown positions, with few distinct points in the photos to serve as control, and have no control over the generation and quality of the photographic print. Based on the information available and the accuracy required choices must be made on the suitable method.

For camera parameters, PhotoModeler requires the focal length, negative format size, and principal point (where the optical axis intersects the negative). The program also accepts lens distortion coefficients for radial and decentering lens distortions. PhotoModeler has the option of using frame fiducially marks (to locate the principal point on the image) which were used for several project cases. NURBS Surfaces are 3D surface with a smooth curved shape.

2.3 Aerial photography

These methods (air photography and satellite pictures) only should be mentioned and won't be described in detail.

The whole country is to be taken up by land surveying in such a way that a mapping is possible in an uniform scale. In addition a basis is created, which consists as evenly as possible of a number of points distributed over the whole country according to the location and the height. Based on this fixed point-net all further measurement work is developed mainly:

- The topographic survey of the entire country
- The production of plans and maps for technical purposes, in particular for the plant of traffic, water -, industry and buildings of settlements as well as different tasks of the administration, the economy and the public life.
- The location of individual properties, their borders and surface sizes.

For air photographs airplanes specially equipped and adopted are used. To produce real vertical air photographs, the pilot must keep a stable horizontal flight. Optimal to take photographs is around midday with highest position of the sun, so that the shade is not too long and suitable lighting conditions for the aerial photograph admission given in the pictures.

The satellite photographs are both black-and-white and colour films. Black-and-white photographic films guarantee a larger detail loyalty compared with the colour films. In contrast to airplanes the overflight/flyover route and time are fixed with satellites.

2.4 Measurement equipment

2.4.1 Tape measure

The measurements are accomplished with 30 m or 50 m roll volumes. At least two persons are necessary to measure with tapes if the point of origin can't be fixed in a different way.

Tape measure equipment:



Fig. 10: Tape measure

2.4.2 Yardstick



Fig. 11: Yardstick

2.4.3 Measuring wheel

From the revolution of the tyre the distance from point A to point B is determined. To measure a grass strip with a measuring wheel could be problematic. To lead the measuring wheel above an uneven surface results in a measuring error. The s-shaped characteristic is another error which could occur. For this method only one person is necessary.

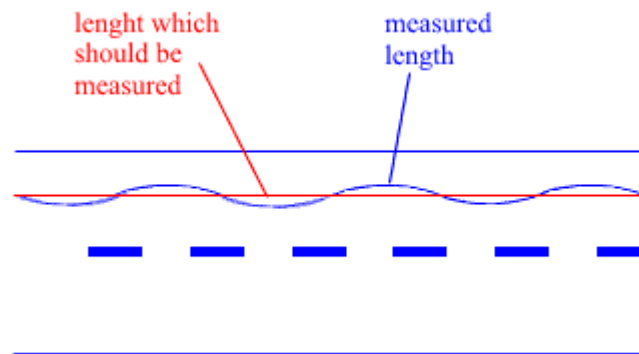


Fig. 12: S-shaped characteristic

Equipment:

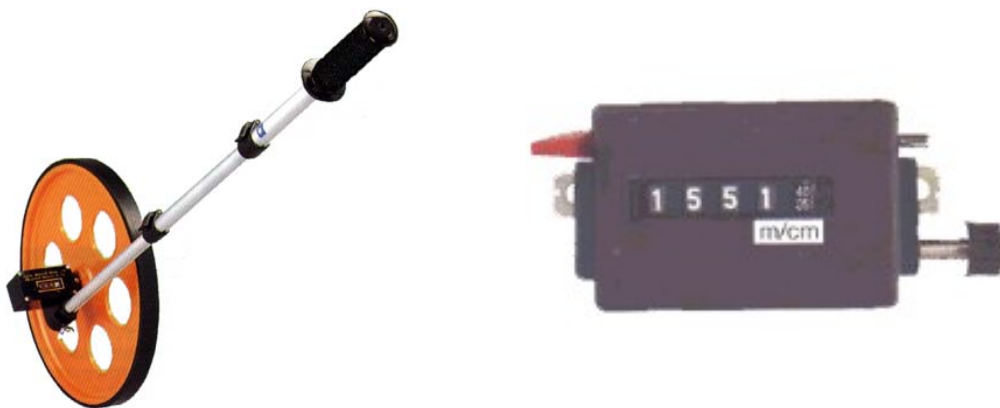


Fig. 13: Measuring wheel with counter

2.4.4 Laser rangefinder

Measure distances with a Laser become more important. The accuracy of such systems is in the range of +/- 5 mm depending on manufacturer and working area. Dust, fog, rain or smoke consists out of small particles or droplets. When they are hit by the laser point, light is reflected to the device and can interfere with the measurement. A reliable measurement is not possible any more. Wind however does normally not have any influence to the measurement result. Sunlight complicates measurements of a laser rangefinder. The reason is that the brightness of the ambient light becomes more and more similar to the brightness of the laser beam.

Equipment:



Fig. 14: Laser rangefinder

This equipment could be used to measure the interior of a car as well. For measuring the accident scene it's better to use reflectors in addition.

The costs of such equipment are at least 300 to 500€ and expensive in comparison to a tape or a measuring wheel.

2.4.5 Camera

Cameras are used to take photos of the accident scene as well as photos from interior and exterior of the damaged cars. Using digital cameras reduce work; no scanning of the photos is necessary. It's possible to look at the picture immediately after taken and could be done again if the result is not satisfactory. With software the pictures could be rectified. On each picture reference lengths are necessary.

Accident scene:

- The surface should be close to planar for the rectification process. If not, the area under consideration should be broken down into smaller areas which can be rectified independently.
- The camera height has a direct influence on the quality of the photo rectification. The higher it is, the better the result of the rectification will be, and the less will be the effect of local scene unevenness. As a general rule the depth of the scene to be rectified should be no more than about 12 times the camera height.
- Orthogonal as well as diagonal reference lengths should be used.
- Reference lengths should be in different areas of the scene.
- In the rectified picture the foreground of the picture is calculated with higher accuracy than the background. Therefore, try to use photographs which have the area of interest in the foreground.
- Only distortion-free camera lenses should be used. For most practical purposes, conventional 35 mm single-lens-reflex (SLR) cameras are suitable.
- When scanning photographs the whole picture must be scanned. A section of a picture, especially one far from the centre of the original, will produce poor results.

Reference length

To measure the accident scene it's easier to use reference length so picture can be rectified. This equipment in the picture below has four meters in diagonal.

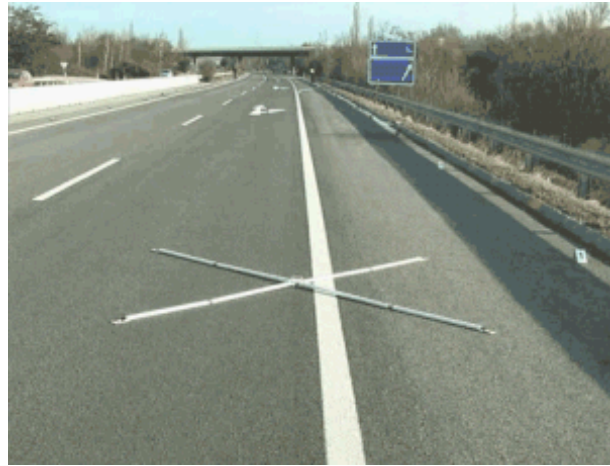


Fig. 15: Reference length equipment

3. Accident evidence

It is very useful to make as many pictures as possible from damaged vehicles and from accident scene. Imagine, if the vehicle is repaired or scrapped no information of the damaged profile is left. Pictures of vehicles should include the damage profile as well as interior pictures like pedals, airbag and facia in fact every interesting part. Parts of interest of the exterior are the damage profile. This includes longitudinals, bonnet, engine, glazing, wheels etc.

3.1 Damage marks

Damage marks result in connection with a traffic accident from the collision of a vehicle with at least one collision opponent. This could be another vehicle, person, obstacle, building, etc. The existing damage traces permit conclusions on driving directions and collision positions of the collision opponents to each other. Speed back calculations can be accomplished by the extent of the deformation (insertion depth).



Fig. 16: Damage marks

3.2 Material marks

Material marks in this sense (traces on/in vehicles or at persons) are at or in the vehicle and/or at persons responsible, imprinted, lying or gotten jammed articles, lacquer fragments or fabric parts (e.g. textile remainders), whereby the material is still clearly recognizable in its form/structure. Material marks can give referring to the impact place (textile fibres). Additionally the identification of participants of vehicles or person is possible. Where could this material marks be located? At first take a look on the bumper, mudguard, doors, exterior mirrors. Important is the breakage of the lightning equipment.

Following picture shows marks of a red coloured object (could be a car, obstacle, etc.) on another.



Fig. 17: Material marks

3.3 Wiping marks

Wiping marks develop, if an article, a person or an animal by the vehicle are touched. Dust and dirt particle are wiped by the surface of the vehicle or the floor pan. Wiping traces can be assigned due to their characteristic form and the determined height over the earth to a causing article so that conclusions on the contact point between the collision opponents can be pulled.



Fig. 18: Wiping marks

3.4 Casting marks

Casting marks result from transmission of a specific surface sample of an article or if dust on the vehicle isn't smeared. The sample of the keep in track-causing article is to be assigned mostly clearly recognizable. The two pictures on the left side have marks from an object and on the third picture the object is shown which made this marks.

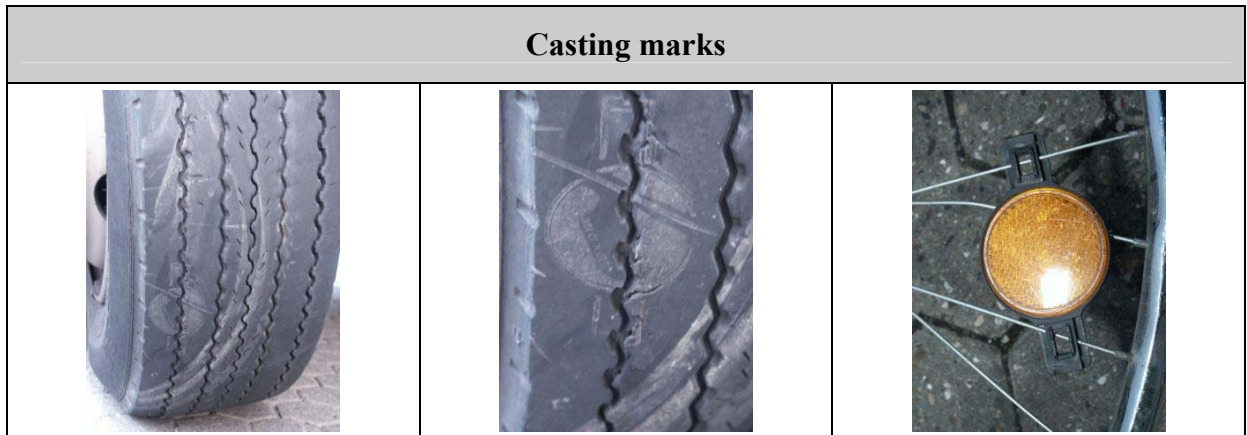


Fig. 19: Casting marks

3.5 Abrasion, melting marks

Abrasion marks develop with contacts of two articles on/in vehicles or on/by persons, whereby abrasion marks from vehicle/obstacle are on each other. Most abrasion marks at the vehicle are lacquers, transferred rubber and plastics in the vehicle are this blood, hair and textile fibres. These traces give information of the direction of motion, the course of motion and the position of the vehicles/persons involved in an accident at the time of the collision. Moreover they serve in addition, for the identification of participants of vehicles (by lacquer investigations and comparison of the trace pictures) and persons and/or the driver (by fabrics -and blood investigations).

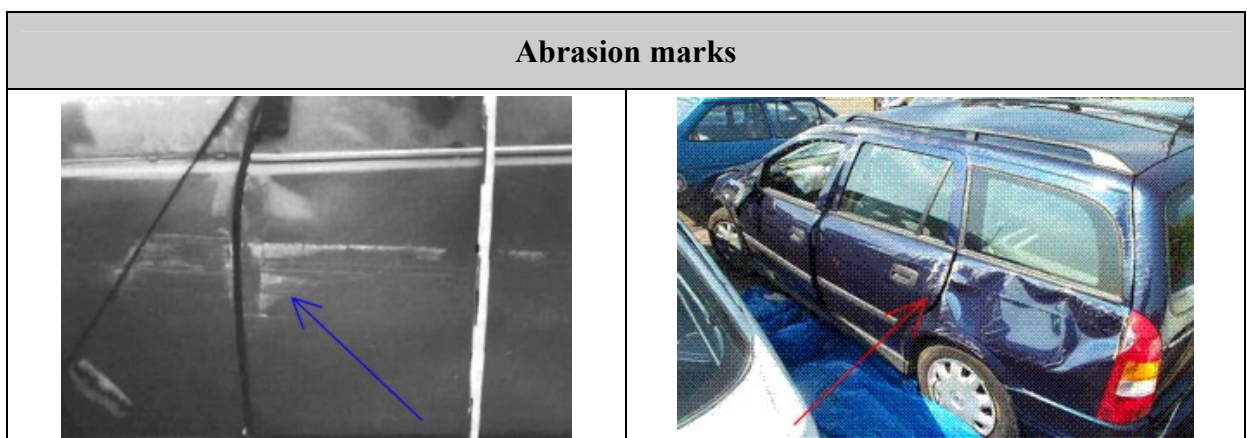


Fig. 20: Abrasion marks

3.6 Biological traces

Biological traces in this sense (traces at/in vehicles or at persons) are separated, withdrawn, abraded or separated materials or parts of an organism (humans, animal or plant). In the context of an accident these are blood, vomit, excrement and urine, hair or feathers/springs, fabrics and secretions, brain mass, body and bone parts, plant parts. Biological traces at or in the vehicle or at persons inform about the accident process (e.g. when finding feathers/springs, hair of animals and parts of plants) and the impact place of people involved. In accidents biological traces serve persons in or at the vehicle (when finding blood, hair and fabrics) also for the identification of a suspect and for the determination of the seating positions.

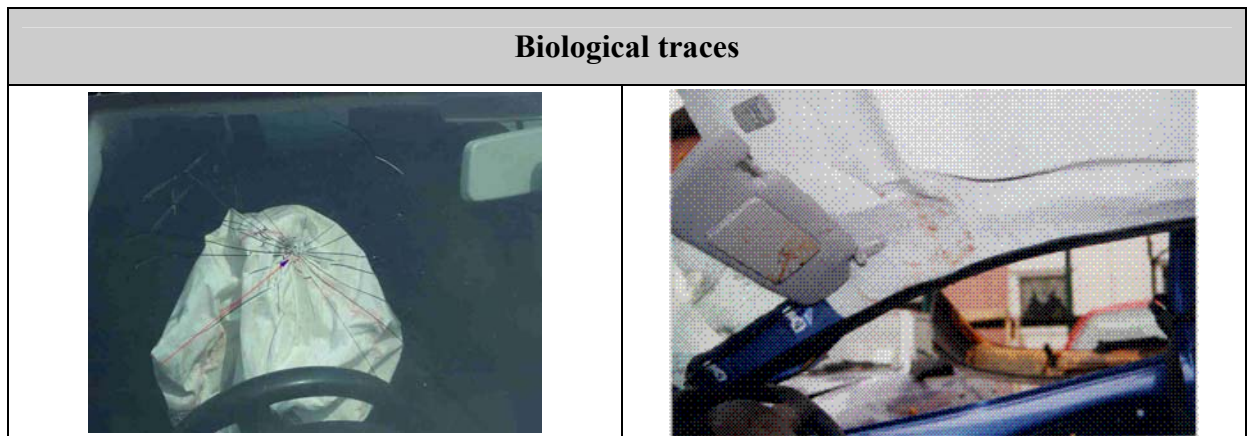


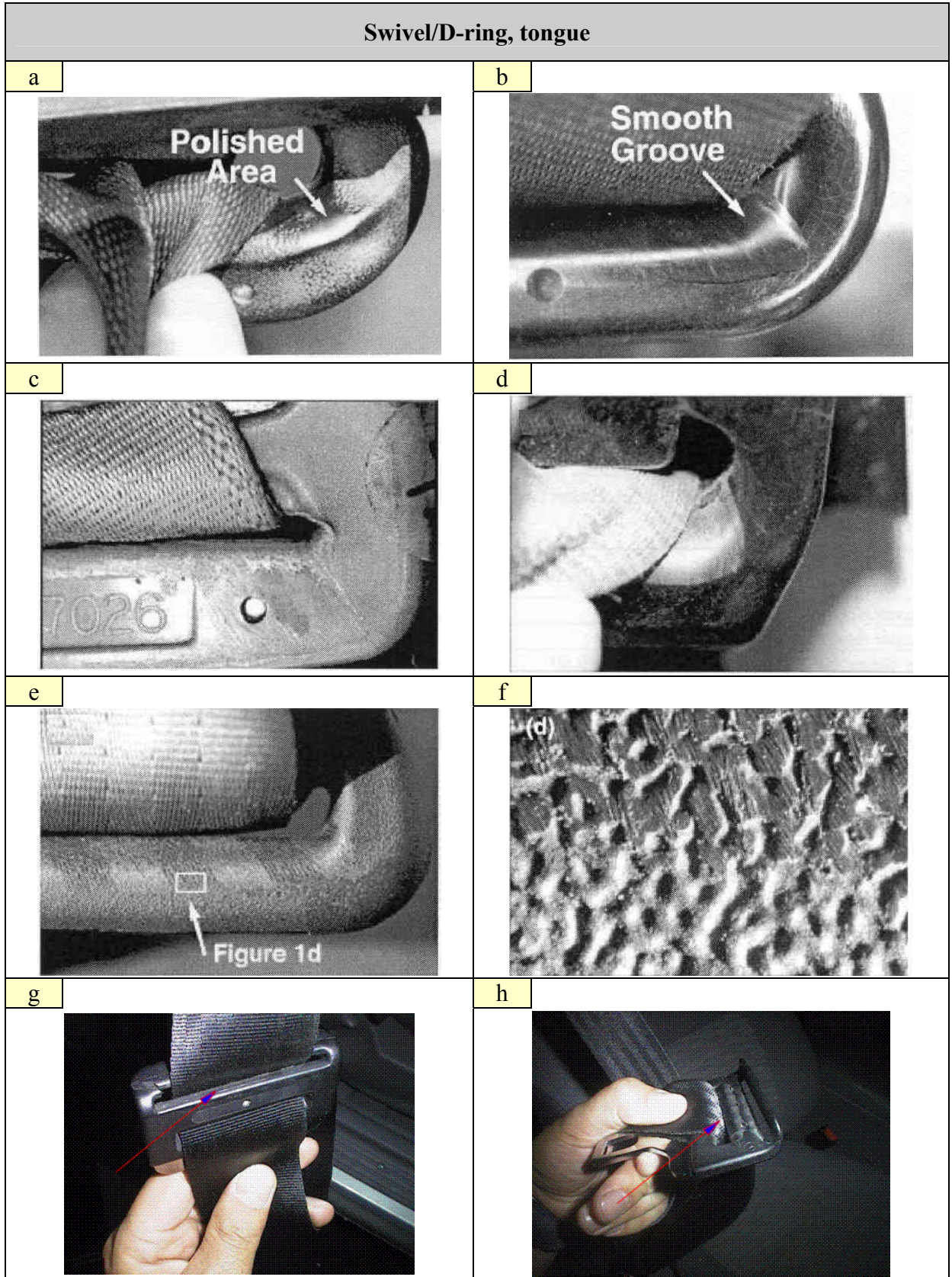
Fig. 21: Biological traces

3.7 Webbing marks

In accidents there could be marks on the tongue and on the webbing. On the webbing there are striations and on the D-ring abrasions and smelting plastics. Such webbing marks will be produced only if big forces were occurred and not under normal conditions. These big forces produce enough heat for these marks.

The first two pictures (a) and (b) below have a polished and a smooth area on the D-ring. For the first consideration this effects must be from the accident but these marks are from general use of the driver or passenger. In case of an accident the material of the D-ring would be found in the seat belt as well.

In the pictures (c) and (d) the material of the seat belt is daubed in the D-ring. Picture (e) shows the weaving pattern of the seatbelt on the D-ring. The force wasn't very high and the accident not severe. Picture (f) shows the microscopic photo of the daubed seat belt material. (g) and (h) demonstrate material of the seat belt on the D-ring whereby in picture (i) and (j) striations are on the belt. Such characteristics can be arguments that the seat belt was used if the driver or passenger doesn't tell the truth. Broken glass causes such traces shown in pictures (k) and (l) if a window breaks and is pitched into the passenger's compartment.



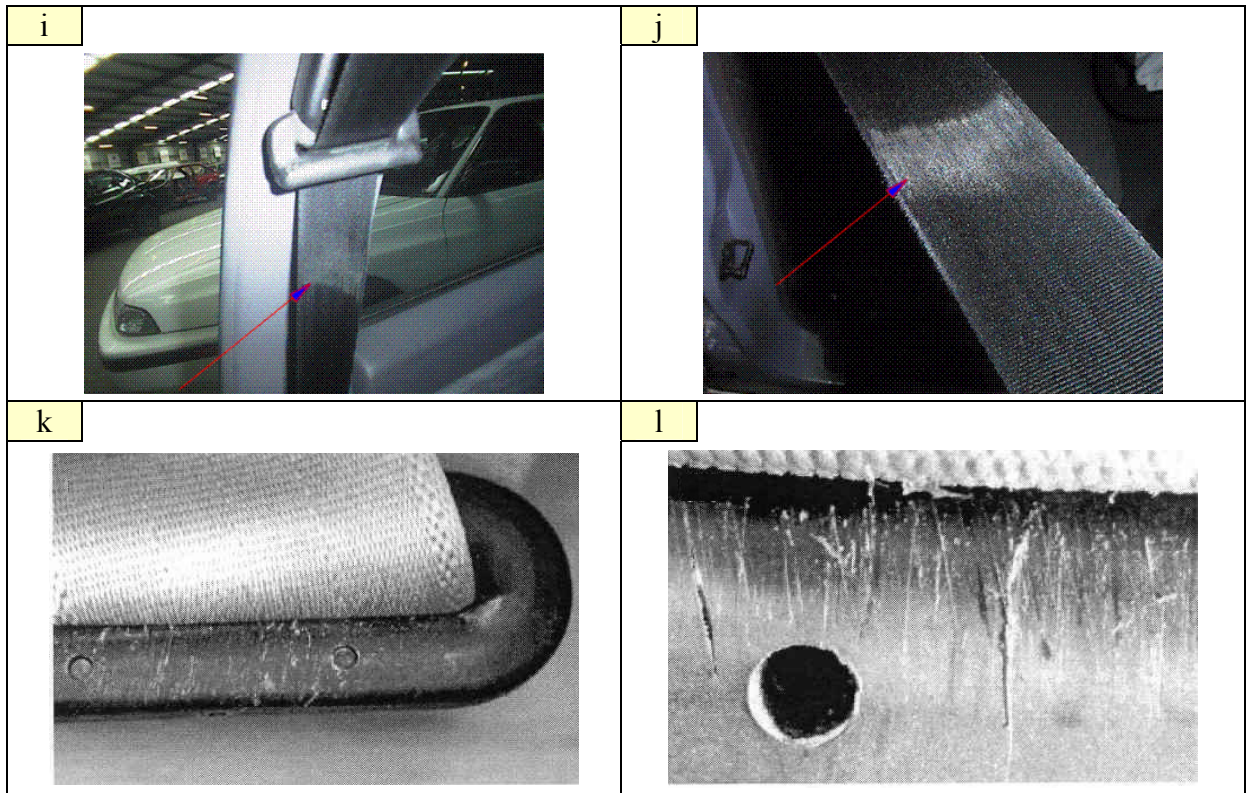
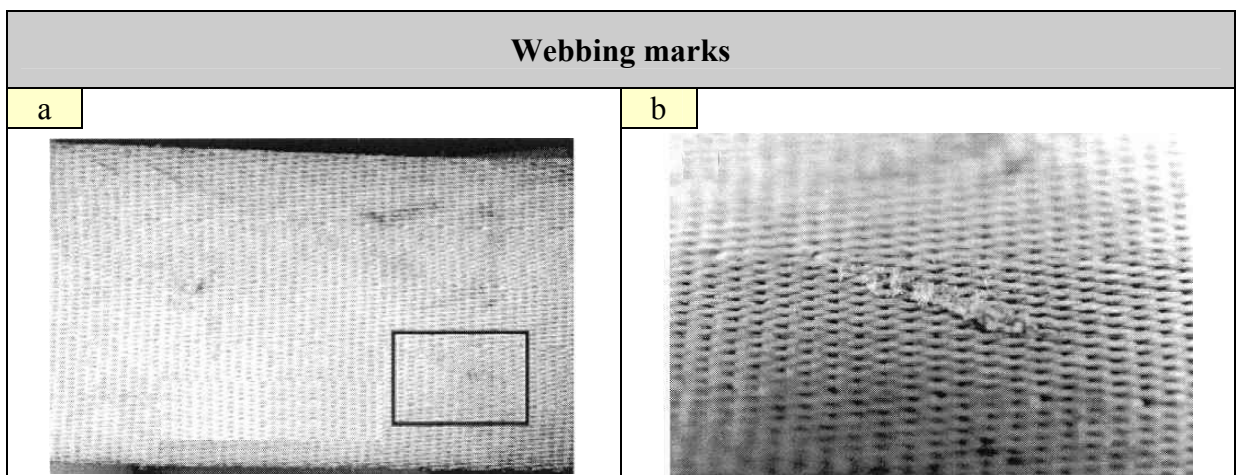


Fig. 22: Swivel/D-ring, tongue

On the webbing there are many different traces which are caused during an accident or of daily use. In picture (a) and (b) the belt was often penned in the door and this was the reason of those marks. The investigator has to be very carefully if he looks at such marks.

If seat belts are used incorrect marks could occur as well (c) and (d). In picture (e) and (f) the seat belt was penned in due to incorrect use. Image (g) demonstrates striations on the seat belt which are rather from a watch, a ring, etc. than from clothes whereby in image (f) the striations are from melted filament of clothes.



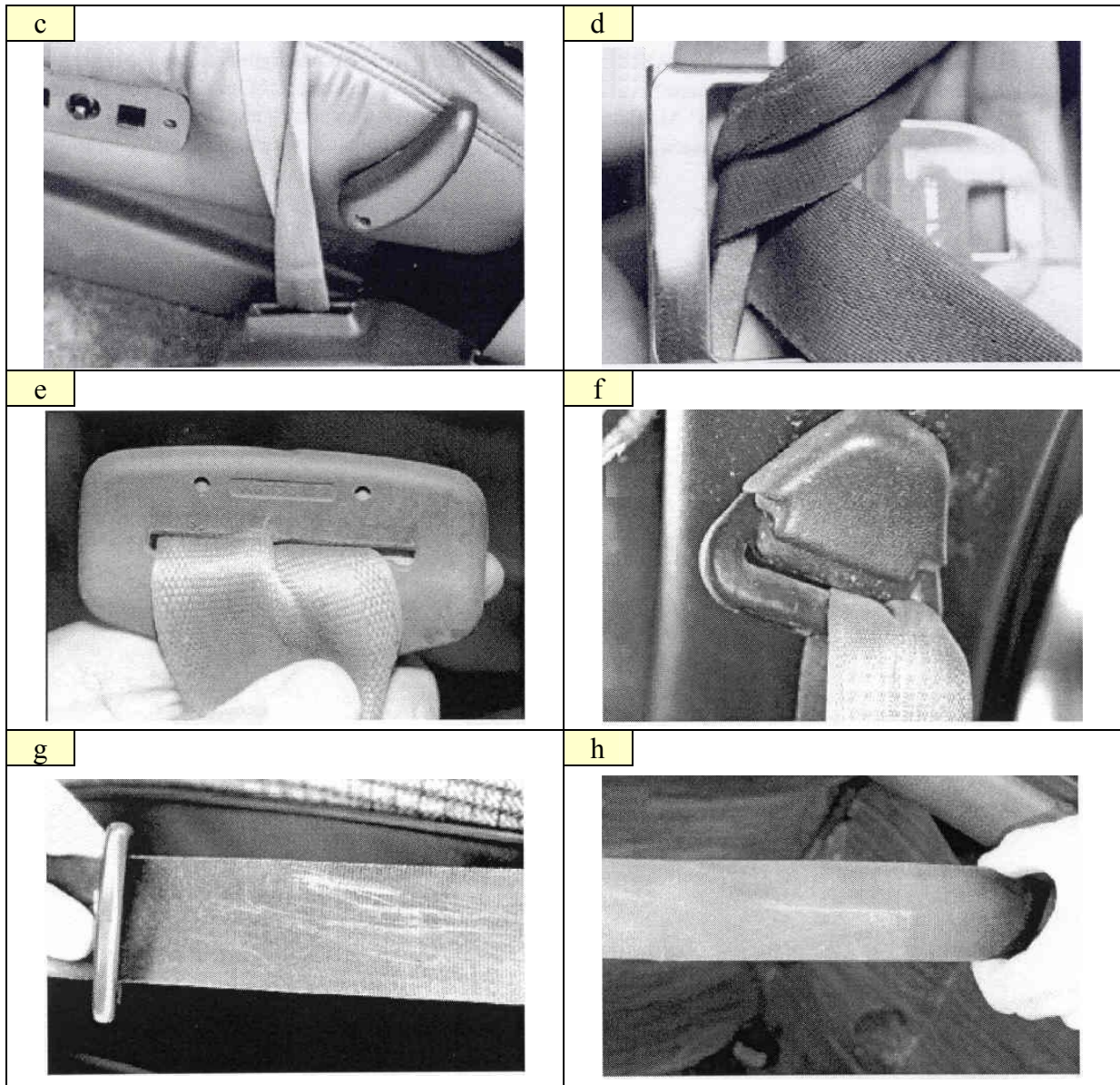


Fig. 23: Webbing marks

Often it is very difficult to find out the driver of the vehicle. If no eyewitnesses are available the evidences described above should give information. In the area of driver's seat and the steering wheel, dashboard, side carpeting and centre control stand are traces visible which are caused by an accident. Fibre from clothes of the driver could be melt with the car interior lining. Similar traces could occur on the passenger's side of the vehicle of course. If the vehicle was fitted with airbags and they were deployed there could be traces as well. There could be biological traces on windows or roof interior which give information about contacts. On the webbing there could be clothing fibre which is good information of source if the person was belted or not.

Based on STAIRS protocol following seating positions are possible:

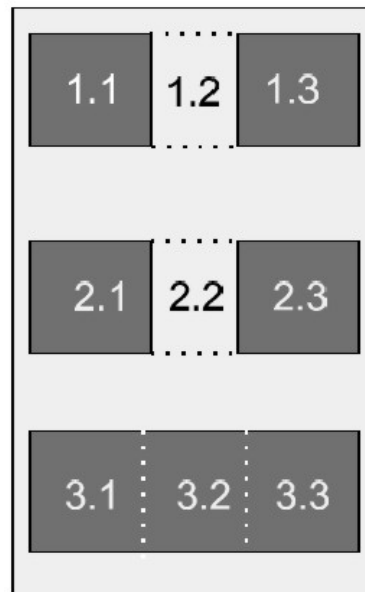


Fig. 24: Seating positions

1.1 is the driver's position, 1.3 passenger's position.

Some cars are equipped with seat allocation recognition systems. The reason for the development of such systems was the high and unnecessary economic costs for deployed airbags. For a velocity range between 25 and 40 kph most of the vehicles could be repaired. In most of these accidents no passenger is in the car but the passenger airbag deployed anyway. One of the essential requirements of these systems was a fail safe behaviour. In case of an error in the system the airbag should deploy even if there is no passenger on the seat.

Systems which are available:

- Capacitive measurement systems
- UHF-sensors
- Thermal infrared sensors
- Optical recognition systems
- Ultrasonic systems
- Piezoelectric cable
- Resistance strain gauges on bending bar
- Force Sensing Resistivity (FSR)

3.8 Airbag control unit

The airbag system consists of modules and a control unit. Modules are in steering wheel, doors, dash board. Furthermore there is a microcontroller which consists of CPU, analogue/digital transducer, storage unit and communication interface. Storage unit consists of a read memory (ROM), read and write memory (RAM) and an electric deletable and programmable storage unit (EEPROM).

Data which are stored in airbag control units (EEPROM):

- System and failure status before and during collision
- Troubles which occurred during impact
- Error times
- Battery voltage
- Energy reserve voltage
- Reference voltage
- Sensor testing results
- Ignition circle error
- Warning lights errors

To get such information it is necessary to contact to car manufacturer. In case of legal procedures it is possible to get that information.

3.9 Throwing range of broken glass

At the accident it's not possible to say if there is either broken glass from headlights or broken glass from the windscreen. Additionally there's hectic on the scene and not every glass splint could be found or glass splint can be carried off through pedestrians or vehicles. Therefore a wide range of broken glass should be used. Tests of DEKRA confirm previous papers which have been made by several accident reconstructionists in the past. An essential difference between broken glass from headlights and broken glass of windscreen couldn't be found although the damage of a windscreen in case of pedestrian accidents happens approximately 0.1 to 0.15 seconds later than the damage of the headlights.

“Glass flour” has no long throwing distance and is good evidence for an impact location.

Mathematical description of the first glass splinter boundary formula:

$$s_{Ge} = 0,00222 \cdot v_k^2 - 0,0117 \cdot v_k \quad 3-1$$

Mathematical description of the last glass splinter boundary formula:

$$s_{Gl} = \frac{1}{2} \cdot v_k \quad 3-2$$

Following picture shows the throwing range of broken glass from headlights based on tests of Schneider (H. Burg, H. Rau: Handbuch der Verkehrsunfallrekonstruktion; Verlag Information Ambs GmbH, Kippenheim):

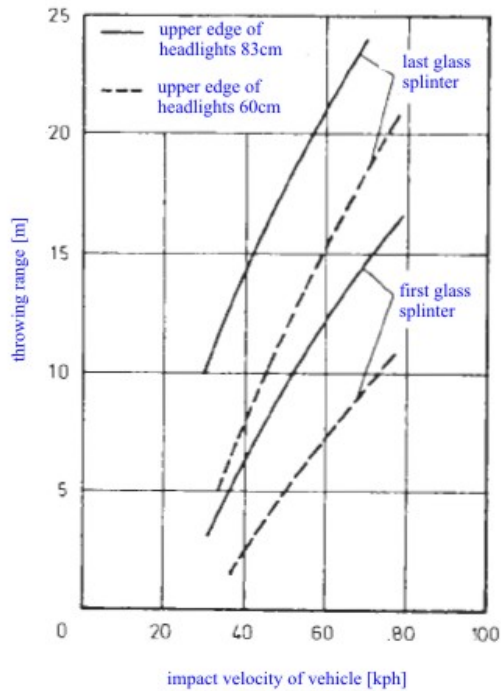


Fig. 25: Throwing range of broken glass from headlights - Schneider

Next pictures are from H. Burg, H. Rau: Handbuch der Verkehrsunfallrekonstruktion; Verlag Information Ambs GmbH, Kippenheim

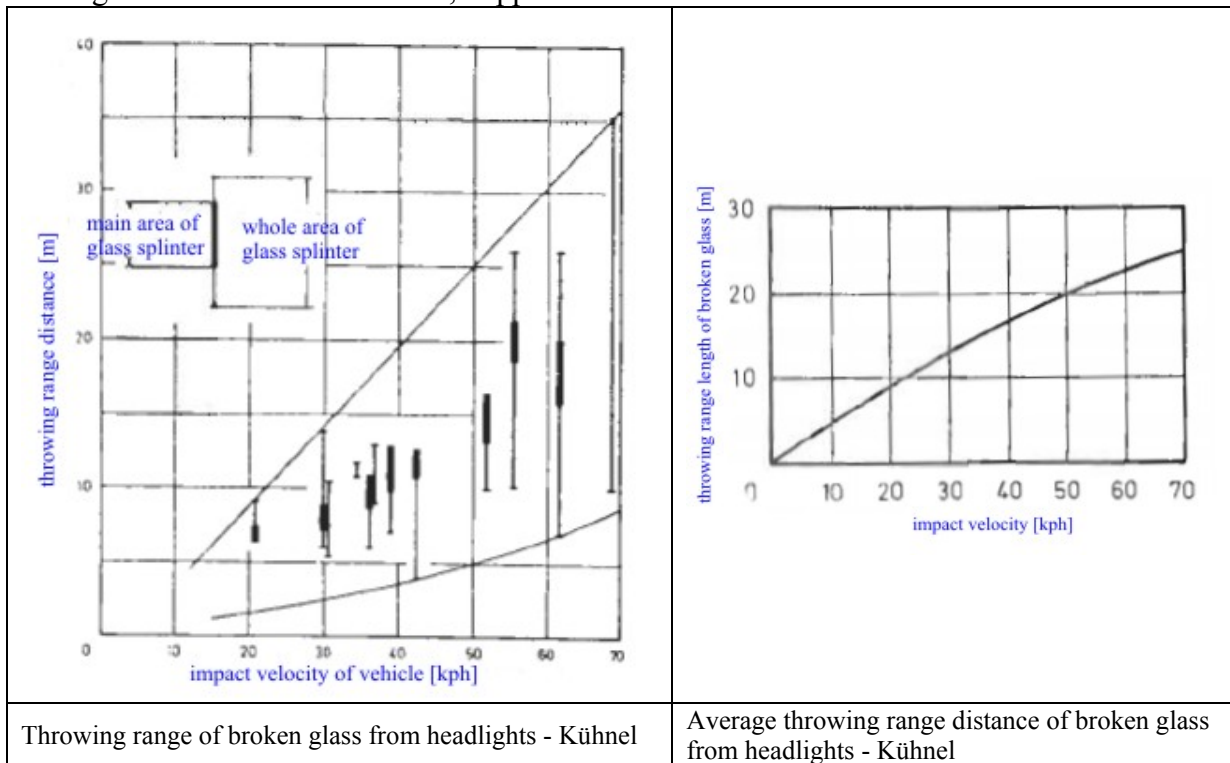


Fig. 26: Throwing range of broken glass from headlights - Kühnel

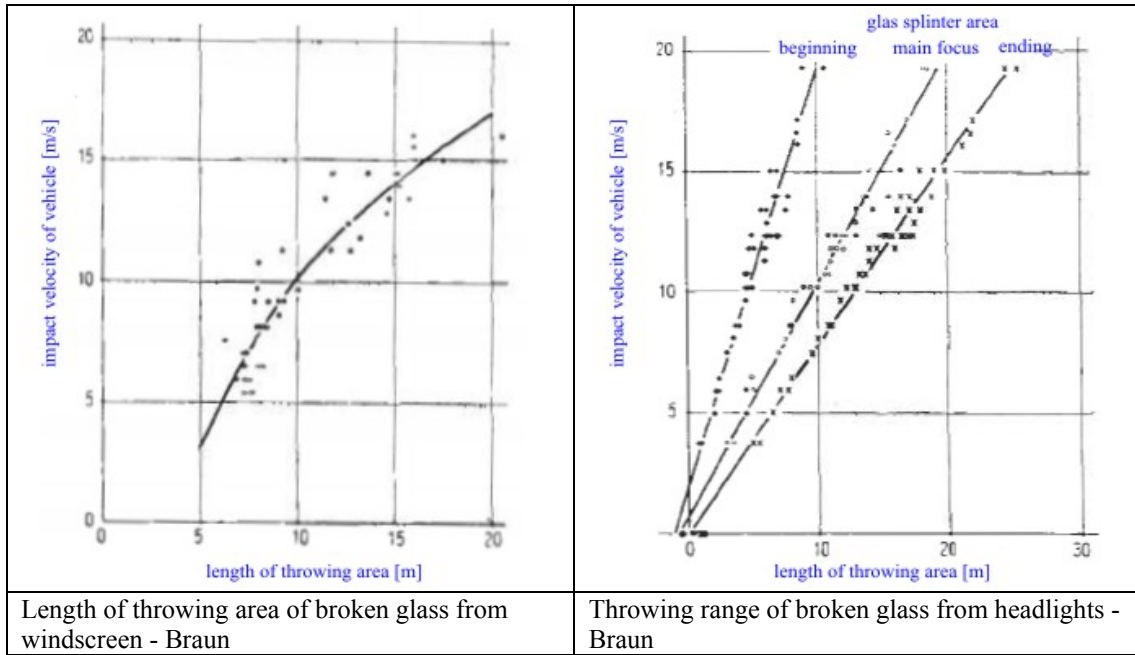


Fig. 27: Throwing range of broken glass from windscreen and headlights - Braun

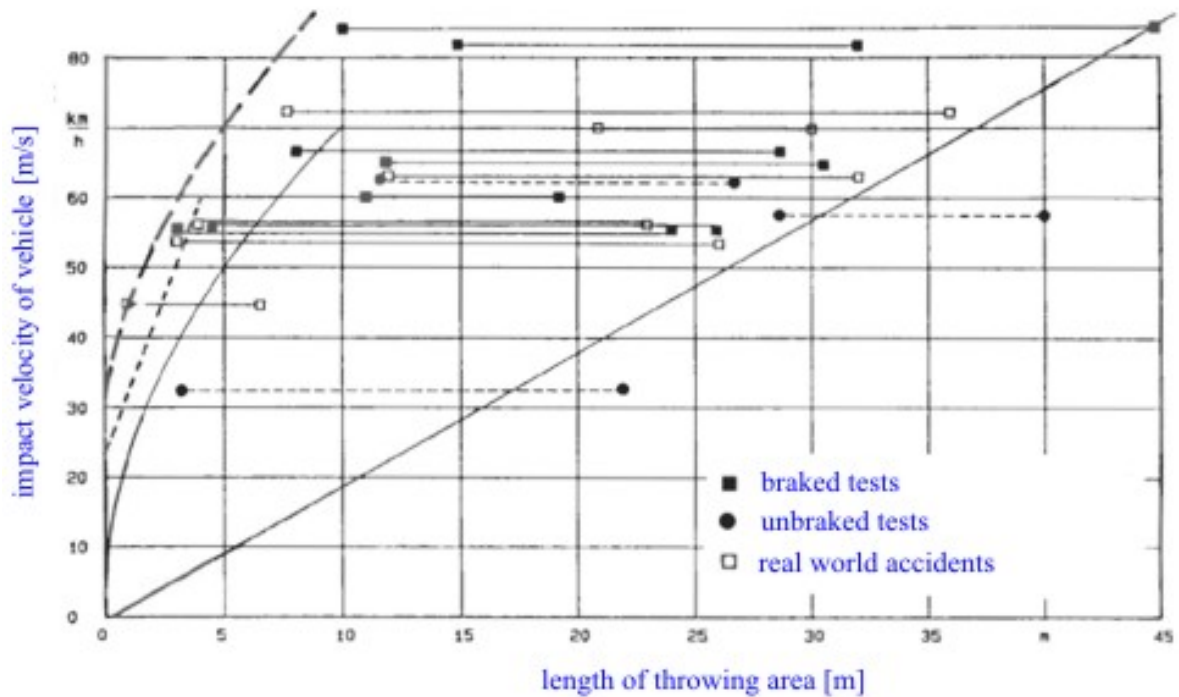


Fig. 28: Modified length of throwing range of broken glass - DEKRA

Based on those tests DEKRA modified the formula for the first glass splinter boundary to:

$$s_{Ge} = 0,0018 \cdot v_k^2 - 0,0544 \cdot v_k \quad 30 \geq v_k \geq 85 \quad 3-3$$

The formula for the last glass splinter boundary hasn't been changed.

4. Tyres and pavement

4.1 Tire-Roadway friction values

Warner et al: The determination of appropriate friction coefficient values is an important aspect of accident reconstruction. Tire-roadway friction is highly dependent on a variety of physical factors. Factors such as tire design, side force limitations, road surface wetness, vehicle speed, and load shifting require understanding if useful reconstruction calculation are to be made.

Definition: The friction force F is defined as the force which exists on a body at its interface with another body, acting in a direction which tends to resist or retard relative sliding motion between the two bodies.

$$\mu = \frac{F}{N}$$

Formula 4-1

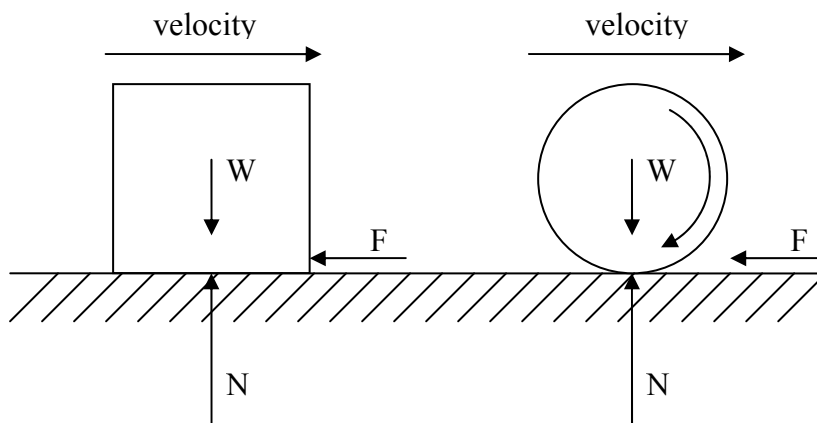


Fig. 29: Friction and normal forces in sliding and rolling

Kind of forces which cause friction:

Mechanical interference, or abrasion, occurs between even the smoothest surfaces as local surface irregularities try to lock together like random gear teeth.

Viscoelastic deformation forces occur because of localized squeezing and relaxation of materials.

Molecular attraction results from the natural attraction existing between surfaces.

Friction types:

Static friction covers all cases where the frictional force is sufficient to prevent relative motion at the interfaces.

Sliding friction occurs where there is relative tangential sliding motion at the interface.

Rolling friction exists where one surface rotates, but does not slide on the other at the point of contact.

In static friction the greatest forces are due to mechanical interference and molecular attraction. Once external forces are sufficient to overcome static friction, motion occurs between the bodies and the realm of sliding friction is entered. When sliding occurs, all three causative factors contribute to the friction force. When rolling occurs, most friction may be attributed to local deformations near the contact zone. Mechanical interference can be minimized in rolling by keeping the surfaces smooth. Adhesion is minimized by keeping surfaces out of widespread contact with each other.

The reconstruction of accidents occurring on roadway surfaces in winter is often complicated by the myriad of factors which affected the selection of the proper tire-to-road-surface coefficient of frictions for use in the analysis. Some of these factors are: the presence of ice or snow, the temperature, the use of snow tires or chains, the application of sand to the road surface, the dispersion of the sand, a fresh snow layer over pre-existing ice, and deep snow where vehicles may unintentionally travel etc.

More information to *Tire-Road Friction in Winter Conditions for Accident Reconstruction* in SAE paper 960657.

4.1.1 Influence of the vehicle speed

In the literature it is suggested, that the dry-pavement sliding frictional force of a tire decrease with increasing sliding speed, although there are some data to the contrary in specific area. This decrease, called the velocity decrement of sliding friction, v , is of relatively small effect for low and moderate highway speeds.

$$\mu = \mu_0 - v \times V \qquad \text{Formula 4-2}$$

- μ_0 low speed friction coefficient
- V sliding velocity
- v value between 0.0027 to 0.008 kph

4.1.2 Interaction between tires and pavement

Tires are part of a dynamic system, the automobile and their interaction with the pavement cannot be viewed in isolation. Tires transmit forces from the automobile to the pavement and the pavement must be able to withstand this forces. The vertical force carry the total load, while the horizontal force provide traction, braking and direction stability. These forces depend on the coefficient of friction between the tires and the road surface. A high coefficient of friction is needed to prevent skidding accidents.

The available friction is the maximum friction force that can be transmitted under the conditions. Friction demand is the friction force needed for performing the intended manoeuvre. It is essential that the available friction exceeds the friction demanded.

Friction demand increases with increasing speed while available friction decreases. Thus speed is a major variable in road safety.

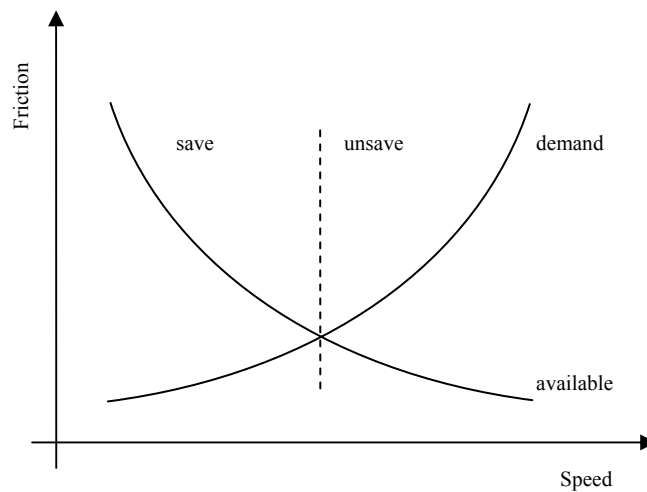


Fig. 30: Available and demand friction on wet pavements

4.2 Skid marks

Skid resistance depends strongly on the type of tire and pavement. Some type of rubber gives much more friction than others.

Reveley et al described following: Tire marks present at an accident scene involving vehicles are one of the most foretelling pre and post crash parameters. An automobile equipped with a conventional brake system often will produce four skid marks on a roadway surface during maximum braking. The utility is further enhanced since the three directions a vehicle may assume are characterized by the type of mark (or lack of mark) produced by the moving vehicle. From skid marks important data could be determined for the reconstruction. For instance: velocity, direction of movement, movement of the vehicles after the collision, final positions etc.

Skid and yaw marks left on the pavement after an accident have occurred may assist accident reconstructionists in determining the course of events that led to the accident and the pre-crash parameters of the vehicles involved.

The determination of whether a tire mark is the result of locked or unlocked wheels it is important for the results of an accurate accident reconstruction. The biggest problem in modern vehicles, from the point of an investigator, is the increasing use of anti-lock braking systems (ABS). In certain conditions it may be true that ABS allows stopping vehicles in a shorter distance, but anti-lock systems are designed to prevent the wheels of a vehicle locking. This allows the driver steering during emergency braking. No locked wheels mean that there are no wheel marks on the road surface which is not helpful for calculating the initial speed. In certain conditions marks will be on the road surface even if the vehicle was equipped with ABS.

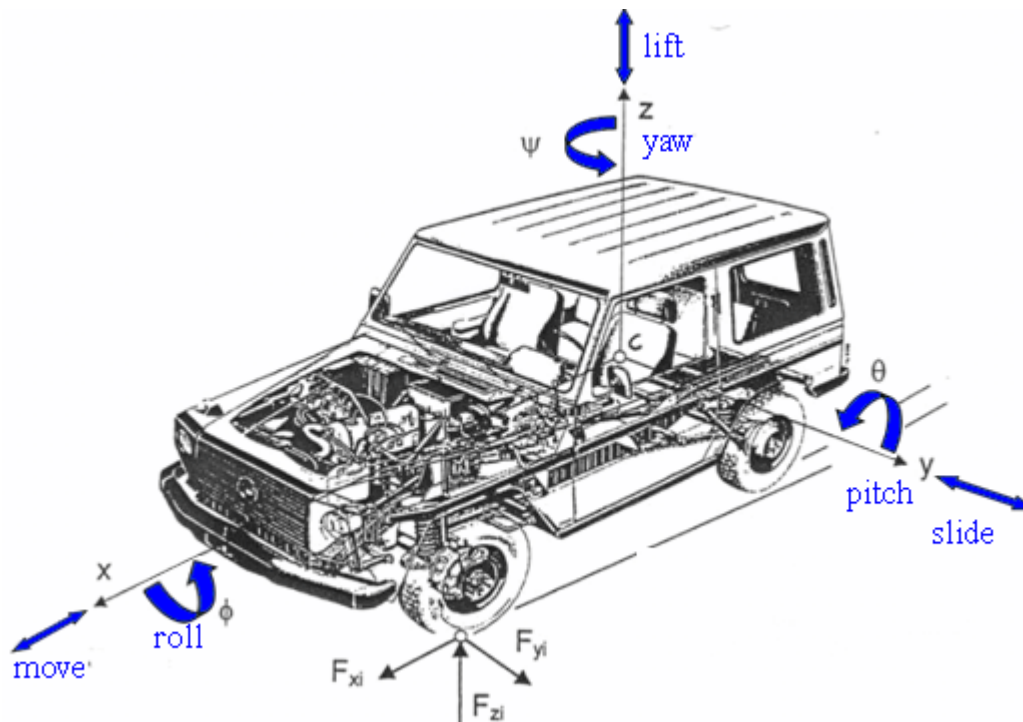


Fig. 31: Axis of possible movement of a vehicle

Yaw is the term applied to a sideways movement of a vehicle, such as when the rear of a vehicle sideslips and moves in a direction other than the direction in which the vehicle is headed. In a fast turn, the centrifugal force tending to keep the vehicle going straight ahead becomes greater than the friction force between the tires and the road. So the tire slips sideways leaving a yaw mark. A yaw mark is a tire mark made on a surface by a rotating tire which is slipping over the roadway more or less parallel to the tire's axis. Common driver occurrences that produce yaw marks would be when the rear end of a vehicle attempt to lead the front end of a vehicle. This yaw is often experienced when driving on slippery road surfaces (wet, snow covered, ice covered) gravel or loose dirt/sand surfaces.

Skid marks are the result of a non-rotating tire slipping over the roadway while the vehicle is still moving. This locked wheel tire print is often referred to as a braking skid mark. The vehicle tends to rotate about the pitch axis of the vehicle as the front axle experiences a load shift due to the sudden deceleration of the vehicle. Severe high speed braking skids will actually remove a significant amount of rubber on the head of the tire often resulting in a flat spot.

Before determining the speed of a vehicle from a tire mark which was left on the roadway, it must be determined what type of tire mark is present. Tire marks left as a result of braking (locked wheels) typically have striations that run parallel to the length of the mark. Tire marks left as a result of sliding, rotating (unlocked wheels) leave a striation that is typically lateral to the length of the mark unless the vehicle has spun around. If the vehicle has spun around with unlocked wheels, the striations in the mark typically will change from lateral to parallel and back to lateral to the length of the mark. Steering input while yawing appears to reflect in the appearance in the yaw mark's striations of a change from lateral to between lateral and parallel to the path of the tire mark.

Marks of movement (e.g. in snow, on the roadside, etc.):

Imprint of the tyre on the surface, typically is the undistorted tread pattern.

Skid-marks from unlocked wheels:

Result from the slip of the wheels with brake; rubber abrasion and keying on e pavement are recognisable. This skid marks have to be taken as soon as possible because they are ruined easily.

Skid-marks from locked wheels:

The wheels are locked and slide on the surface of the pavement. If the vehicle velocity is more than 100 kph the wheels would be damaged. This kind of tyre marks arises at the end of the phase of swelling. On a planar surface the movement of the centre of gravity in case of unlocked wheels is a straight line.

Accruelement of marks from locked and unlocked wheels:

- on concrete roadways by abraded roadway dirt and tire abrasion
- on plasters by shifted stones and depending upon kind of plaster rubber abrasion
- on sand -, crushed stone and grass surfaces only by shifting or turning up the surface of the underground
- on bitumen roadways by exude of the bonding agent - bitumen at the roadway surface due to heating up by the over there-sliding or under large slip still partly rolling tire and by exude of the tire rubber likewise dissolved by friction heat

Sliding marks:

It often happens that marks appear from stones. Offsets within the skid marks indicate always points of collisions. Both the course of motion and the position of the vehicle for direction of motion can be completely arbitrary. Often sliding marks process arched whereby the traces of the individual tires can change the distance and the skid marks must not be looking similar over the whole length regarding to the vehicle turns around the vertical axis.

Accruelement:

A centrifuge trace develops with a completely uncontrolled movement of the vehicle, if the border of the road grip is exceeded.

Milling traces:

The milling trace results from the friction of a strongly pressure-reduced or in addition, pressure-free tire on the road surface. If one can assign the milling trace to the introduction phase of the accident, then the tire concerned was already pressure-free before the collision and is possibly applicable as cause of accident. If one tightens the milling trace however in the rundown phase, then the pressure-free of the tire might be caused by the accident.

Accruelement:

The milling trace results from the friction of a strongly pressure-reduced or in addition, pressure-free tire on the road surface. Milling traces develop more or less in truck accidents than in passenger car accidents.

Drift traces or transverse sliding traces:

Result from the resistance of the sole profile of a tire against the vehicle's centrifugal force while driving in a curve. The vehicle is at the detention border and did not exceed. During excess the detention border turns the vehicle around the vertical axis and changes into a centrifuge movement. Drift traces make statements about the reaction and brake behaviour, the speed dismantling, the direction of motion and a computation for the speed possible.

Accruement:

Drift traces or transverse sliding traces result from the resistance of the sole profile of a tire against the vehicle's centrifugal force while driving in a curve.

4.2.1 Skid mark interferences

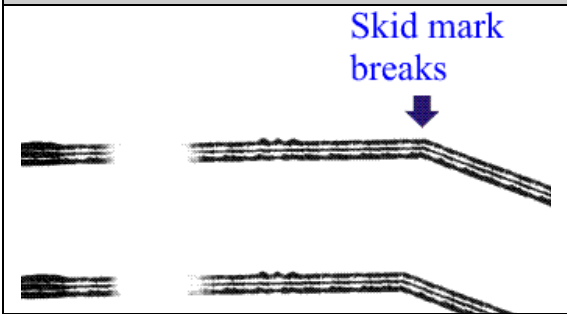
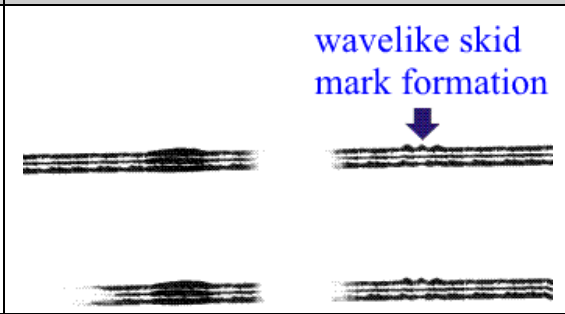
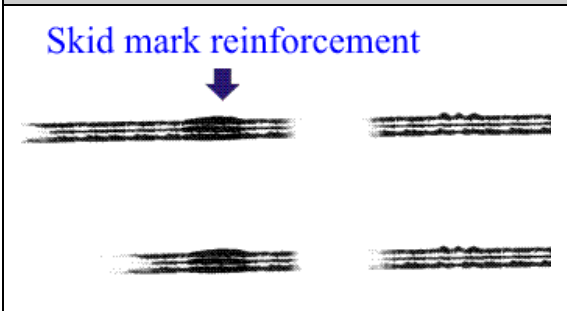
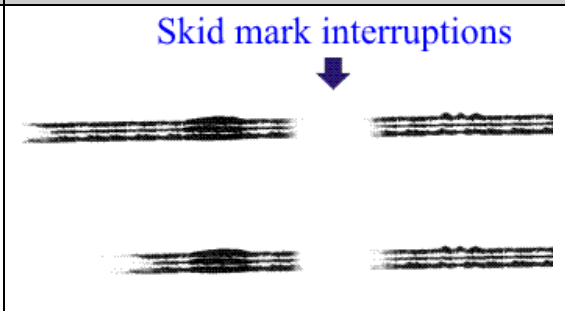
Skid mark breaks occur due to change of direction of the braking and traces drawing vehicle. This shows up in the trace in form of a change of direction, a trace break. Usually the direction indicates the driving direction of the vehicles to the trace deviation.

Changes of direction step also before or after the collision with a vehicle on (e.g. by impact against curb or other obstacles) and produce likewise during the braking trace breaks, which however under no circumstances may not rated as the collision location.

Wavy trace can also develop, if a defect at the wheel suspension is present (usually from the beginning of trace and runs up to the end of track), by uneven roadway surfaces.

Trace reinforcement also arise, if keeping in track drawing wheel an increase in the roadway surface (e.g. bump) over-drives or the carriageway surfacing (e.g. by repairs) changes.

In rare cases also short *trace interruptions* are to be observed due to the collision. It could be possible that a wheel takes off from the roadway and interrupt the skid mark.

Skid mark breaks	Wavelike skid mark formation
	
Skid mark reinforcement	Skid mark interruptions
	

Tab. 2: Skid mark interferences

4.2.2 Influence parameter for skid marks

Influences of skid marks are multifarious for instance tyres, surface of the road, temperature, weather or braking slip. DEKRA developed a track intensity scale which describes recognizability of traces. Minimum is 0% (no trace) and maximum 100% (maximum distinct trace). Most important is the intensity of traces.

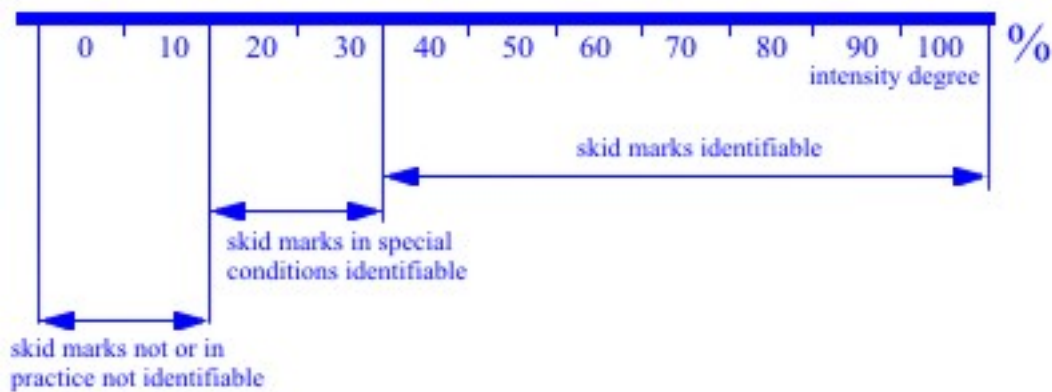


Fig. 32: Skid mark apperance – intensity degree

Skid marks with an intensity degree of 40% are recognizable. For special conditions e.g. the vehicles are in the end position and if the securing of evidence has been made carefully skid marks with an intensity degree of 20 to 40% are identifiable. An intensity degree of 0 is not identifiable.

Trace development:

Mark development alongside of the braking distance.

Border mark:

Distinctive development of the mark from the border of the tyres.

Filling:

Marks between the borders of the tyre.

Spacing mark:

Interrupted marks alongside of the braking distance.

In the following pictures show how skid marks could look like. If a vehicle brakes traces will occur on the pavement. Picture (a) illustrates an uninterrupted skid mark where the border mark isn't different from the filling and the filling is strongly pronounced. The difference of filling and border marks is shown in (b) and (c). The skid mark is uninterrupted. In picture (d) there is an interrupted skid mark demonstrated.

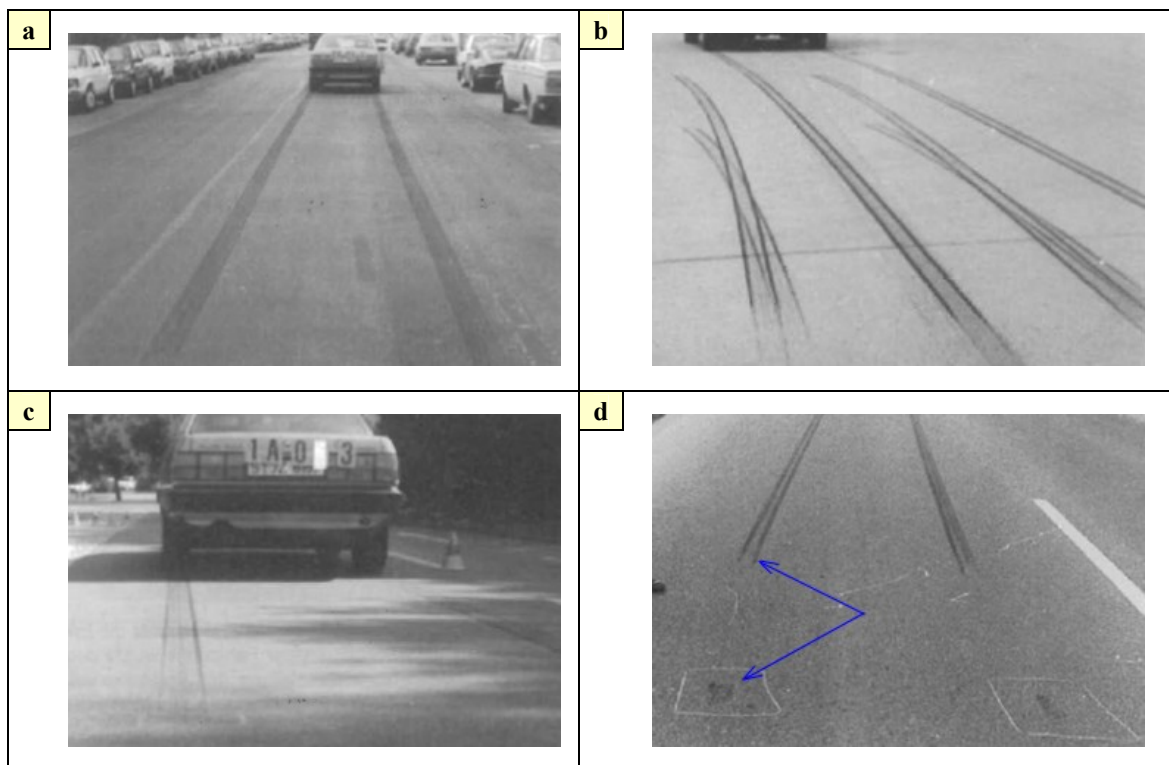


Fig. 33: Skid marks

4.2.2.1 Pavement

Condition of the pavement:

A fine roughness which will be caused by fine-grained crushed stones benefits developing of marks. Due to relative movement between the tyres and the pavement (slip) rubber will be emerised from the tyres and will be visualized on the road surface. The conspicuity of such marks is only for about half an hour up to an hour. Skid marks which occur from vehicles with ABS are called “rule traces”.

Situation of the pavement:

In case of a water film on the surface blocking traces won't be developed neither will rule traces. Dry dirt and dust on streets benefit rule traces because of the slip between tyres and pavement. The dust and dirt will be smeared to visible traces.

In following table the maximum acceleration values in correlation road surface and road condition could be found. This study has been made by Danner and Halm in 1994.

		road surface			
		asphalt	concrete	paving stone	gravel/sand
road condition	dry	8,8 [m/s ²]	10,0 [m/s ²]	8,2 [m/s ²]	5,8 [m/s ²]
	wettish	8,0 [m/s ²]	9,0 [m/s ²]	7,4 [m/s ²]	5,2 [m/s ²]
	wet	7,5 [m/s ²]	8,5 [m/s ²]	6,8 [m/s ²]	7,0 [m/s ²]
	snow	4,1 [m/s ²]			
	hoarfrost, icy	2,0 [m/s ²]			

4.2.2.2 Tyres

New tyres which have less than 50km mileage cause slightly rule traces because the fine rubber particle on the surface of the tyre will be smeared to a visible trace on the pavement. This is more or less irrelevant for reconstruction.

4.2.2.3 Brake initial velocity

If there is a full braking with blocked tyres, the vehicle doesn't have ABS; the intensity of the marks on the surface of the road will increase. This effect arises because the footprint of the tyres is the same (tyres are blocked) and the rubber heats up. The melted rubber cause marks. In case of vehicles with ABS where the tyres are not blocked the fusion boundary won't be reached and there are no rule traces on the pavement it doesn't matter how fast the initial brake velocity was.

4.2.2.4 Development of skid marks during collision

If the vehicles slide during the collision sliding marks can be developed. In pedestrian accidents it's very difficult to estimate the point of collision.

Goal of the analysis:	Marks of:	Marks on:	Determination:	Conservation of evidence:
Determine of the driver	Clothing (trouser, jacket, shirt, sweater, etc.)	Seat, dash board, side carpeting, centre console, etc.	Marks of filament on seats	Take pictures of passenger compartment and clothes
	Shoes	Brake pedal, clutch, accelerator pedal	Marks on sole of the shoes, marks on pedals from shoes	Take pictures from pedals and shoes
	Hair, blood	Roof interior, side windows, seats, covering	Marks from blood, hair	Take pictures
Marks on skin of vehicle	Clothes	On skin of vehicle (front-, side-, rear area), wing mirror, lightning, etc.	Marks of filament, etc.	Take pictures
	Lacquer, other materials		Lacquer	Take pictures, reference lacquer
Marks on objects	Lacquer, glass, plastics, vulcanized rubber, etc.	On the exterior of the object and the surrounding area	Adherence of lacquer and other materials, breakage of glass	Take pictures
Marks on persons	Lacquer, vulcanized rubber, plastics, dirt, oil	Clothes, shoes, accident scene	Adhesion of material on clothes, rifts, crushes, missing of parts of clothes	Take pictures, shoes, measurement of accident scene and objects
Marks on accident scene	Lacquer of vehicle, tires, plastics and vulcanized rubber parts, dirt from vehicle	On and next to the road surface, safety fence, obstacles next to the road	Adhesion of lacquer, parts of glass, rubber and plastics parts, tire marks, skid marks, dirt, parts of vehicle	Take pictures, measurement of the scene, sketch, protection of vehicle parts and obstacles
Webbing	Seat belt	Clothes, swivel, D-ring, tongue	Striations on clothes, seat belt;	Take pictures
	Clothes	Seat belt		

Tab. 3: Accident evidence

5. CRASH3 measurements

CRASH3 measures are taken to provide a damage profile for the crash programme. These measurements are taken across a measured width or length to a measured datum. Usually the crush measurements are obtained by measuring a damaged vehicle and then comparing these with similar measurements taken from an undamaged vehicle. CRASH3 defines three options for the crush measurements. Two, four or six crush measurements are taken which are labelled C₁ through C₆ as appropriate. One, three or five crush zones are designed to approximate the damage profile. For PENDANT it has been agreed to use six measurements which are referred to C₁ C₂ C₃ C₄ C₅ C₆.

C₁ is always on the left side for a front or rear impact.

C₁ is always at the rear in a side impact.

C₆ or the last measure is always on the right side for a front or rear impact

C₆ or the last measure is always at the front for a side impact.

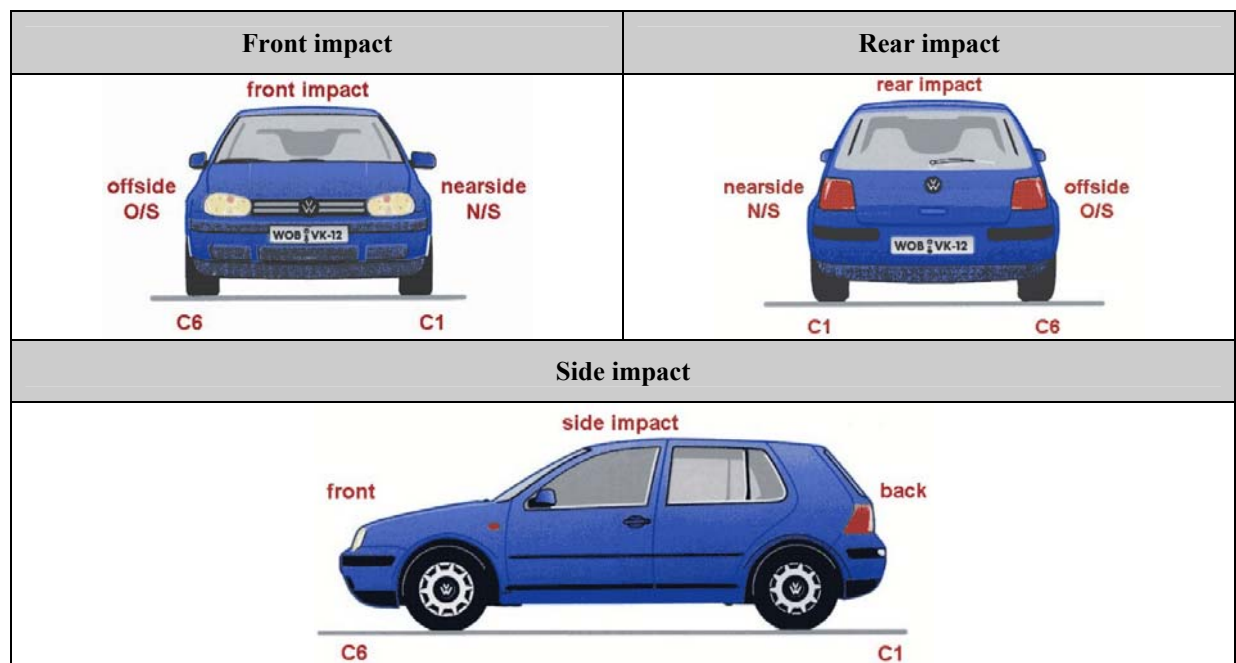


Fig. 34: Crash measurement

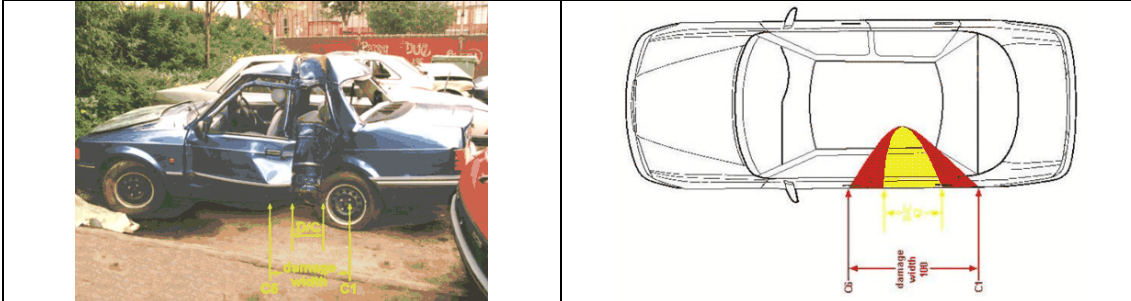
5.1 Damage width

The distance between C₁ and C₆ measures is the damage width. This damage width is simply the point of zero crush or the end of the vehicle, to the point of zero crush or the end of vehicle.

Unlike direct contact, D/C, which is a measure along the part of the vehicle that has come into contact with an object, damage width is a measure of all crush. As this crush is often as a result of transmitted forces pulling the body shell inwards the C₁ to C₆ measures are more likely to be over a greater width than the D/C. Crush

measurements should be taken at frame height around the vehicle. For front and rear impacts this will be at bumper height and for side impacts at sill height.

Below the D/C from a narrow pole impact is only 42cm but transmitted forces have pulled the sills doors and other bodywork inwards making C_1 to C_6 , i.e. the damage width, 100cm.



In the next example the vehicle has an offset frontal impact to the left side. The D/C is 77cm but there is measurable crush across the whole width making damage width the full width of the vehicle



Tab. 4: D/C

5.2 Damage measurement

The energy dissipated by a damaged vehicle is roughly proportional to the square of depth of crush: double the crush means four times the energy. The change of velocity parameters Delta-V and ETS are roughly proportional to crush: double the crush means double the impact velocity.

The stiff frontal structure of many contemporary passenger cars now lie some distance behind the most forward point of the front bumper bar. The front bumper region can be largely filled by plastic, fibreglass, foam, and fresh air. If an impact results in the bumper being torn away or shattered, with little or no damage to genuine frontal structures, how should the crush profile be measured? Two options are possible for this case. First option is to set the reference line at the original front of the car measure crush depths right through to the first structural components encountered. This entails a wide damage field w_1 and a deep maximum crush d_1 . The second option is to set the reference line at the original position of the undeformed stiff structure and measure only structural crush. This entails a narrow damage field w_2 and a shallow maximum crush d_2 . These two options are illustrated in the following picture.

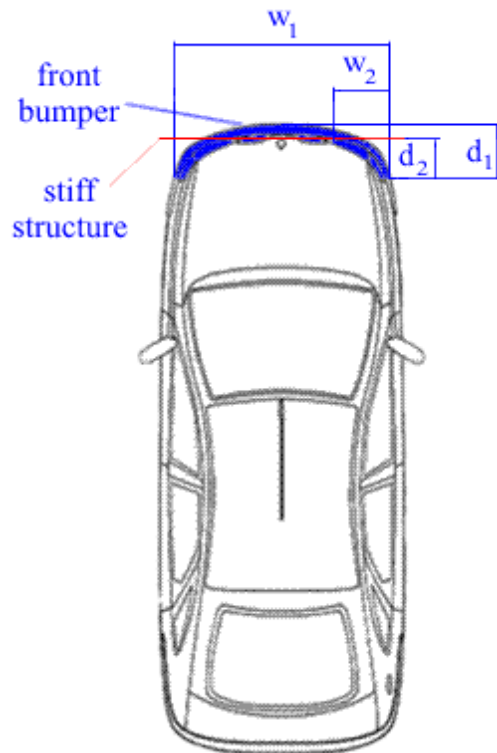


Fig. 35: Crush of stiff frontal structures

Users need to have a thorough understanding of the way in which crush damage is measured. The arrow shows in which direction C_1 to C_6 will be measured. Depending on the crush zone C_1 to C_6 is taken from the rear to front, right to left or from left to the right side of the vehicle.

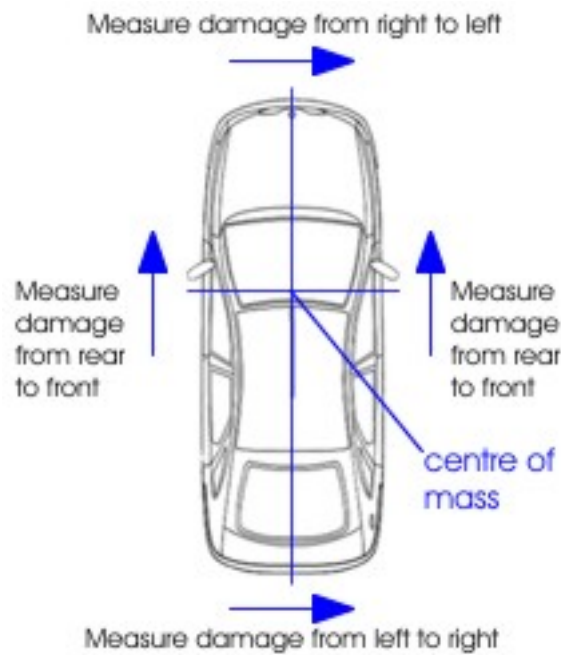
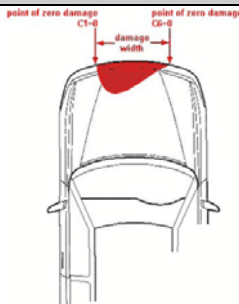
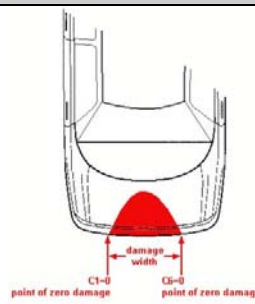
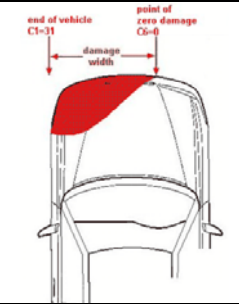
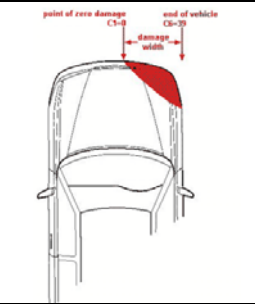
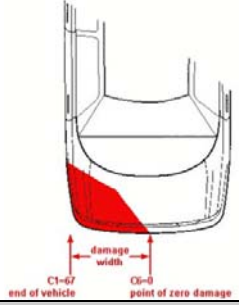
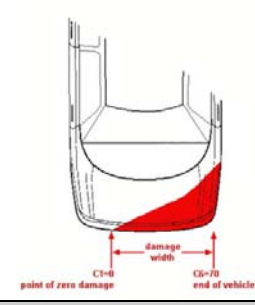
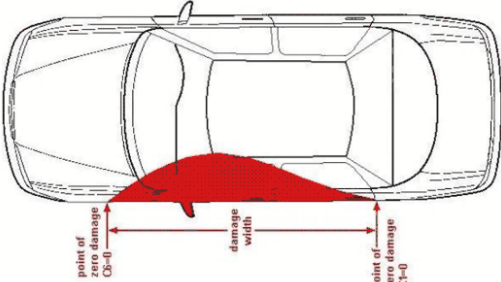
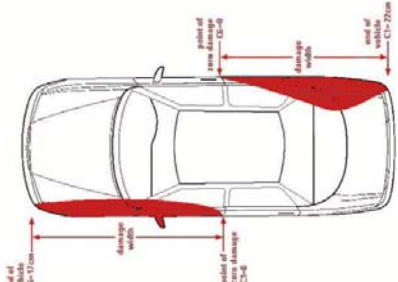


Fig. 36: Damage measure

The table shows some examples of C_1 to C_6 measurements for

Front-,
Rear-,
Side-impacts

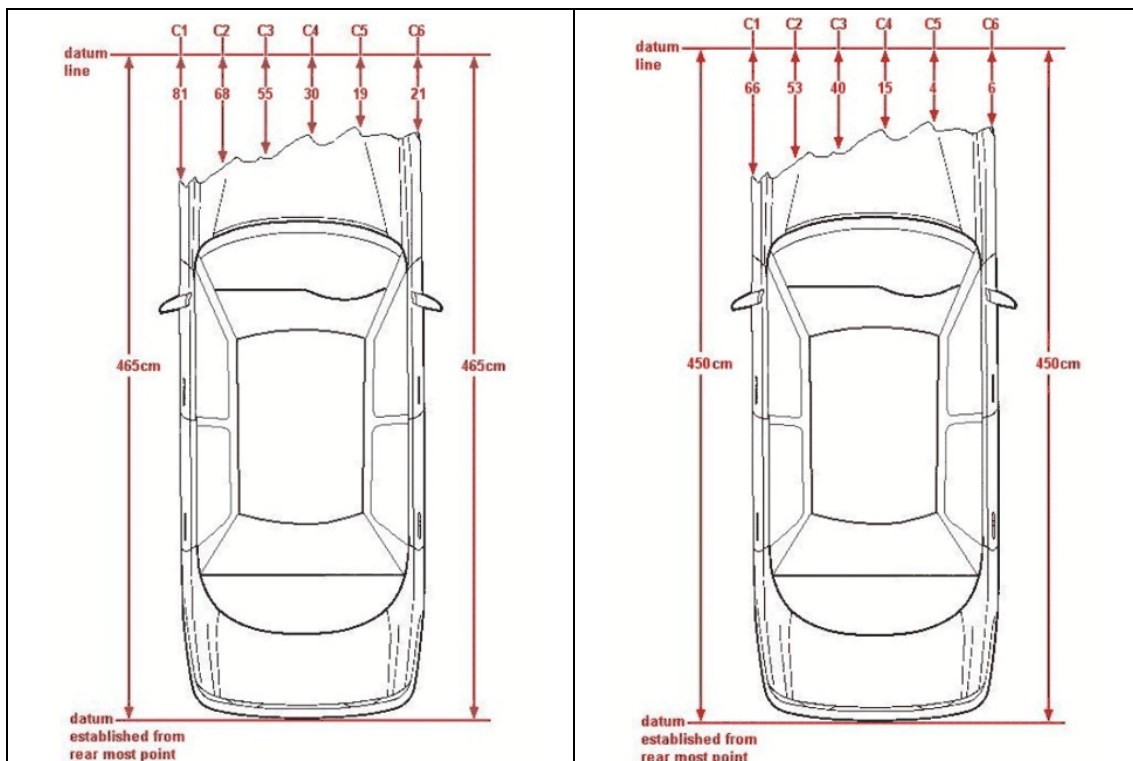
Front and rear impacts	
	
Front impacts	
	
Rear impacts	
	
Side impacts	
	

Tab. 5: Examples of damage width

5.3 Setting a datum

5.3.1 Front and Rear impacts

A datum is set from the undamaged end to either the U/D length of the vehicle or to a known length. The C₁ to C₆ figures can then be adjusted depending on whether the datum was longer than or shorter than the U/D vehicle. Original dimensions could be found on www.aiexperts.com. Length, height, width, wheelbase distance and other things are available. This database is not complete but could help if no dimension of the undamaged vehicle is present.



Tab. 6: Setting a datum for front and rear impacts

The above scenario represents a large frontal impact on a Rover 600. Undamaged length of the Rover is 465cm, in the first example this undamaged length is known so the datum line is set at 465. The damage width is over the full width, 172cm, with the C₁ to C₆ measures being 81, 68, 55, 30, 19, 21, these measures would then be entered into the Crash programme.

In the second example the undamaged length is not known so the datum is set at 450cm with the C₁ to C₆ measures being 66 53 40 15 4 6. The datum in this instance is 15cm shorter than the undamaged length so the crash figures must each be added to 15 before being inputted into the Crash programme

5.3.2 Side impacts

<p>In the first diagram below it is easy to set a datum using tape stretched between the two undamaged points C₁ to C₆.</p>	<p>If no undamaged points exist, as below, then datum line is established across the vehicle width:</p>

Tab. 7: Setting a datum for side impacts

5.3.3 Bowed vehicles in side impacts

Side impacts could be divided into two groups, those which do not cause significant bowing and those which do. Bowing is defined as a vehicle which distorts during the impact so that the ends of the vehicle curl round towards each other.

The following picture presents what could happen in a side impact. In the left picture a vehicle hits the other one. Result of this accident, depend on velocity and stiffness of the car, is a bowed and damaged second vehicle. The blue coloured picture is the original vehicle and the red one shows the vehicle after the accident happened; blue lines shows the distances of the parts which moved sideways during the impact.

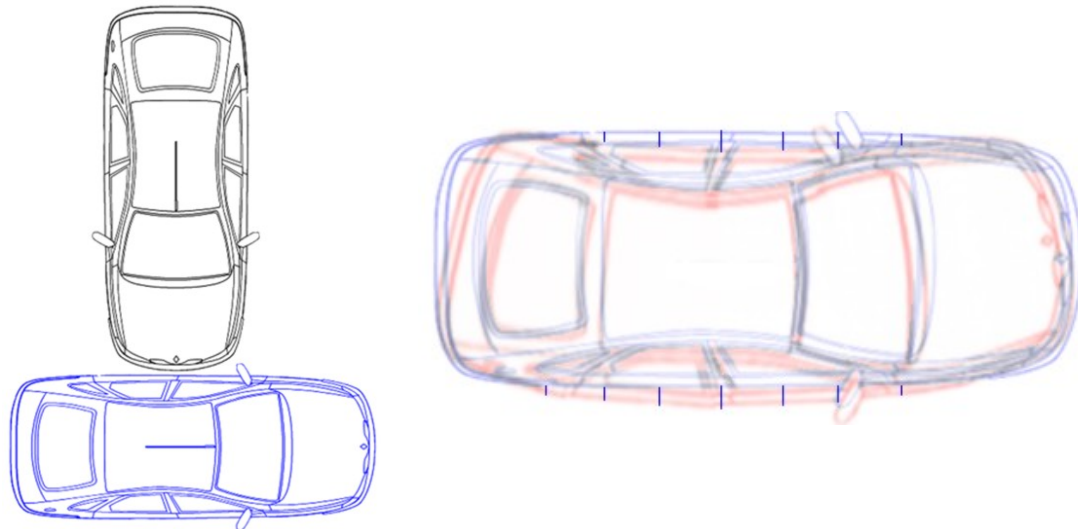


Fig. 37: Bowed vehicle due to side impacts

The yellow field describes the area of direct contact. Yellow and red field describes the whole damage zone of the vehicle. The datum line should be set at the front and rear lateral bumper corner. C_1 and C_6 will be spaced into five equal lengths whereby C_1 and C_6 have a value of zero.

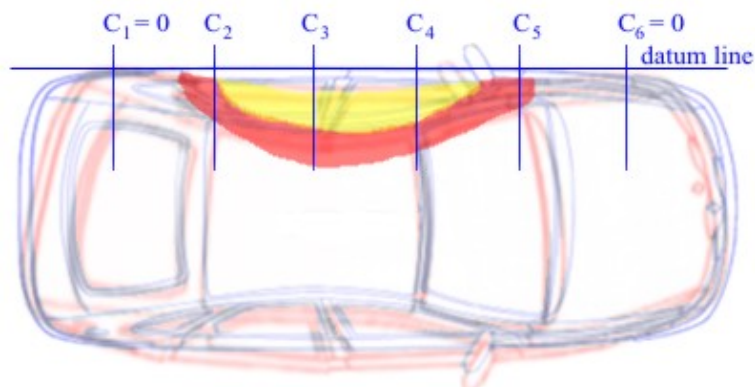


Fig. 38: Spacing of bowed vehicles

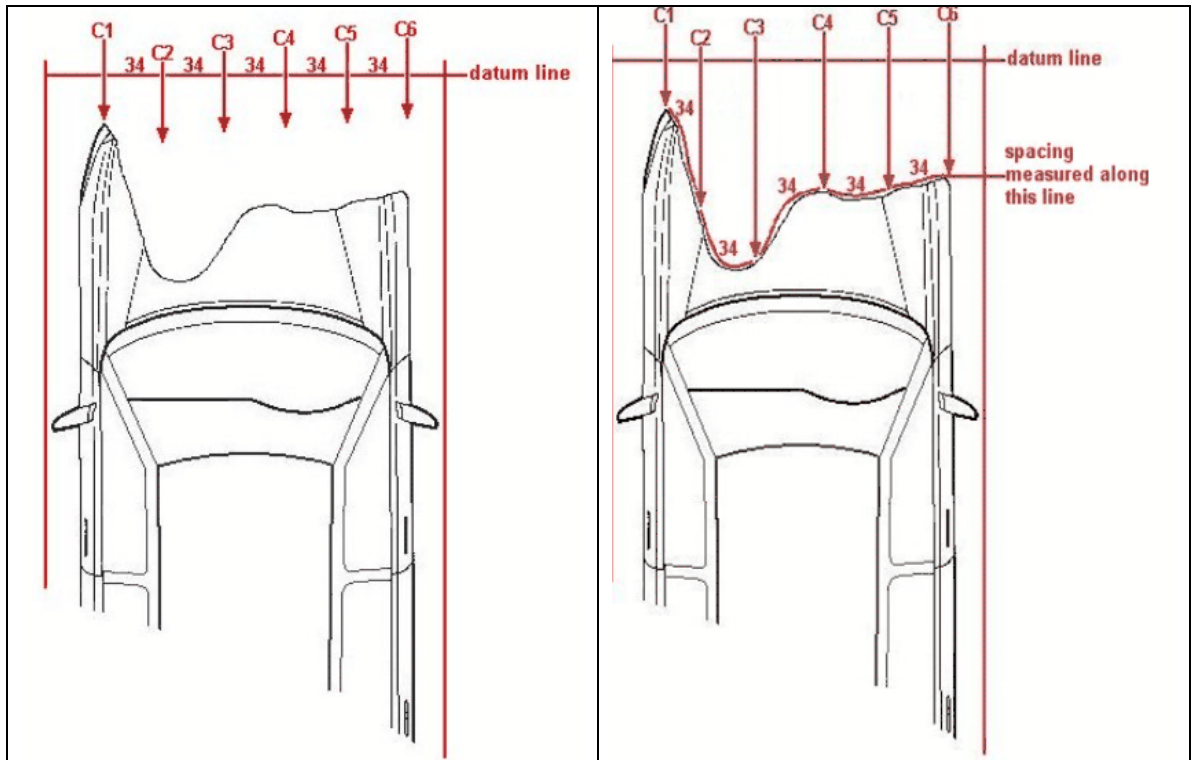
5.4 Spacing C_1 to C_6 measures

In the pictures below there are two systems shown how a damage profile could be measured. In the first option five equal distances are within the damage field from C_1 to C_6 at the datum line. In the second option the measure points are taken along the damage width.

In the example the damage width is the full width of the vehicle 172cm. C_1 is at the very left side with the remaining measures taken every 34cm. This spacing of 34cm should be measured along the damage profile not the datum line.

It is very difficult to measure deformations at the damage line and divide this distance into five equal spaces.

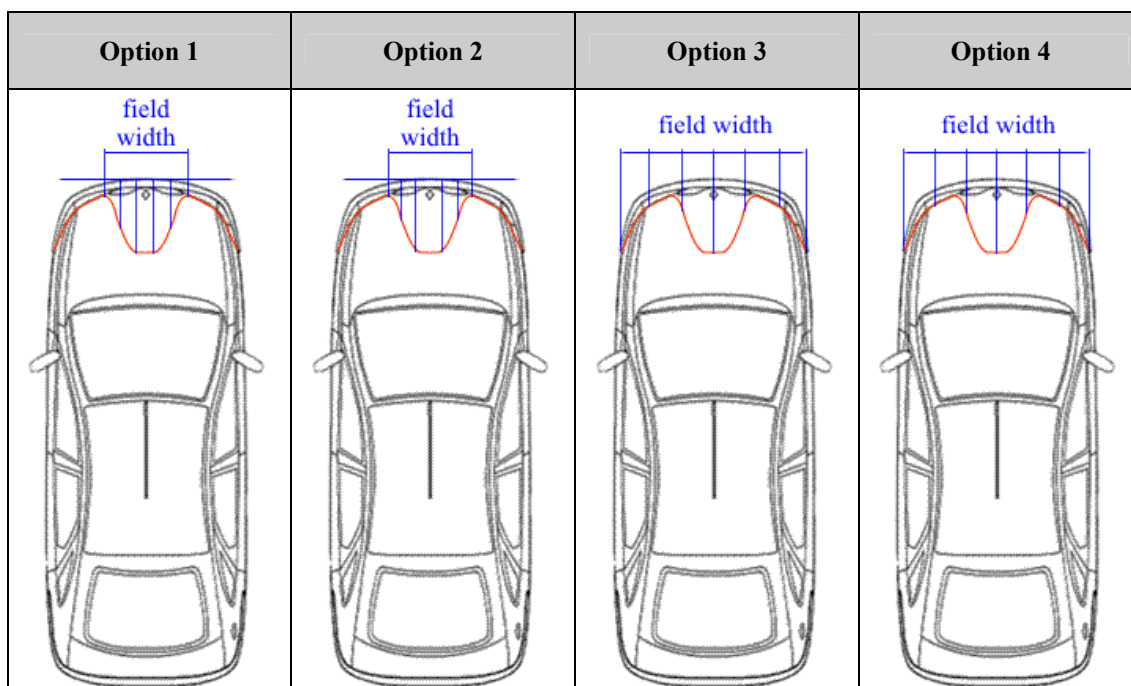
To avoid that different partners use different methods the first option should be taken, divide the vehicle width into C_1 to C_6 . Measure the depth of the crush at those points.



Tab. 8: Spacing C_1 to C_6 measures

5.4.1 Spacing narrow penetrating profile

In case of an accident with a narrow object there are some different possibilities to measure the crush profile. Following pictures shows four options:



Tab. 9: Spacing narrow penetrating profile

In those pictures the vehicle hit a narrow object which caused the front corners of the vehicle to be dragged inwards and backwards (red line). Now it's possible to space the damaged profile in four ways.

The first option measures to six points that are equally spaced along a reference line, but are not equally spaced along the perimeter of the car. The second option measures to six points equally spaced along the damaged perimeter of the car, but not equally spaced along the reference line of the car. The third option measures to six points equally spaced over the original width of the car but not equally spaced along the perimeter of the car. For the last option the measures are taken to six points equally along the damaged perimeter over the width of the car but not equally along the reference line.

Four different options how to measure deformations caused by narrow objects. To get results which can be compared with different partners' one option need to be chosen: option 1 should be taken.

The reference line is set at the original position of the front bumper. If there is no damage at the rear of the vehicle it's more or less easy to find out the length of the original car.

5.5 Offset of the crush location

Collisions do not extend over the whole of the vehicle width, particularly those involving side impacts. The reason that the offset measurement is important is that this, together with the PDoF, determines the moment arm of force. If a force has a distance to the centre of mass it tends to produce rotation as well as translation. In case of same force is acting, a larger moment arm produces a lower Delta-V but higher rate of rotation.

The offset is entered in centimetres, positive or negative values. The measurement should be taken from the centre of mass but it's very difficult to know where this point is located. The distance can be taken from the centre of the wheelbases as well. Next picture shows you whether if it's a positive or a negative value.

The car is divided into four sections which consist of two sections each. In two sections always negative or positive values are taken and the other two sections consist of both, negative and positive values.

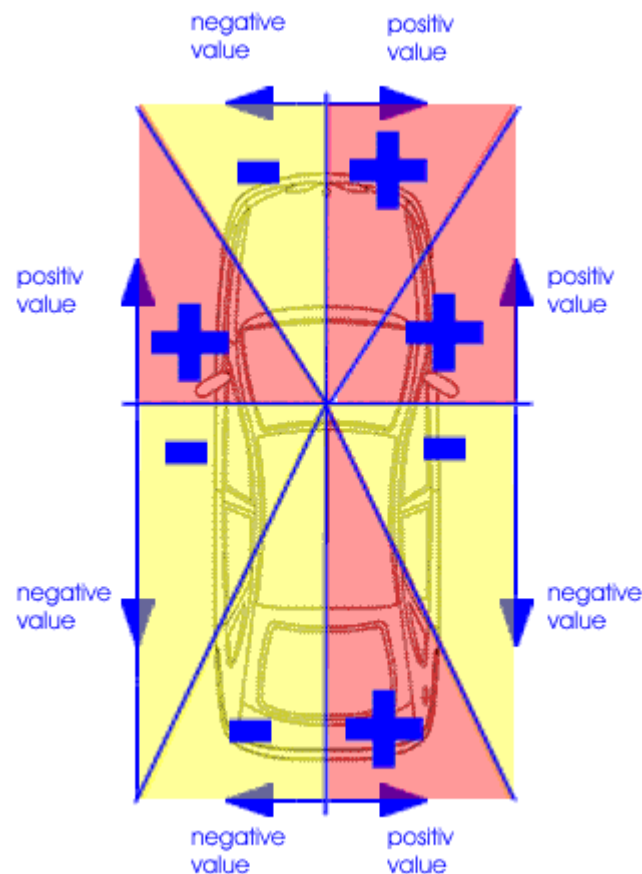


Fig. 39: Offset measurement location

The mid-point offset locates the damage field within the whole side of the vehicle. The value of these parameters has no effect on the calculated value of energy dissipated, since (for a give direction of force) this depends only on the width and depth of crush. It affects the calculation of change of velocity Delta-v and equivalent test speed ETS, since these both depend on the location of the impact force. When the impact force is away from the centre of mass of the vehicle more spin and less Delta-

v occurs. The mid-point offset is the distance along the side of a car between the centre of mass and mid-point of the *direct damage* portion of the whole damage field.

The reason that the offset measurement is important is that this, together with the PDoF, determines the moment arm of the force. Force acting at a distance from the centre of mass tends to produce rotation as well as translation.

Example:

For the crush zone of a vehicle the distance of the crush zone to the centre of mass (centre of wheelbase) a positive distance value will be taken according to the picture above. The centre of the crush zone is located on the right side of the centre line. If it will be on the left side a negative value will be taken. Imagine this example is only a fictitious vehicle with a fictitious crush zone.

In case of the side impact the value will be negative.

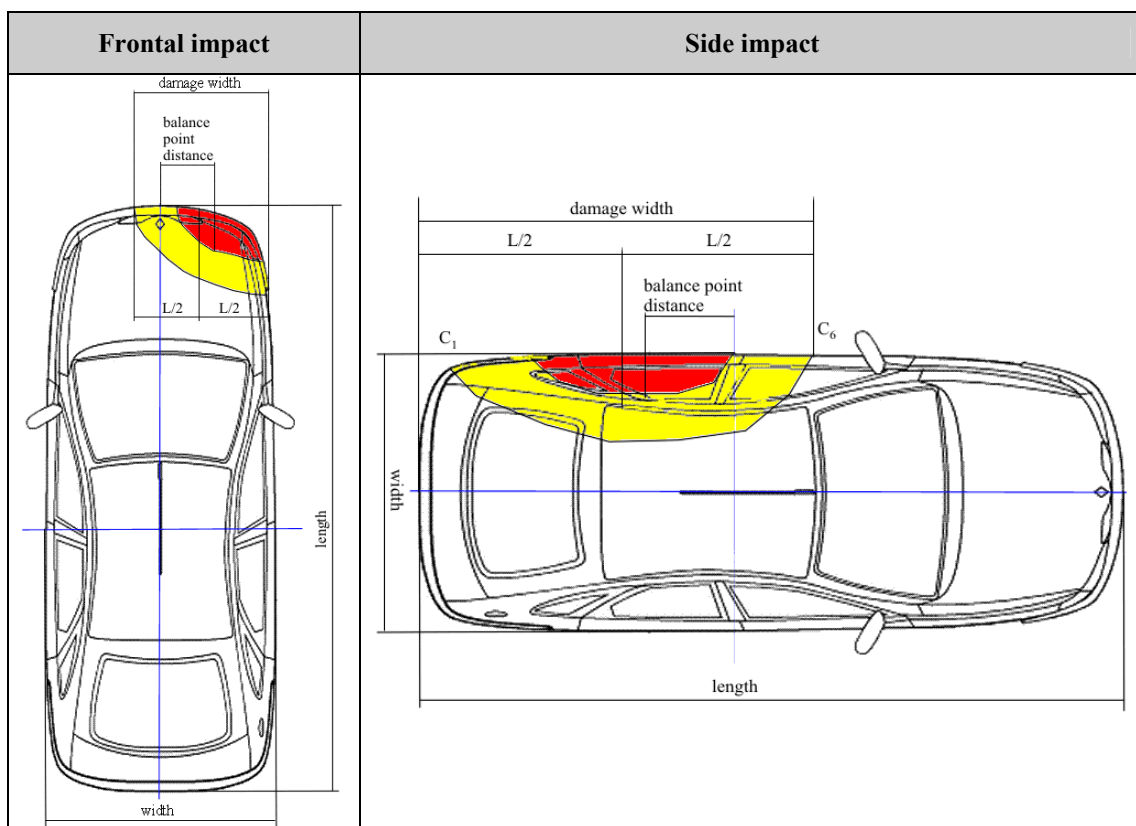


Fig. 40: Balance point for side and frontal impacts

6. Reconstruction methods

In general, four categories of reconstruction methods can be distinguished. The most common one is the reconstruction by hand. Simply some of the principles of mechanics are used within this method. The computer method is another one. Its development started in the 70's and this method allows a combination of calculations in a short time. It is also based (as every mathematical reconstruction method) on the same principals of mechanics as the method by hand. Some modern methods are the reconstruction based on the data produced by crash data recorders and the video analysis of accidents recorded by a video camera outside the vehicle or most commonly, attached in the occupant compartment.

It is very important that a reconstruction method or tool will provide realistic results when it is used for an accident reconstruction. The accuracy of the results depends on various parameters such as the accident analyst (level of knowledge, experience), the accident data available (completeness and quality) and the accuracy of the reconstruction method/tool. There have been several workshops for validating the reconstruction methods/experience of accident analysts from different countries. There are also publications, in which a reconstruction tool is validated. A limited number of publications, referring to direct comparison of tools, were found.

In-depth investigations differ also per study. This is mainly related to whether or not the scene of the accident is investigated, and – if yes – when. This results in three main categories of in-depth research:

on-scene-in-time:

The accident investigation team is immediately notified and goes to the scene of the accident instantly. Dependent on the local rules this happens with "blue light" and siren. A disadvantage of this method is that no matter how quick the team is, for many accidents the vehicles and certainly the victims may be removed already.

later-on-the-scene:

The team is notified and investigates the accident scene as soon as possible, but within a certain time (24 or 48 hours) after the accident actually occurred. An agreement with the police is commonly made that they mark the vehicles and victim positions as well as possible with chalk or paint, so that the investigators still have a good insight in these parameters.

retrospective:

The scene of the accident is not investigated at all. For this method most of the insight in the accident is gained by the inspection of the vehicles.

In the next sections, the different reconstruction methods and their validations will be described.

6.1 Reconstruction by hand / empirical method

In order to determine the uncertainty in measurements (e.g. skid marks, deformations, etc), assumed parameters (EES, vehicle deceleration, etc) and calculations, the researcher can use the next three methods (Brach, 1994):

- Establishment of upper and lower bounds through calculation of the largest and the smallest possible values of the quantity being estimated for all combinations of the input variables
- Use of differential calculus and places variation (sensitivity analysis, error analysis, design of experiments) of the variables into a differential equation derived from the mathematical formula
- Development of approximate means and variances (or parameter distribution) for cases where statistical information is known about the input data.

Validation of reconstruction by hand

The reliability of the hand calculated reconstruction is based on the analyst who applies it. The equations that are used within this method are the basic equations that describe laws of physics. The error that will possibly occur, is an outcome of assumptions that the user makes. This does not mean that the analyst is the responsible for the error. The fact that parameters (e.g. friction coefficient, crush energy dissipation), which are unknown or can not be accurately defined after the crash, are mainly responsible for the error. Also the applied laws might be a simplification of the real situation.

The basic parameters of an accident (pre-/ post-crash velocity, velocity change) can be calculated with the use of the principal of the energy and/or momentum conservation. Before using the two conservation laws, the analyst has to assume some other sub-parameters, which are essential for the accuracy of the reconstruction. These parameters are:

- the friction coefficient between surface of objects involved in the accident (tires, the body of the motorcyclist, the pavement, etc)
- the energy dissipated by the deformation of the vehicles/objects
- the restitution coefficient between the crashed objects
- the masses of the vehicles/object

At this point the method is not 100% accurate (as every other reconstruction method), the analyst has to assume the minimum and maximum bound and these bounds are based on known values from previous similar accidents or tests or databases. An error will always occur, because the accident configuration and conditions are never known with 100% certainty.

The uncertainty in the variation in the input variables can be treated with the use of three techniques, as it is explained in the previous page. Each technique has some limitations (Brach, 1994), which makes it not always suitable for application.

Computing upper and lower bounds is the simplest and the most general of the three, but provides the least information. Since the likelihood of simultaneously reaching the extreme values of the variables is not taken into account, the results can be unrealistic.

The second one (sensitivity, error analysis) using the differential variations is more sensitive to the mathematical form of the equation being used and is more illustrative in comparing relative uncertainty due to the different variables.

The third, using mathematical statistics, provides the most information about uncertainty and requires the most input information, namely, quantitative statistical descriptions (distributions) of the independent variables. Being an analytical method, it is necessary to use approximate distributions for non-linear formulas. It can work well for simple to moderate complex reconstruction equations, but becomes impractical for complex reconstruction problems. More sophisticated methods, such as Monte Carlo can be used for those problems.

The hand calculated reconstruction can be applied for complex accidents, where many from the input variables are missing. The analyst has to make many assumptions in order to give some answers. In this case the reconstruction requires less time with this method instead of the use of a computer tool. The experience says that the time needed to enter the assumed data in the computer and the time needed for the calculations is more than the time needed just using the hand calculated method. The result from both methods/tools will be anyway an assumption.

Within the MAIDS project, two workshops have been organised by the project coordinator, in order to compare the results of hand calculated reconstruction of motorcycle accidents by research institutes from different countries. The conclusions that have been drawn are:

- for low speed accidents and with many input variables known, the calculated results were approximately the same. The calculated speed for example was lying within a 10km/h range (+- 5km/h)
- for high speed accidents and with some input variables unknown, the results differed remarkably. One of the reasons is that the unknown variables had to be assumed by the reconstructionists, based on their experience and on their own databases. Another reason is that the analysts were not familiar with the motorcycle dynamics during a high speed impact and with the amount of energy absorbed by the vehicles during the crash. If the analysts followed a training program, the differences in results should be decreasing. These differences therefore are not a weakness of the method as such.

6.2 Computer methods

In this section some important examples of accident reconstruction software are treated. These software packages are worldwide available. Following capture should be an overview and explanation of existing systems. PENDANT in the context of a project don't have any interest in any software. Every user is responsible for his system.

6.2.1 CARAT

CARAT (Computer Aided Reconstruction of Accidents in Traffic) is a simulation computer program, available for Microsoft Windows applications. The user can model cars, trucks, trailers and tractors/semi-trailers and he can simulate the pre- and post-crash dynamics and the collisions in a graphical environment. CARAT is time forward kinetic simulation, but can also be used to perform kinematic calculations forwards and backwards in time. A momentum-based collision algorithm is implemented.

CARAT-3 has been released in the mid-90's by H. Burg. It is a three degree-of-freedom (3 DOF) model, with three dependent DOF's and operated mathematically in a two-dimensional (2D) graphical environment. The impact forces can only be modelled in the yaw plane and no dynamic tire behaviour is implemented.

CARAT-4 is a three-dimensional (3D) mathematical model. It can model heavy trucks, including articulated vehicles. It implements 3D multi-body models with 10 DOF's for the car model and up to 26 DOF's for the truck and trailer. CARAT-4 utilises multi-body system modelling, defined by linked singular rigid bodies. The dynamics (translation and rotation) of a body in the system are influenced by external forces, including the connections (joints) between the body and the linked bodies in the system and the body in turn influences the kinematics of those bodies. This pattern is traced back to the root body. Friction in the connections is not modelled for simplification. The program does not utilise generated differential equations but utilises articulated total body models for all types of vehicles (Fittanto, 2002). CarSim (Gillespie, 1999) is the base of the mathematical description of the car suspension. A tire model is also used for the vehicles tires (ArcSim, 1997). The impact forces can be considered in three dimensions.

Validation of CARAT

A validation of the program made by the developer and the Ruhl forensic agency has been found (Fittanto, 2002). Twelve two-vehicle collision RICSAC (Research Input for Computer Simulation of Automobile Collisions) tests in various configurations were used for the validation of the CARAT-4. The separation velocity and the Delta-V of the simulations were compared to the test result and to the outcome of the SMAC simulations for the same test.

Tab. 10 contains the input parameters for these tests, the crush as reported by RISCAC at the centroid (Ccentroid) of the damage area (both perpendicular to the vehicle) and as measured along the PDOF (Principal Direction of Force). The last column contains the crush as reported by CARAT, based on the position of the vehicles and the location of the contact point.

Tab. 11 Comparison between the CARAT-4/ SMAC results and the RISCAC data shows the difference in percentage between the CARAT-4/ SMAC calculated results and RICSAC measured data.

Test, Vehicle	Impact		RISCAC		CARAT
	Speed (kph)	Angle (degrees)	Ccentroid (m)	PDOFadj (m)	PDOFadj (m)
1.1	31.70	-30	0.38	0.44	0.38
1.2	31.70	90	0.30	0.33	0.29
2.1	50.37	-30	0.42	0.42	0.41
2.2	50.37	90	0.60	0.66	0.57
3.1	33.96	0	0.05	0.05	0.05
3.2	0.00	10	0.13	0.13	0.13
4.1	61.96	1	0.29	0.31	0.29
4.2	0.00	10	0.66	0.67	0.66
5.1	63.57	0	0.07	0.07	0.23
5.2	0.00	10	0.93	0.93	0.90
6.1	34.44	0	0.06	0.07	0.18
6.2	34.44	120	0.49	0.49	0.45
7.1	46.67	0	0.16	0.18	0.26
7.2	46.67	120	0.45	0.45	0.42
8.1	33.15	0	0.09	0.10	0.20
8.2	33.15	90	0.23	0.26	0.38
9.1	33.96	0	0.32	0.36	0.36
9.2	33.96	90	0.12	0.14	0.13
10.1	53.27	0	0.36	0.42	0.48
10.2	53.27	90	0.13	0.16	0.30
11.1	32.67	171	0.45	0.45	0.45
11.2	32.67	0	0.53	0.55	0.55
12.1	50.37	171	0.70	0.71	0.71
12.2	50.37	0	0.67	0.69	0.71

Tab. 10: Input data and CARAT-4 reported crush

	CARAT-4			SMAC		
	Average magnitude	Standard deviation	Maximum deviation	Average magnitude	Standard deviation	Maximum deviation
Separation velocity	19.7%	27.6%	134.8%	16.8%	24.0%	110.3%
Delta-V	9.2%	5.2%	18.6%	7.4%	4.1%	14.3%

Tab. 11: Comparison between the CARAT-4/ SMAC results and the RISCAC data

From the Tab. 11, it can be concluded that the program provides results reasonably consistent with the crash test data and similar to another crash-modelling program (SMAC). The maximum deviation for the separation velocity occurred in the test 9. It was believed that a secondary “sideswipe” collision, which was not modelled in the CARAT simulation, was the reason for the great inconsistency. After modelling the secondary collision, the new result was closer to the test one, but it is still highly deviating. It is stated that the exact reason for the deviation is not known.

CARAT is designed to analyse the resultant effect of the impact phase, but is not designed to analyse the time-history of this phase, such as SMAC.

6.2.2 MADYMO

MADYMO (Mathematical Dynamic Model) can simulate the dynamic behaviour of physical systems, with a focus on the analysis of 4-wheeled vehicle collisions and the sustained occupant injuries. MADYMO is also very flexible to reconstruct motorcycle and bicycle accidents and to study the performance of restraint systems such as seat belts and airbags. It has been developed by TNO Automotive in The Netherlands in the early 80’s and has been continuously up-dated since then.

MADYMO combines in one program the multi-body techniques (for the simulation of the gross motion of systems or bodies connected by joints) and the finite elements techniques (for the simulation of structural behaviour). A model can be made with only finite elements models or only multi-bodies or combination of both. The program allows 2-D and 3-D modelling.

Validation of MADYMO

The MADYMO models have been validated many times in the past. There are articles about vehicle models, occupant models and pedestrian models, published by different scientific institutes around the world. This survey will refer only to some validations of the most recent MADYMO models.

Morsink et al (2001) have studied the accuracy of the MADYMO model of a Ford Explorer, comparing the simulation results with the test results of a full overlap frontal impact against a rigid wall. Fig. 41 shows in four steps the simulated impact phase.

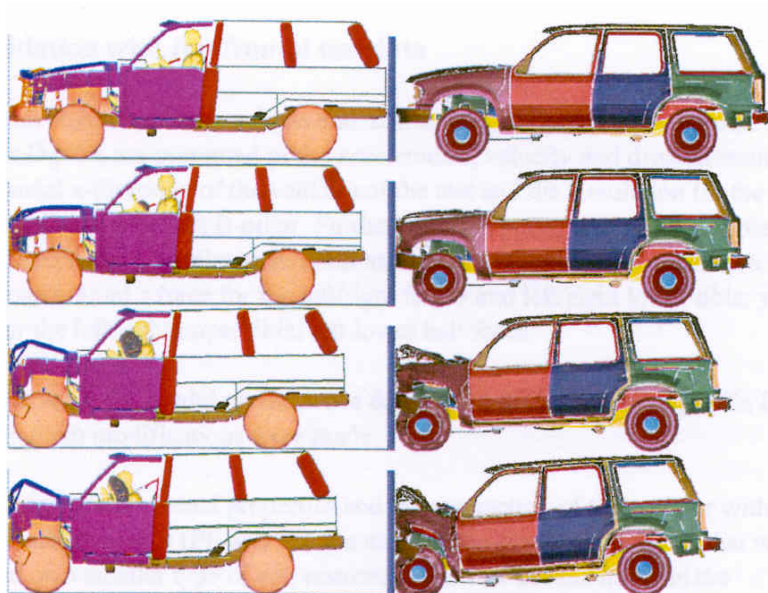


Fig. 41: Crash phase of Ford Explorer Multi-Body (left) and Finite Element (right) model at $t=0$, 20, 40 and 60 ms (top-down)

The comparison showed a good match for the engine and b-pillar velocity, acceleration and displacement and the head and chest accelerations, but MADYMO predicted less accurate the sternum displacement and the forces applied to the right and left tibia. In conclusion, the estimates derived from the MADYMO vehicle model were reasonably good, if it is also taken in consideration that the interior, seat belt and airbag model are generic models, which were modified according to the characteristics of the actual Ford Explorer features in this case.

The accuracy of MADYMO vehicle models has been also studied by Zweep et al (2003). Test results from NCAP frontal impact tests for four passenger cars have been compared with the simulation results. The four vehicles are a Ford Taurus, Ford

Explorer, Geo Metro and a Chrysler Neo. Simulation results from two MADYMO versions (5.4.1 and 6.0.1) were available for this validation. The validation showed that the simulation estimates were close to the test results in most of the cases, but there were also cases, where MADYMO results were less representative. In Fig. 42, some of the simulation and test results are showed. A conclusion of this study is that the model designed in the newer MADYMO version (6.0.1) provides more accurate results than the models designed in the older version (5.4.1).

A scaleable mid-size male pedestrian model has been extensively validated by TNO Automotive (Hoof, 2003). The model parameters were derived from published data and a large range of impactor tests. The biofidelity of the model has been verified using an extensive range of full pedestrian-vehicle impact tests with a large range in body sizes. The simulation results were objectively correlated to the experimental data (see Appendix).

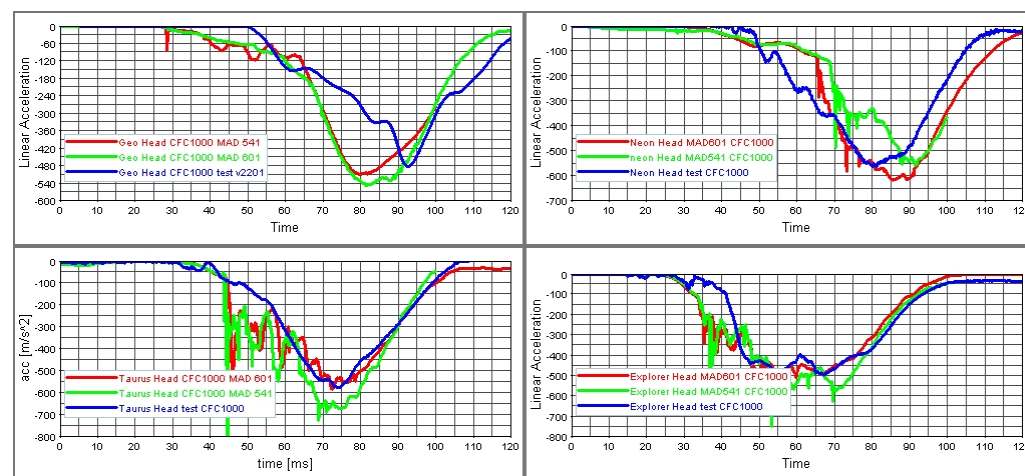


Fig. 42: Comparison of head acceleration

Overall, the model predicted the measured response well. In particular the head kinematics were accurately predicted, indicated by global correlation scores over 90 % for the head impact location. The correlation scores for the bumper forces and accelerations of various body parts were significantly lower (47-64 %), but still acceptable considering the complexity of the tests simulated. This was mainly attributed to the limited information available on the vehicle contact characteristics and the initial conditions in the tests (pedestrian posture, impact velocity). In addition, in a number of tests signals were missing due to recording problems, indicating the complexity of these kinds of tests.

Consequently, it can be concluded that besides biofidelic pedestrian models, accurate representations of vehicles and test conditions, also reproducible test data are required for realistic predictions of pedestrian-vehicle interactions.

In general MADYMO seems to be able to reproduce reasonably accurately various measured test results. However, for reconstruction of real-world crashes most of the times less detailed information is available on various parameters. In general, this fact will result in a less accurate reproduction of the actual situation. In this case, however, this is clearly not due to limitations in the accuracy of MADYMO but to the intrinsic uncertainties in accident reconstruction calculations.

6.2.3 PC-Crash

PC-Crash is an accident computer simulation program, developed at the early 90's by the DSD (Dr Steffan Datentechnik) research company in Austria. The program is based on Microsoft Windows. The user can model cars, trucks, trailers and tractors/semi-trailers and he can simulate the pre-, post-crash and the collision phase in 2D or 3D. Simulations can be performed forwards and backwards in time. The software allows reconstructing rollovers and accidents with road side barriers. In the newest version of PC-Crash which will be available in autumn 2004 textures has been implemented which increases the environmental design.

PC-Crash uses a discrete time approach to solve for the trajectory of a specified vehicle with user-defined initial conditions'. The vehicle dynamics are defined by Newton's Second Law, and the vehicle and tire kinematics are updated for each time step. The collision model is an impulse-momentum model. Linear momentum and angular momentum are conserved, and energy loss during the collision is estimated with the use of a restitution coefficient. Sliding impacts are handled with an inter-vehicle contact plane and a friction coefficient. Based on the inputs, a crash impulse vector is calculated, which causes a linear and angular velocity change of the vehicles. Multiple impacts can be simulated in PC-Crash. A limitation of the impulse-based collision model is that there is no collision duration and the fact that the collisions are based on the same shape of crash pulse. Nevertheless a force based model is also included, which allows to resolve the contact forces over time.

Pre- and post-crash vehicle movements are calculated with a trajectory model, which is based on a time-forward vehicle dynamics kinetic simulation. Tire-ground forces, steering and individual wheel brake or acceleration factors, weight transfer due to roll, pitch and yaw motions are taken into account during the simulation. Two different tyre models can be chosen: The linear Tire Force Model or the TM Easy Model. TM.-Easy allows non-linear tire effects including differences between lateral and longitudinal parameters. The values for lateral and longitudinal tire forces are base on the tire force model curve. The program allows the optimization of the calculated data by applying one of the linear, genetic (or evolutionary) and Monte Carlo methods.

The program allows the optimization of the calculated data by applying one of the linear, genetic (or evolutionary) and Monte Carlo methods. An optimizer tool in PC-Crash is designed to minimize reconstruction time and error by automatically varying a selected number of impact parameters, comparing the resulting simulation for each combination of parameters with the actual incident. For each simulation, it calculates a weighted total error that is based on differences between the actual vehicle positions and angles and those obtained in the simulation. In each subsequent simulation, it changes values in an attempt to minimize the weighted total error. Hundreds of different combinations can be compared in a few minutes. Three different methods are available: Linear Method, Genetic Method, Monte Carlo Method.

Parameters that can be varied by the optimizer are:

- Pre-impact speeds
- Position of impact in x-y direction
- Position of impact in z direction

- Contact plane angle ϕ in the x-y plane
- Pre-impact headings
- Vehicle positions at impact
- Coefficient of restitution
- Contact plane friction.

Within PC-Crash, an occupant MADYMO model and a pedestrian multi-body model are integrated. The occupant model is a 50%-tile Hybrid III (HIII) dummy. The interior of the vehicle is simplified to plane, cylinder and ellipsoids and the program allows the interaction between the occupant and the interior. Two different restraint systems are available (which can be combined), a three point seatbelt with or without pretensioner and an airbag module. A finite element model is used to model the belt, allowing slippage between the seatbelt and the occupant body. The input data for the MADYMO simulation is the crash pulse result calculated from the PC-Crash reconstruction. The pedestrian model is a multi-body system consisting of several rigid bodies. The pedestrian model in PC-Crash uses a multi-body system consisting of several rigid bodies to simulate the movement of the pedestrian. The different bodies, which represent the different parts of the pedestrian like head, torso, pelvis etc., are interconnected by joints. For each body different properties like geometry, mass, contact stiffness and coefficients of friction can be specified. The geometry for each body can be specified by defining a general ellipsoid of degree n . The number of bodies and joints used influences the calculation time needed. Therefore a compromise has to be found between calculation time and model detail. 24 bodies are interconnected by 15 joints. The interaction between one rigid body vehicle and the pedestrian is done by contact forces. However, the multi-body module in PC-Crash can deal with an unlimited number of bodies and joints. Besides the definition of several properties for each body, the size and the weight for the whole pedestrian can be specified in the program. The initial conditions like position and orientation for each body as well as the velocities can be entered by the user to define the parameters of motion before the impact. However, the relative position of two bodies connected by a joint is defined by the joint location.

Body properties: For each body of the multi-body system the following properties can be specified independently.

- *Geometry*: Each body is represented by a general ellipsoid, the length of the semi-axes a , b , c and the degree of the ellipsoid can be specified.
- *Mass and Moments of Inertia*: For each body of the multi-body system the mass and the moments of inertia have to be specified.
- *Stiffness coefficients*: A body stiffness coefficient has to be specified, which is used when calculating contacts. The stiffness coefficients for different body parts can be determined experimentally.
- *Coefficients of friction*: Two coefficients of friction can be specified. One is used for ellipsoid to vehicle contacts, the other one is used for ellipsoid to ellipsoid or for ellipsoid to ground contacts. These coefficients of friction are assumed to be independent of the amount of penetration

Validation of PC-Crash

One obvious requirement of a simulation program is that it must correctly model simple slide-to-stop and roll-out trajectories.

Cliff and Montgomery compared the results of twenty car-to-car test crashes with the results of the PC-Crash reconstructed crashes (Cliff, 1996). Three sources of staged collision data were used for evaluation. The first source was seven staged collisions conducted by Ishikawa at the Japan Automobile Research Institute. Inc. (JARI). The second source was the twelve staged collisions (commonly referred to as the RICSAC tests) outlined by Smith and Noga and earlier summarized by Shoemaker. Brach also referenced these tests and conducted some useful analysis of the data. The final source of test data was a single locked-wheel staged collision from McHenry. Cliff and Montgomery's evaluation of PC-Crash was conducted in two stages. The first stage was to assess the trajectory model by reconstructing only the post-impact phase of the collisions, the second stage was to assess PC-Crash's ability to model the entire event from initial contact to rest.

Conclusions:

- Based on comparisons with h and calculations, RICSAC, JARI and McHenry staged' collisions, PC-Crash simulation predicated speeds were found to be in good agreement with real world results. For the staged collisions, errors larger than about +/- 5 km/h could be attributed to inaccuracies in reported wheel brake factors, the inclusion of cases unsuitable for this type of analysis, or tire losses between the initial contact point and where the post-impact simulation was started.
- In cases where there was little post-impact rotation and long rollout trajectories, the wheel brake factors were critical in order to assess the speeds accurately.
- When there was significant post-impact spinout (more than about 90 degrees) reasonably close results could be obtained by matching the tire marks during the initial spinout without matching the rest position.

H.H. Spit validated PC-Crash during his three-month traineeship at TNO Accident Analysis group (Spit, 2000). A well-documented car-to-car side-impact test (done by TNO Crash Lab) has been selected for this validation. The simulation (input) parameters: impact speed, EES, and restitution coefficient have been defined by the reconstructionist. The impact velocity, restitution coefficient and friction coefficient between the cars have further been used as optimisation parameters in the "Collision Optimiser" feature. The initial velocity and the end position, derived from the optimisation process, have been compared with the test measurements. The simulation speed was 2,3% lower, which was a satisfactory result and the rest position deviated about 13,2% from the actual rest position, due to the difference in heading. Spit has also looked at the influence of small changes in magnitude of the input parameters (sensitivity analysis). He concluded that relatively small changes in the magnitude of important input parameters (e.g.: mass of vehicle, centre of gravity, restitution coefficient) can result to relatively large differences in the calculated pre-impact speed and rest position of the vehicles. For this reason, TNO and NFI (Nederlands Forensisch Instituut) developed a tool (MC-Crash), which can statistically estimate the best value from the interval of parameters that the

investigator has specified in advance. The tool uses the Monte-Carlo simulation technique.

PC-Crash has also been validated for frontal (30% overlap) and car-to-car side-impact, occupant kinematics and pedestrian accidents, by the institute that has created it (Geigl, 2001) (Steffan, 1999) (Moser, 1999). In the frontal impact, the impact velocities and the rest position of the vehicles were predicted accurately. The visual comparison of the whole crash scene kinematics showed also a good correlation between simulation and experiment. The occupant simulation produced accelerations to head and chest of the human model, which agreed on timing and peak acceleration with the test results.

PC-Crash predicted reasonably well the impact velocities and the post-crash motion of the vehicles in the side impact. There was also a good correlation between the simulated occupant head and chest accelerations and the test ones, except a second head acceleration peak which was observed in the test, but it was not predicted by the simulation.

Collision optimizer:

Twenty staged collisions (12 RICSAC, 7 JARI and 1 McHenry) were reconstructed with the optimizer tool in PC-Crash. These staged collisions had been previously reconstructed with a combination of manual linear momentum calculations combined with the trajectory model in an earlier version of PC-Crash.

Conclusions:

- For sixteen of the twenty cases reconstructed, the accuracy of the pre-impact speeds determined using PC-Crash's optimizer was better than +/-5 km/h. The accuracies in general were a significant improvement over those obtained in a 1996 study (Cliff and Montgomery), in which only PC-Crash's trajectory model (and not its impact model) was used.
- When reconstructing cases without considering damage energy, accuracy was worse for head-on collisions with little post-impact vehicle movement.
- The impact coefficient of restitution ϵ ranged from 0 to 0.25 in the reconstructions, with an average of 0.12, indicating the commonly used value of 0.10 is a good starting point. Fixing the value of ϵ at 0.10 decreased the accuracy markedly in two of the twenty cases.

Occupant kinematics:

In the automotive industry various simulation programs are used to determine occupant movement and loads during car accidents. Two approaches are currently used to perform this type of calculation: A Multi-Body approach as used by Adams or MADYMO [MAD97], or the Finite Element Method as used by PAM Crash, Radioss, Dyna3D and several other simulation programs. MADYMO was chosen for modelling the occupant movement. A big advantage of this program is the database of validated dummy models included in the software package. For side collisions, the accuracy of the HIII dummy is not perfect. But as long as the major result of the simulation is only a comparison between different restraint systems or the possible movement of the dummy, the results which can be expected are quite satisfactory. For the neck a two joint model was used. This model also gives quite good results for

frontal and rear end impacts. This model, which is part of the MADYMO database, has been validated through several test series and publications [MAD97].

The interior of the vehicle is specified through the general shape of the vehicle. At the moment there are only a few options for influencing these parameters.

The occupant kinematics has also been validated for car-to-car rear-impact. The comparison between simulation and experiment showed that the head peak accelerations are reasonably similar. An advance in the phase of the simulation acceleration graphic was observed, which was caused by the fact that the impact point is not identical with the point of first contact in the simulation. A time of 30 to 60ms for the pre-impact vehicle crush must be added.

Limitations, which have to be improved in the future, these are:

- The current dummy model is based on the standard HIII dummy and not on the real human
- There is no definition of vehicle acceleration during the impact
- There is no option for modifying the interior of the vehicle
- The HIII dummy is not validated for side impacts
- Only one dummy can be handled within a simulation and therefore dummy interaction is not possible
- No option for modifying the vehicle interior is available
- Restraint systems are mainly predefined

Conclusions:

The interface, which was developed for the simulation of the occupant movement during vehicle collisions, predicts occupant movement quite well. The major advantages of the model are that the well known and validated simulation software MADYMO is now made available for accident reconstruction. Although several limitations exist, many accident situations can now be simulated. The movement of the occupants during the accident can be shown in three dimensional form and graphically. This tool cannot be used to determine an accurate HIC or certain other injury parameters, as there are too many undefined parameters. However, the software can be used to gain a better understanding of the mechanisms causing certain injuries.

Pedestrian model:

To validate the pedestrian model and to estimate body properties for the pedestrian model several crash tests have been performed. Six different common vehicle shapes have been used in the simulations. A good correlation between the crash tests and the simulation results in general was found. Especially the total post impact travel of the pedestrian as well as contact locations, where the pedestrian hit the car, were predicted in the simulation runs. The simulation runs also showed which body parts of the pedestrian had contact with the car at which time. Also the influence of the pedestrian onto the post impact movement of the vehicle could have been seen in the simulation runs. To analyze the pedestrian kinematics and contact locations on the car three crash tests with different vehicles have been used (Annex).

Test 1 (55 km/h VW Polo)

Test 2 (50 km/h Polski Fiat 125P)

Test 3 (40 km/h Skoda 1203)

The six different most common vehicle shapes (DIN 75204):








Wedge shape	Trapezoidal shape	Pontoon	Box shape	Bonnet height	Bonnet angle	Front angle
				$\leq 0.7\text{m}$	$\leq 20^\circ$	
						
					$\leq 20^\circ$	$\leq 70^\circ$
					$> 20^\circ$	$\leq 70^\circ$
				Ellipsoidal front Front vehicle edge R > 0.25m		
						$> 70^\circ$
				Box shape Upright contact plane		

Fig. 43: Geometrical front shape classifications (DIN 75204)

Restrictions/Limitations for the validation of pedestrian:

There are some limitations, which apply to the pedestrian model at the current stage. Some of these limitations will be eliminated in future improvements of the pedestrian model, others may be neglectible.

- The stiffness coefficients of vehicles are assumed to be much higher than the stiffness coefficients of body parts of the pedestrian
- Deformations on the car body surface are neglected.
- In pedestrian to environment contacts the stiffness coefficients of the environment are assumed to be much higher than the stiffness coefficients of the pedestrian.
- Contact forces onto the environment do not result in any motion of the environment.
- Body parts of the pedestrian model will not separate during the simulation. Therefore there is no force limit for the interconnecting joints.
- Remaining deformations of different body parts of the pedestrian model are not taken into account for the calculation of further contacts.

Conclusions:

The pedestrian model in PC-Crash has shown to be a good tool to analyze pedestrian accidents. The post impact movement of the pedestrian can be predicted very well; contact locations on the vehicle as well as contact locations of the pedestrian on the ground can be calculated. Even if the scene data is not very accurate the additional information about pedestrian injuries and con-tact locations can be used to reconstruct the accident.

From the above mentioned validations, it can be concluded that PC-Crash can predict accident parameters well enough. Cliff and Montgomery used a large sample of tests (12 RICSAC, 7 JARI and 1 McHenry) to validate the program. Therefore, more tests are needed for identifying the accuracy of PC-Crash in the occupant kinematics and pedestrian (three tests have been done) accidents although the accuracy of the pedestrian model is good. There is also a need for PC-Crash validation for simulations

with other types of vehicles than passenger cars (e.g.: heavy trucks, articulated vehicles).

6.2.4 CRASH

During the 70's, a computer algorithm called CRASH (Calspan Reconstruction of Accident Speeds on the Highway) was developed at Calspan for the U.S. Department of Transport. This program can estimate the impact velocity and the Delta-V of a vehicle in a crash, based on information from the vehicle and the crash scene.

CRASH has been updated several times. In the early 80's, CRASH2 was renamed to CRASH3 by updating the stiffness coefficients of the vehicles. In January 1997, CRASH3 changed to SMASH (Simulating Motor Vehicle Accident Speeds on the Highway) by updating again the stiffness coefficients and by allowing the use of vehicle specific stiffness coefficients. SMASH also allows the input of specific vehicle dimensions.

CRASH (SMASH too) has two options of speed estimation, the damage-only and the trajectory method. The resulting Delta-V calculated from the damage-only algorithm represents the change in velocity of the vehicle's centre of gravity at the time of the maximum crush and it does not include rebound velocity. The calculation is based on the conservation of momentum and the energy absorbed. The energy is calculated by measuring the residual crush of the vehicle and applying an estimate of the stiffness to the measured crush area. Stiffness categories contain stiffness coefficients that define a linear force-deflection curve for a specific vehicle category (mini, compact, etc). The categories are listed in CRASH. In offset crashes, the Delta-V estimated by the damaged-only algorithm is also modified to account for rotation of the vehicle during the impact.

The trajectory algorithm (second option) requires detailed information from the crash scene and multiple assumptions regarding the energy dissipated in e.g. tire-road friction to calculate post crash dissipation. The calculation of the impact speed is based on the laws of the conservation of momentum.

Validation of CRASH / SMASH

There are a large number of publications about the CRASH program. Crash is probably the first accident reconstruction program ever made in the world. It is used by NHTSA and it is also used by many other agencies in the US. Therefore, attention had to be paid to the accuracy of the program. The different versions of the program are often validated by institutes that introduced an improved (on a specific issue) version of CRASH (e.g.: CRASHEX). In the following paragraphs, there will be no reference to these improved versions, but only general validations will be discussed.

Stucki and Fessahaie (1998) attempted to quantify the differences between CRASH3 velocity change (Delta-V) and measured velocities from test. Data derived from a study conducted by IIHS (Insurance Institute for Highway Safety) and by NHTSA, has been used for that purpose. The IIHS compared test speeds in collinear, offset impacts, both car-to-car and car-to-deformable barrier, to CRASH3 results. NHTSA

compared the measured velocity change with the CRASH3 Delta-V in collinear and oblique, offset car-to-car crash tests. The result of the comparison can be found in Tab. 12.

Car-to-Car Impacts							
Facility	Make/Model	Impact Direct.	Model Year	Vehicle Wt. (Kg)	% Overlap	Velocity Change (kmph) Test	CRASH3
IIHS	Lincoln Town Car	In-line	92	1860	46%	56	42
IIHS	Lincoln Town Car	In-line	93	1883	46%	57	42
IIHS	Chrysler LeBaron	In-line	89	1413	48%	56	43
IIHS	Chrysler LeBaron	In-line	89	1408	48%	57	43
IIHS	Chrysler LeBaron	In-line	89	1417	62%	64	58
IIHS	Chrysler LeBaron	In-line	89	1426	62%	64	58
IIHS	Oldsmobile Cutlass	In-line	85	1380	50%	55	42
IIHS	Oldsmobile Cutlass	In-line	85	1431	50%	55	40
IIHS	Oldsmobile Cutlass	In-line	86	1342	52%	56	50
IIHS	Oldsmobile Cutlass	In-line	86	1395	52%	56	48
IIHS	Oldsmobile Cutlass	In-line	89	1376	52%	55	45
IIHS	Oldsmobile Cutlass	In-line	88	1376	52%	56	45
IIHS	Oldsmobile Cutlass	In-line	89	1342	57%	55	47
IIHS	Oldsmobile Cutlass	In-line	89	1357	57%	55	46
IIHS	Oldsmobile Cutlass	In-line	89	1367	62%	55	45
IIHS	Oldsmobile Cutlass	In-line	89	1371	62%	56	45
IIHS	Oldsmobile Cutlass	In-line	89	1344	55%	63	55
IIHS	Oldsmobile Cutlass	In-line	89	1345	55%	64	55
NHTSA	Ford Taurus	In-line	91	1574	51%	56	45
NHTSA	Ford Taurus	In-line	93	1569	51%	56	45
NHTSA	Chevrolet Corsica	L.Obliq.	93	1315	56%	52	35
NHTSA	Chevrolet Corsica	L.Obliq.	93	1270	56%	62	42
NHTSA	Ford Taurus	L.Obliq.	94	1574	50%	59	38
NHTSA	Honda Accord	R.Obliq.	91	1370	100%	50	34
NHTSA	Honda Accord	R.Obliq.	91	1370	100%	59	39
NHTSA	Ford Taurus	R.Obliq.	92	1574	100%	59	38
Car-to-Deformable Barrier							
IIHS	Chevrolet Cavalier	In-line	95	1362	40%	64	37
IIHS	Subaru Legacy	In-line	95	1380	40%	64	39
IIHS	Ford Contour	In-line	95	1431	40%	64	38
IIHS	Honda Accord	In-line	95	1452	40%	64	40
IIHS	Mitsubishi Galant	In-line	95	1459	40%	64	47
IIHS	Saab 900	In-line	95	1489	40%	64	46
IIHS	Nissan Maxima	In-line	95	1507	40%	64	43
IIHS	Toyota Camry	In-line	95	1511	40%	64	48
IIHS	Chrysler Cirrus	In-line	95	1553	40%	65	48
IIHS	VW Passat	In-line	95	1557	40%	64	43
IIHS	Ford Taurus	In-line	95	1565	40%	64	44
IIHS	Volvo 850	In-line	95	1565	40%	65	44
IIHS	Toyota Avalon	In-line	96	1584	40%	64	45
IIHS	Mazda Millenia	In-line	95	1593	40%	64	41
IIHS	Chevrolet Lumina	In-line	95	1645	40%	64	42
IIHS	Ford Taurus	In-line	96	1651	40%	64	42
IIHS	Lincoln Town Car	In-line	91	1880	40%	64	55
IIHS	Lincoln Town Car	In-line	90	1897	40%	64	57
IIHS	Lincoln Town Car	In-line	92	1924	40%	64	49
IIHS	Ford Ranger	In-line	88	1379	40%	64	58
IIHS	Ford Ranger	In-line	89	1419	40%	64	51
IIHS	Ford Ranger	In-line	90	1448	40%	64	52
IIHS	Ford Ranger	In-line	89	1495	40%	64	52

Tab. 12: Comparison of CRASH3 Delta-V estimates with test results

From Tab. 12, it can be concluded that CRASH3 produces low estimates in comparison to test results. Especially for oblique impacts, the average error exceeds the 34%, which can be considered as a great error. In order to minimise the error, relationships between actual measure and the CRASH3 estimates were developed as adjustment factors. Factors have been developed for collinear and oblique crashes. Adjustment factors for offset impacts are contained in “WinSmash”, a successor to CRASH3.

It is also concluded that CRASH3 cannot provide reliable estimates of the Delta-V in Deformable Barrier tests (DFB). The deformable barrier provides a much softer impact surface than in impacts with fixed objects such as trees, median dividers, etc.

IIHS, in its detailed study (Nolan, 1998) (the data of this study have been also used by the authors of the previous validation) has concluded that the estimates from CRASH3 are lower than the true Delta-V. Among new vehicles tested by IIHS, the average CRASH3 Delta-V are 33% lower than impact velocities for passenger cars, 22% lower for utility vehicles and 10% lower for passenger vans. CRASH3

underestimates Delta-V, because of poor pre-assigned stiffness and size category coefficient.

Lenard et al (2000) have also treated the accuracy of CRASH3, comparing results from 137 passenger cars crash-tests to the CRASH3 estimates for these tests. The range of tests includes front, side and rear impacts against other cars, rigid barriers and deformable barriers. In Fig. 44, the comparison between CRASH3 estimates and test results for all vehicles is shown.

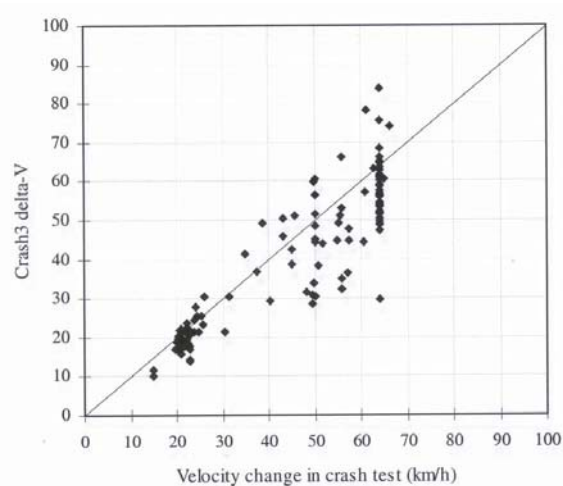


Fig. 44: Comparison between CRASH3 results and crash-test measurements

Overall, velocity change was underestimated by 9% (4km/h) with a standard deviation of 15% (8km/h). The rigid barrier results were most underestimated, because of the fact that contemporary European passenger cars are stiffer than the vehicles originally used to calibrate the program (vehicles from the American market). However, the Delta-V for the frontal car-to-car impacts was slightly overestimated. The deformable barrier crash-test results remain tentative, until the energy dissipated by the EuroNCAP barriers has been experimentally verified. Therefore, comparison of results for this type of tests with CRASH3 estimates could lead to wrong conclusions.

In general, it is concluded that CRASH3 underestimates the crash velocity. It can be accurate in its estimations, if the stiffness and the vehicle type can be pre-defined, according to the real values. Stiffness data for all vehicle types are not available and therefore known values from similar vehicle types have to be used as reference, which of course leads to inaccurate Delta-V estimates. CRASH3 cannot predict the Delta-V for low overlap (15% or lower) impacts, or under-run impacts, because the stiffness is actually unknown (tests have never been performed for these accident configurations).

Ai Damage

AiDamage is just one of the programs within Collision Suite which relies heavily on fairly complex physical principles for its operation. In addition the user input must be accurate before you can rely on the results produced. AiDamage is based on the Crash3 algorithms. The CRASH algorithms were refined over several years and are

now known as CRASH3. Data entry into the AiDamage program requires a statement as to the primary force direction. This is the direction from which the user considers the force which caused the damage was directed.

Throughout the data entry phase an active edit window gives you visual feedback on the data as it is entered. This allows mistakes to be spotted, and corrected immediately.

AiDamage calculates the change in velocity of a vehicle from the amount of crush sustained in an impact. By taking measurements from the damaged vehicle and comparing them with an undamaged one, the crush can easily be measured. Two measurement protocols are included, CRASH3 and AiDamage. Documents can be converted between either measurement systems. Users can also choose whether to use the original Crash3 crush coefficients or the later coefficients which have more vehicle classes.

Crush measurements are limited to any number between 2 and 100 and all measurements are taken from left to right with reference to the side of the vehicle being measured. Total damage width is not required, instead the width of the crush zones is entered, from which the program calculates the total width. Offsets are measured with either a plus or minus figure relative to the centre of the crushed area.

The program has the ability to perform two dimensional momentum calculations in addition to any crush analysis. AiDamage cannot perform post-impact calculations. Instead the user is left to determine the post-impact velocities by some other means and these are entered directly as a speed and direction of the centre of mass immediately post-impact. Delta-V is calculated, using the crush analysis, are subtracted from the post-impact velocities, to produce pre- impact velocities.

AiDamage performs all its calculations in metric and uses metric crush coefficients.

The program includes an option for researchers which allow access to specific Crash3 technical data. This data can be exported to databases as a CSV file. AiDamage requires either Windows XP, 2000, NT4 or 98

6.2.5 SMAC / EDSMAC

SMAC (Simulation Model of Automobile Collisions) is a reconstruction program sponsored by NHTSA and produced by Calspan in the early 70's. The program has been developed by different organisations through the years. In 1986, Day and Hargens created EDSMAC, a PC version of the SMAC 1974 version, converted to the BASIC computer language. In the late 90's, an improved version of the EDSMAC (the EDSMAC4) was introduced. In both SMAC and EDSMAC4, the trajectory and the damage method are available and can be combined, allowing a more accurate calculation of the momentum-based results.

SMAC is a time-domain mathematical model in which the vehicles are represented by different equations derived from the Newtonian mechanics combined with empirical relationships for some components (e.g. crush properties, tires) that are solved by numerical integration. The user has to specify parameters such as dimensions and inertia of the vehicle, crush and tire properties, initial speed and angles and the program produces detailed time history, including the collision responses, through step-wise integration of the equations of motion.

EDSMAC4 is an interactive, menu-driven program developed for PC (Day, 1999). Its collision algorithm is 2-dimensional. Cars and articulated vehicles can be simulated and the program allows the simulation of unlimited number of vehicles. The vehicle model is a 3 DOF, simulating X-Y translation and yaw rotation. Motion in the Z direction and roll and pitch orientation are calculated on a quasi-static basis. A tire model (Fiala, 1954) and the friction circle are used to compute the force at each tire.

Validation of SMAC / EDSMAC

The EDSMAC4 is validated by the Engineering Dynamics Corp., using RICSAC 2-car collision test (Day, 1999). The simulation results have been compared with the test results and also results from the version EDSMAC have been compared with those derived from EDSMAC4 (Tab. 13: Comparison of simulation results and test results).

Test	Method	Vehicle 1				Vehicle 2			
		V impact (mph)	X,Y, Ψ (ft, ft, deg)	CDC	dV (mph)	V impact (mph)	X,Y, Ψ (ft, ft, deg)	CDC	dV (mph)
Test No. 9	Measured	21.2	4.0, 35.3, 104.0	11FDE W2	21.4	21.2	-5.0, 49.5, 152.0	02RFE W2	8.9
	EDSMAC		7.7, 16.8, 74.1	11FDE W4	20.2		-34.0, 54.9, 193.7	02RYE W3	8.6
	EDSMAC4		3.8, 38.1, 111.5	11FDE W4	20.8		-4.3, 48.1, 152.9	02RYE W2	9.1
Test No. 12	Measured	31.5	22.3, -5.5, 118.0	12FDE W4	40.1	31.5	6.8, 2.6, -12.0	12FYE W4	26.4
	EDSMAC		22.7, -9.9, 134.8	12FYE W4	40.3		8.0, 1.7, -4.0	11FYE W3	27.3
	EDSMAC4		20.4, -6.4, 116.7	12FDE W3	40.4		6.5, 1.6, -17.9	12FYE W3	27.5

Tab. 13: Comparison of simulation results and test results

The conclusions can be summarised as follow:

- As it can be seen from Tab. 13, the simulation results are comparable to the test results. Only the EDSMAC prediction for the vehicle position deviates significantly from the test results
- There are some differences between results of EDSMAC and EDSMAC4. Some of the reasons for these differences are the extensions to the model in the EDSMAC4. The primary difference in collision-phase results was due to the extended force-deflection model that it was to simulate the contact of the truck and the trailer in a jack-knife situation. The difference in post-collision trajectories was mainly due to the addition of load transfers
- The reduced deformation, the higher and earlier occurred acceleration peaks and the shorter duration of the collision phase in the EDSMAC4 compared to the EDSMAC were produced due to changes of the force-deflection model
- Interpretation of the 3-D damage profile might be required, because the direction of deformation is always towards to the vehicle CG, which does not always occur during real crushing. The damage profile was produced using a

2-D algorithm, which of course did not change the z (e.g: elevation) damage co-ordinates

The EDSMAC4 has been also validated by M.M. Leonard et al (2000). They have compared the HVE (Human Vehicle Environment) EDSMC4 collision module of the 3-D computer simulation program with instrumented crash tests. In each test, one vehicle was a pickup truck pulling a trailer. From the comparison of the results was found that:

- EDSCAM4 predicts reasonably well the trends of the damage profile, rest positions, acceleration, velocities (Delta-V too) and velocity directions
- The stiffness coefficients are sensitive to the impact configurations and therefore have to be refined accordingly
- Inaccuracies in the trailer model response did not appear to affect the tow vehicle negatively
- The stiffness and damping properties of the vehicle-to-trailer connection can not be adjusted. The ability to improve these parameters would improve the accuracy of the results

The method is validated by Ruhl forensic agency. The Tab. 11: Comparison between the CARAT-4/ SMAC results and the RISCAC data shows that SMAC predicts the separation velocity and the Delta-V reasonably close to the test measurements. In comparison to the CARAT-4 results, the SMAC predicts more accurately the two parameters.

6.2.6 HVOSM / EDVSM

HVOSM (Highway-Vehicle-Object Simulation Model) is a simulation model developed at Calspan for the Federal Highway Administration during the late 60's and the early 70's. EDVSM (Engineering Dynamics Vehicle Simulation Model) is introduced by Engineering Dynamics Corp. in the late 90's and it uses the HVOSM model with an improved tire-road modelling.

The EDVSM is an HVE-compatible (Human Vehicle Environment) (HVE User's Manual, 1996) 3-dimentional simulation analysis of a single vehicle. The vehicle model includes front and rear suspension; both solid axle and independent suspension systems are supported. The model includes 14 degrees of freedom: six degrees for the sprung mass (body X,Y,Z, roll, pitch, yaw) and two degrees for each unsprung mass (wheel, spin and jounce/ rebound). The suspension model accommodates ride and damping rates, anti-sway bars, jounce and rebound stops, camber change, half-track change, anti-pitch and roll steer at each wheel. Close-loop driver control parameters include steering, braking, throttle and gear selection. The terrain is modelled automatically by the HVE environment model (Day, 1997).

The similarities between HVOSM and EDVSM are that both share the same basic vehicle model. Both programs require the same input and produce the same output. The calculation procedure is also the same. Differences are the programming language and the road surface and the tire properties definition.

Validation of HVOSM / EDVSM

The HVOSM and EDVSM have been validated by Engineering Dynamics Corp. by comparing the simulation result obtained by the two programs, as well as by comparing the results with field measurements (Day, 1997). Five well-instrumented vehicle handling test (found in the literature) have been used for the validation purposes. These handling studies were as follows:

- sinusoidal steer
- braking in a turn
- alternate ramp traversal
- turning manoeuvre into curb (rollover)
- wet pavement skid into soil (rollover)

Sinusoidal steer

Direct comparison of the results of the two programs revealed that the results were quite similar, even though that the tire and suspension model in EDVSM was not found in the SMI1 of the HVOSM. The differences might have been larger if the manoeuvre had been more severe (peak lateral acceleration was about 0.3g). The test results have been very similar to those of the computer simulations too.

Braking in a turn

Both program results were matching reasonably well. The simulation results were also matching with the test results in most cases. Some simulation and test result disagreement have been observed for roll angle and the left front wheel deflection. It is suspected that an error during the test measurements has been occurred. However, this finding is not certain and additional testing would be required to confirm the simulation results.

Alternate ramp traversal

Similar simulation results have been also revealed in this validation. Both HVOSM and EDVSM produced results that matched well. The simulation results were also matching to the test results, despite that some of the initial data (tire data, tractive effort and initial heading angle) have not been measured during the test and they had to be assumed or estimated for the simulations. An inconsistency that has been observed is a phase shift in the run, suggesting that the simulated vehicle was travelling a little bit slower than the actual vehicle. This might have happened due to lower acceleration and wheel deflection.

Turning manoeuvre into curb (rollover)

For this test, only the EDVSM results have been compared with test results. The simulated vehicle behaviour was in substantial agreement with the experimental results, including the rollover phase at the end of the run. Some advance or delay of the phase of the simulated results has been indicating that the tire characteristics of the simulated vehicle were slightly different than the tire characteristics of the measured vehicle.

Wet pavement skid into soil (rollover)

Again, only the EDVSM results have been compared with test results. The comparison showed a good agreement of the results. However, the problem that

plagued the previous test (considered to be related to the tire parameters of the simulated vehicle) was more pronounced in this test.

In general, it can be concluded from the validation of the simulated results that:

- The EDVSM and the HVOSM required the same input and produced the same output
- EDVSM is capable to drive directly over any 3-D surface
- EDVSM is able to visualise the 3-D response of a vehicle in real time (while the calculations are being performed)
- The EDVSM model has to be improved in order to simulate rollover crashes that result in the vehicle's upside down body contacting the earth
- The EDVSM tire model has to be improved in order to provide a more robust modelling of curbs and deformable soil
- The simulated results agree well with the test results. However, there is a phase lag of the simulated results in some cases (see Appendix)

6.2.7 PHASE / EDVDS

PHASE is a heavy vehicle simulation program developed at the University of Michigan in 70's, sponsored by the U.S. federal government. Different versions have been introduced the last decades and the most recent one is the PHASE4. PHASE4 model is a 3-dimensional simulation, allowing pitch, yaw, and roll movement. It is possible to simulate driver's action, such as steering, accelerating and braking (including anti-lock braking). Simulations with towing vehicles and single, double and triple trailers (the first trailer is a semi-trailer, the others are full ones) can be performed. Front and rear suspension may have single or tandem axles. Tandem axles can be of the 4-spring or walking beam variety. The user has to specify the vehicle parameters, driver control, play load data and the initial conditions. The model applies these data to a physical/ mathematical model to determine the instantaneous external forces acting on the vehicle. The resulting forces and moments are used to calculate the accelerations for each degree of freedom. With double integration of the accelerations, the speed and position can be determined for a small fragment of time.

The Engineering Dynamics Corp. using the PHASE4 model developed a new simulation tool, called EDVDS (Engineering Dynamics Vehicle Dynamics Simulator). EDVDS shares the PHASE4 mathematical model, ported to the HVE platform. This change allows the tires to travel over any 3-D terrain of arbitrary complexity. The C programming language has been used for rewriting the model and the input and output routines have been replaced with HVE input and output interface functions.

Validation of PHASE / EDVDS

The PHASE4 and EDVDS have been validated by Engineering Dynamics Corp. (Day, 1999a). Five experimental validation studies were performed:

- straight truck - step steer
- triples – combined steering and braking
- tractor-trailer – heavy steering and braking

- 2-axled vehicle – loss of control
- tractor-trailer – combined steering and braking

In the first three studies, the results from PHASE4 and EDVDS have been compared. In the fourth, the results of the two programs and the results of the EDVSM have been compared. In the last study, there was a comparison of the EDVDS simulation results and test data.

The conclusions that have been drawn from the five studies validation are:

- The resulting EDVDS model is significantly different from PHASE4, although the EDVDS model is derived from the PHASE4 one
- Results from the two programs revealed differences. These differences ranged from negligible to significant, depending on the severity of the manoeuvre
- EDVDS simulation results and experimental data have been in a good match
- EDVDS may be used for rollovers, because the resulting vehicle dynamics model did not incorporate the small angle assumption for sprung mass roll and pitch
- EDVDS was not valid for rollovers, during the vehicle body contacted the pavement or jack-knife, wherein the vehicle bodies contacted each other. This is because the resulting model did not include a contact model for the exterior body of each unit, either with the ground or between bodies
- The semi-empirical tire model permitted the study of severe handling manoeuvres, wherein tire-slip angle approached and exceeded 90 degrees. Results were comparable with another validated model (EDVSM)
- A problem in the PHASE4 mathematical model, permitting earth-fixed dolly yaw angles to exceed ± 90 degrees, was identified
- The EDVDS ability to drive on a 3-D surface of arbitrary complexity allows its use for studies such as pavement edge drop-off
- The semi-empirical brake model, brake anti-lock model and table look-up tire model, which are included in PHASE4, should be implemented for the EDVDS too
- In general, there is a good correlation of the trends of the time history (see Appendix)

6.3 Conclusions

There are many reconstruction methods/tools available for the estimation of accident parameters. These vary from the traditional reconstruction by hand till the sophisticated multi-body techniques or the advanced crash data recorders (black boxes).

The hand-calculated reconstruction can provide all information needed for an accident. The advantage of this method is that no hardware is required for the calculations. The disadvantages are that human error can occur during the calculations and that much time is required if different scenarios have to be reconstructed for the same accident.

The computer tools are validated as reasonably accurate in general. If important input parameters (e.g.: vehicle rest positions, stiffness, friction coefficient) can be closely defined to the actual values, the programs will produce accurate estimates. CRASH3, MADYMO and PC-Crash are extensively validated. In addition to the general validation of PC-Crash the collision optimizer, pedestrian model and occupant kinematics have been validated too. Some of the other programs should be validated with the use of multiple well-documented tests and not only with one or two experiments, as it has been until now.

Some of the reconstruction software is damaged based and with others it is possible to simulate the accident in 2D or 3D. CRASH and Ai Damage are damaged based reconstruction programs and requires a statement to the force direction. The impact velocity and Delta-V of a vehicle is calculated from the amount of crush sustained in an impact. Ai Damage cannot perform post-impact calculations. The user has to determine the post-impact velocities by some other means.

PHASE model is a 3D simulation which allows yawing, pitching and rolls movement and is more or less for heavy vehicle simulation. The Engineering Dynamics Corp. developed a new tool (EDVDS) which allows the tires to drive over any 3-D terrain of arbitrary complexity.

PC-Crash includes single vehicle simulation as well as vehicle to vehicle simulations. A kinetic driving model allows the consideration of dynamic influences such as suspension characters, tire characteristics and weight transfer. Different road conditions and different driver inputs can be taken into account. Collisions often result in suspension deformation and tire damage. PC-Crash takes these effects into account, while keeping the number of input parameters as low as possible. Furthermore it is possible to simulate the behaviour of occupants whereby a MADYMO model is used. PC-Crash allows reconstructing trailer and pedestrian accidents too. The trailer model is also based on a kinetic driving simulator. Finally the user can use an optimizing method (linear, genetic, Monte Carlo method) to minimize reconstruction time and error by varying of impact parameters. For an effective presentation of the results, 3D animations can be created directly from the calculated results.

SMAC is a time-domain mathematical model. The collision algorithm of EDSMAC is 2-dimensional; articulated vehicles and cars with an unlimited number of vehicles can be simulated. In both, SMAC and EDSMAC the damaged and trajectory method can be combined.

CARAT is a 3D mathematical model and can model cars, trucks, trailers and tractors/semi-trailers. CARAT can be used as time forward kinetic simulation but also for kinematics calculation forwards and backwards in time.

MADYMO is potentially a very powerful reconstruction program, because it allows information of different level of detail for the accident scenario, the vehicle damage and the occupant crash behaviour. However, this high detail level can be also considered as a disadvantage. As disadvantages can be considered the different models required for the different accident configurations, the long time for the adjustments/calibration of models and the need of specialised in body modelling

personnel to operate the program. The long running time for simulations of high detail level is also a disadvantage. With the rapid development of the multi-body models and the increasing computer processor speed, multi-body (e.g.: MADYMO) and Finite Elements techniques might become more popular in the accident reconstruction field in the close future. Primary focus of MADYMO is the analysis of 4-wheeled vehicle collisions, restraint performance and analysis of injuries. To reconstruct an accident the vehicles involved have to be modelled first with all information from crash tests or from models which are already available. With an optimization tool (e.g. MADYMIZER) you try to optimize towards for example end positions and deformation measurements or absorbed energy derived from crash pulses.

A very good solution for estimating many parameters within a simulation is the coupling of different programs. Examples of that are PC-Crash – MADYMO where occupant kinematics are simulated or the combination of EDSMAC4-EDVSM-EDVDS.

7. Collision Classification

7.1 CDC – Collision Deformation Code

In order to describe the damage pattern in a manner that is universally agreed upon and readily recognised, the Society of Automotive Engineers (SAE) has devised a descriptive coding method, which conveys the essential features of the collision damage in a seven-digit code. This method of coding is fully described in a booklet entitled 'SAE Recommended Practice J224b'.

The code is known as the Collision Deformation Classification or CDC. The code describes the nature and location of direct contact to the vehicle for each collision it sustains. However, in accordance with the protocols of STAIRS, this system has been enhanced to an 8 digit alphanumeric code

The first two columns, fifth and last columns are numbers. Columns three, four, six and seven are letters.

The first two columns are made up of two digits which describe the direction of force (DoF) of the impact. This is determined by the super-imposition of a clock-face onto the vehicle. The DoF is thus split into twelve 30-degree sectors as on a clock-face, so that a DoF of 12 o'clock implies that the impact was applied longitudinally from the front of the vehicle, as is often the case of a head on collision. Thus a DoF of 06 o'clock implies that the impact was applied longitudinally from the rear of the vehicle. For each side of the vehicle there are potentially 7 directions of force.

If an impact should occur at an angle greater than 15° to the horizontal of the vehicle (at the time of the impact) then the 00 DoF is used.

7.1.1 CDC 1&2 - DoF – Direction of Force

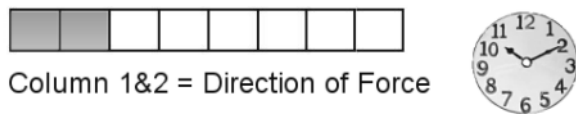


Fig. 45: CDC 1&2 – Direction of Force

PDof – Principal Direction of Force: the force acting on a vehicle that cause crush deformation acts along the impulse line between the two vehicles. During most collisions, the instantaneous direction of force or the impulse line varies over time relative to the vehicle axis. The impulse line is also called the principal direction of force (PDof) line of action. The Delta-V vector also acts along the PDof line of action. A general rule is that the occupants are initially projected along a path opposite the PDof. When the PDof's are not perpendicular to the damaged surface, the crush depths along the PDof will be greater than the crush deformation measured by an investigator, because deformation measured perpendicular to the original undamaged surface. The PDof angle effect can exert a sensitive energy and Delta-V calculations, such as during damage only analysis programs. Consideration should always be given to the damage characteristics and motion of the vehicles which occurred after the impact in order to correctly assess the PDof's of the vehicles.

DoF – Direction of Force is part of the CDC (Collision Deformation Code) Code. The first two columns are made up of two digits which describe the Direction of Force (DoF) of the impact. The investigator has to estimate the Direction of Force which is very difficult but can be useful in occupant kinematics (in which direction the occupant(s) will tend to move). Some useful indications to estimate PDof are longitudinal which could crumble or bend during an impact.

This is determined by the super-imposition of a clock-face onto the vehicle. The DoF is thus split into twelve 30-degree sectors as on a clock-face, so that a DoF of 12 o'clock implies that the impact was applied longitudinally from the front of the vehicle, as is often the case of a head on collision. Thus a DoF of 06 o'clock implies that the impact was applied longitudinally from the rear of the vehicle. A direction of impact force falling upon any one of the boundaries between clock sectors could be interpreted to be in either sector and still be essential correct. For instance, an impact exactly 15 deg clockwise of straight ahead falls on the division between the 12 o'clock and 1 o'clock sectors. Both, 12 or 1 o'clock would be valid assessments. The user should recognize that there are practical limits with which the direction of force can be assessed and deviations of as much as +/- 5 deg can occur in even expert judgements.

For PENDANT it was agreed to use a clock face split into twelve 30-degrees sectors.

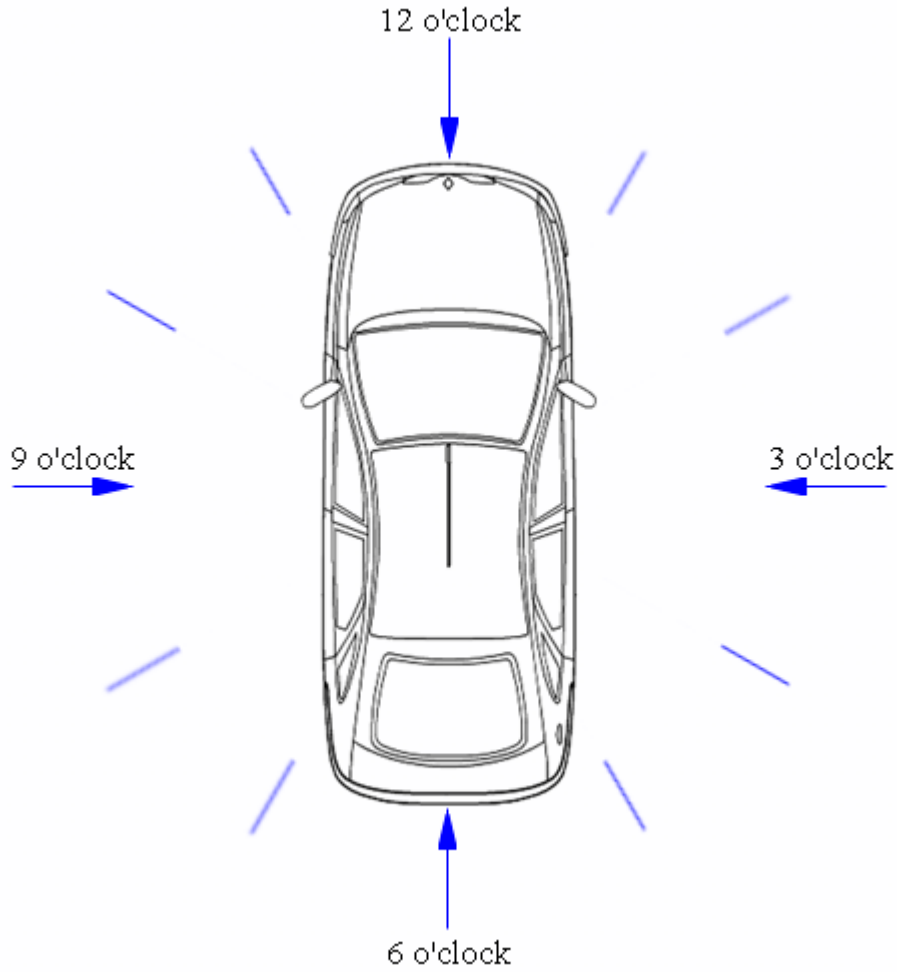


Fig. 46: Direction of Force – clock face

These characters of CDC expression define the force which produced the deformation pattern classified in the remaining columns. Definition, however, is related to the direction of force rather than the magnitude of force.

The picture shows a 90 deg intersection impact configuration

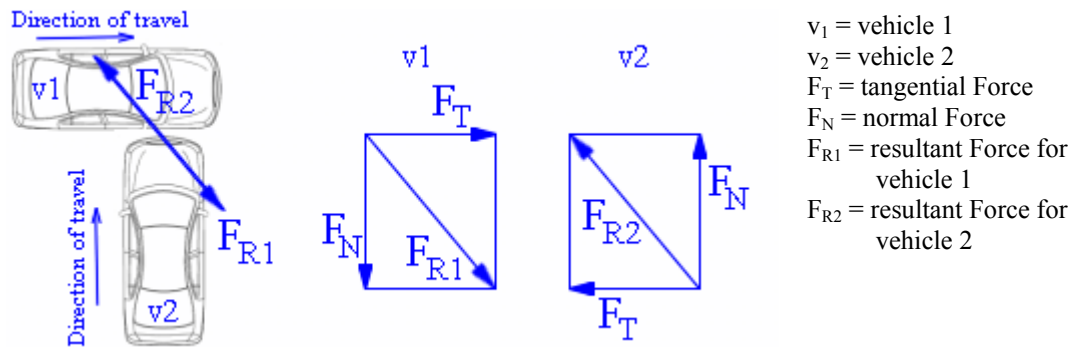


Fig. 47: DoF – Direction of Force

The direction of this force typically is not perpendicular to the surface of the vehicle. The PDoF is established by the angle α between the normal force F_N and the resultant force F_R .

The angle between two colliding vehicles at impact and the direction of force should always be considered together, as they are not independent. It can be quite difficult to determine the direction of impact force applied to a crashed vehicle. Often it is easier to visualize the orientation of two colliding vehicles relative to each other at impact. There is a very simple and useful technique for using the angle between two colliding vehicles at impact to refine assessment of the direction of force: this is illustrated in the next picture.

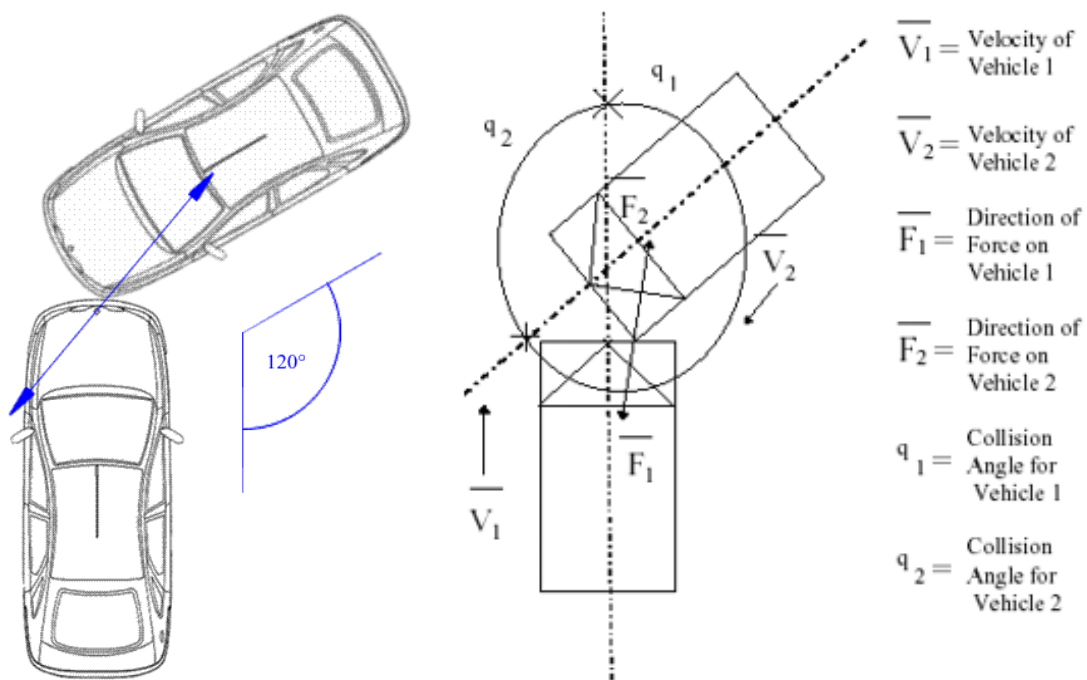


Fig. 48: Relationship between Vehicle Orientation and DoF

The mutual forces applied by the vehicles to each other must always be exactly opposite in direction (collinear) a direct implication of Newton's 2nd Law that to every action there is an equal and opposite reaction. In the example, the angle between the longitudinal axes of both vehicles is 120 degrees and assumed that this orientation is strongly supported by the vehicle damage and accident scenario. In now vehicle one is assigned a 12 o'clock DoF, vehicle two must be given 10 o'clock DoF. In case of vehicle one is given a DoF of 1 o'clock vehicle two must be given a DoF of 11 o'clock. To say they both had a DoF of 12 o'clock and were orientated at 120 degree is incoherent. This technique is especially useful for side impacts because side struck vehicles tend to fit the description of being hard to diagnose for direction of force. If the direction of force to the striking vehicle and the orientation of the two vehicles is more accessible, as is usually the case, the direction of force to the struck vehicle can be inferred.

When examining a damaged motor vehicle, one often has a difficult time in correctly assessing the principal direction of force vector. Cosmetic damage inspection can be very misleading nearly always the correct assessment is made following a thorough

inspection of all damage components. And understanding which direction all of those components have moved.

It is important to understand when inspecting a damaged motor vehicle, for the purposes of determining the principal direction of force, that impact force has direction but also has sense. As the impact force begins to be absorbed by the motor vehicle, the direction in which the force enters the vehicle sometimes can be associated with the structural strength of the components in the damaged zone.

Some of the lighter components, especially in a front-end assembly, on being deflected rearwards from a frontal impact, can move sideways when those components strike a more heavily constructed component. This includes frame rails, firewall bulkhead, etc. Lighter components will then shift sideways. If the investigator was to establish the principal direction of force based on the post-impact position of these lighter components, it could be an error.

Therefore, the most accurate direction of force assessment would be based on more heavily constructed components if the impact was of sufficient magnitude.

If one was able to specify the initial position of the front of one of the vehicle's frame rails or unibody frame rails, and draw a line between that point and the post-impact position of that components, it would likely be the principal direction of force vector, as opposed to noting the pre-impact position of a headlight assembly and the post-impact position of a headlight assembly. The line between those two points might not necessarily be an accurate representation of the principal direction of force vector, as the headlight assembly may have been deflected into that position by a stronger component.

There are many ways to gain a stronger visual perception of the principal direction of force. One of the more handy tools to use is a 35 mm camera with a telephoto lens. Align the datum line of the lens when taking the photograph, with an undistorted line of the vehicle. The developed photo will allow the investigator can get a more magnified understanding of the way that the damage components have moved in relation to an undistorted plane of the vehicle.

Accident collision type classification

Richter et al classified accidents into twelve types. With the help of an accident collision type an accident situation regarding the positions of the vehicles involved could be specified.

Generally an accident can be classified into four types:

- frontal,
- rear,
- side impacts and
- rollovers

The clock-face is divided into four areas. A frontal impact can be within the red area which is between the left and the right corner of the bumper and the centre of gravity (CoG). It is very difficult to find out the CoG; therefore a diagonal was made from the

right/left corner of the front bumper to the left/right corner of the rear bumper. The point of intersection of both lines is in the middle of the car and the centre point of the circle which divides the car in these four sections. This arrangement is enough for our purpose. Within the green section rear impacts happened. In case of a rollover within all four sections damage could be occurred depending on the rollover movement of the vehicle.

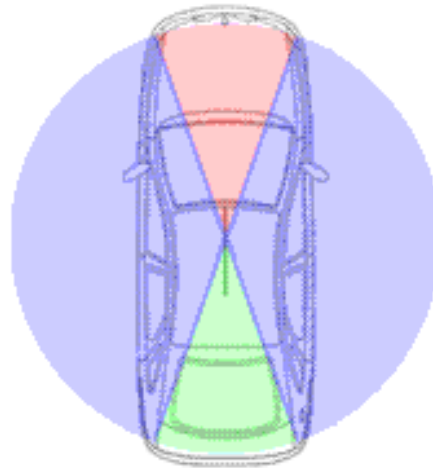


Fig. 49: Vehicle sections

Frontal impacts can be divided into full overlap impacts and impacts with an offset for DoF of 12 o'clock. An offset impact can be either on the driver's or passenger's side.

Frontal impacts generally can be divided into left and right side of the vehicle (offset).

7.1.2 CDC 3 - General Location

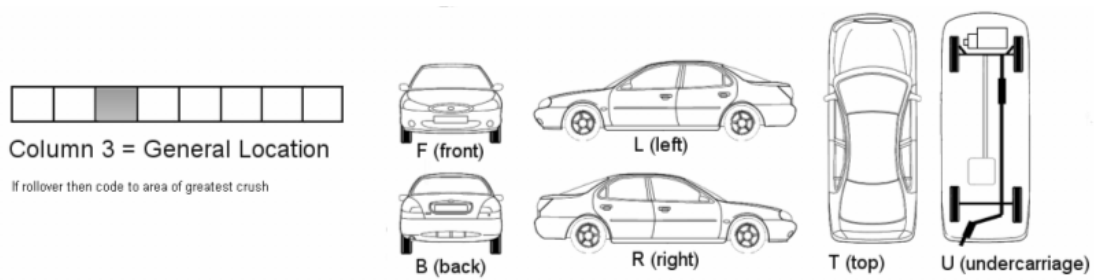


Fig. 50: CDC 3 – General Location

The third column describes the side of the vehicle most damaged by the direction force of the impact.

Broadly defines which projected area of the vehicle contains the deformation. Code the area which contains the most deformation. The windshield is included in 'F' and the rear screen is included in 'B'. 'U' is defined as the bottom plane of the vehicle, including all projections, but excluding wheels and tyres. Impacts involving wheels and tyres are classified as 'FW', 'BW', 'LW' or 'RW'. 'X' is reserved for catastrophic impact configurations in which the projected area of involvement cannot be determined.

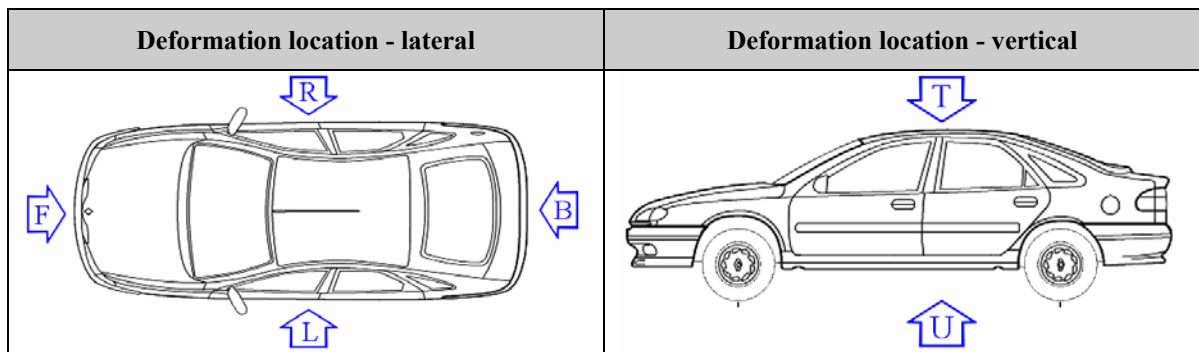


Fig. 51: Deformation Location

Side of vehicle most damaged by DoF
F = Front
B = Back
L = Left side
R = Right side
T = Top
U = Underside

Tab. 14: Side of vehicle most damaged by DoF

7.1.3 CDC 4&5 - Horizontal Location

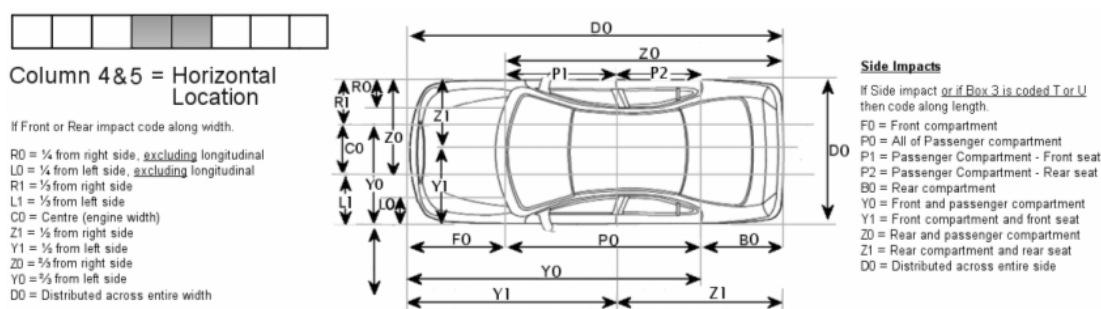


Fig. 52: CDC 4&5 – Horizontal Location

The fourth and fifth columns describe the horizontal location of the direct contact damage by splitting the vehicle width or length into bands as follows:

Specific Longitudinal or Lateral Location of Deformation - defines the region of deformation within the deformation location. When defining the region on the side of the vehicle, define the passenger compartment area, P0, first to establish F0 and B0. P0 is defined as extending from the base of the windshield to the rear of the rear most (forward facing) seat. For off-road and estate vehicles which have seats within the load area, do not include such seats as being within the passenger compartment. If previous variable contains F(W) or B(W), in this column use R0, L0, C0, R1, L1, Y1, Z1, Y0, Z0 or D0. If previous variable contains L(W), R(W), T or U, in this column use F0, P0, P1, P2, B0, Y1, Z1, Y0, Z0, or D0.

Front/Rear Impacts	Side Impacts
R0 = ¼ from right side <u>excluding</u> longitudinal	F0 = Front compartment
L0 = ¼ from left side <u>excluding</u> longitudinal	P0 = All of Passenger compartment
R1 = ½ from right side	P1 = Passenger Compartment - Front seat
L1 = ½ from left side	P2 = Passenger Compartment - Rear seat
C0 = Centre (engine width)	B0 = Rear compartment
Z1 = ½ from right side	Y0 = Front and passenger compartment
Y1 = ½ from left side	Y1 = Front compartment and front seat
Z0 = ⅔ from right side	Z0 = Rear and passenger compartment
Y0 = ⅔ from left side	Z1 = Rear compartment and rear seat
D0 = Distributed across entire width	D0 = Distributed across entire side

Tab. 15: Horizontal location of the direct contact

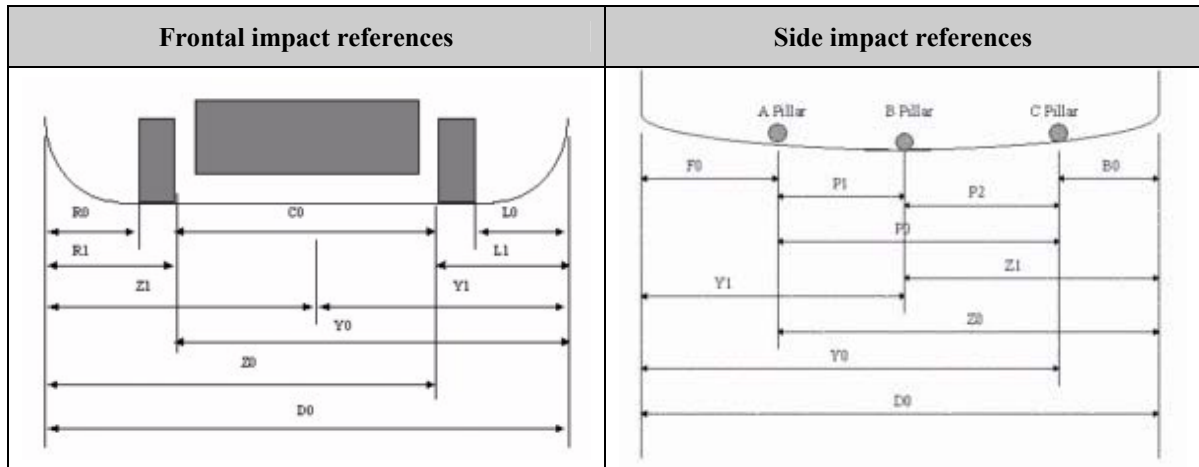


Fig. 53: Impact references – frontal and side

7.1.4 CDC 6 - Vertical Location



Column 6 = Vertical Location

- A = all
- G = belt line & above
- H = above longitudinal to top of vehicle
- M = above longitudinal to belt line
- E = everything below belt line
- L = longitudinal and below (including undercarriage)
- W = wheels & tyres only

If box 3 is coded T or U then code across width

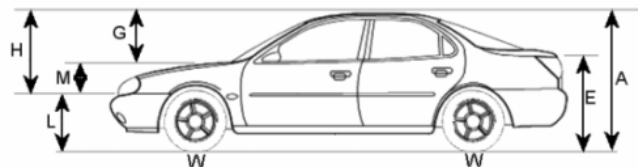


Fig. 54: CDC 6 – Vertical Location

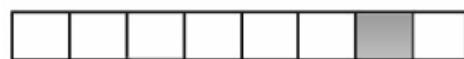
The sixth digit describes the vertical location of the direct contact damage. The height of the vehicle is split into bands as follows:

Specific Vertical or Lateral Location of Deformation -defines the region of deformation within the deformation location. If “Deformation Location” contains F, B, L or R, in this column use A, E, G, H, L, M or W

Vertical location of the direct contact damage
G = Glass Level & Above
M = Middle Section Only
L = Lower Section Only
W = Wheel/s only
E = Middle & Lower Level
H = Middle & Glass Level
A = All Three Levels

Tab. 16: Vertical location of the direct contact damage

7.1.5 CDC 7 - Damage Pattern



Column 7 = Damage Pattern

- A = Gross Underrun (2 step)
- O = Rollover
- N = Narrow <41cm not including a corner
- E = Narrow <41 including a corner
- W= Wide >41cm
- S = Side or end Swipe (10cm or less)

Fig. 55: CDC 7 – Damage Pattern

The seventh digit describes the nature of the impact type once its location has been described. The codes for these are:

General Type of Damage Distribution - provides a description of the type of damage sustained by the vehicle. ‘S’ = sideswipe (or end swipe). ‘O’ = rollover. ‘A’ = overhanging structure shaped like an inverted step, in which the vertical surfaces are more than 760mm apart (both surfaces must have contacted, but not necessarily at the same time). ‘E’ = corner (damage width is less than 410mm). ‘W’ = wide object (damage area is more than 410mm wide). ‘N’ = narrow object (damage area is less than 410mm wide). ‘U’ = no residual deformation (column 8 must be 1 if ‘U’ is used).

Nature of the impact type
W = Wide Impact (>41cm)
S = Sideswipe or endswipe (<10cm)
A = Under-run Impact
N = Narrow Impact (<41cm)
O = Rollover/Overturn
E = Corner Impact (<41cm)

Tab. 17: Nature of the impact type

7.1.6 CDC 8 – Crush Extent

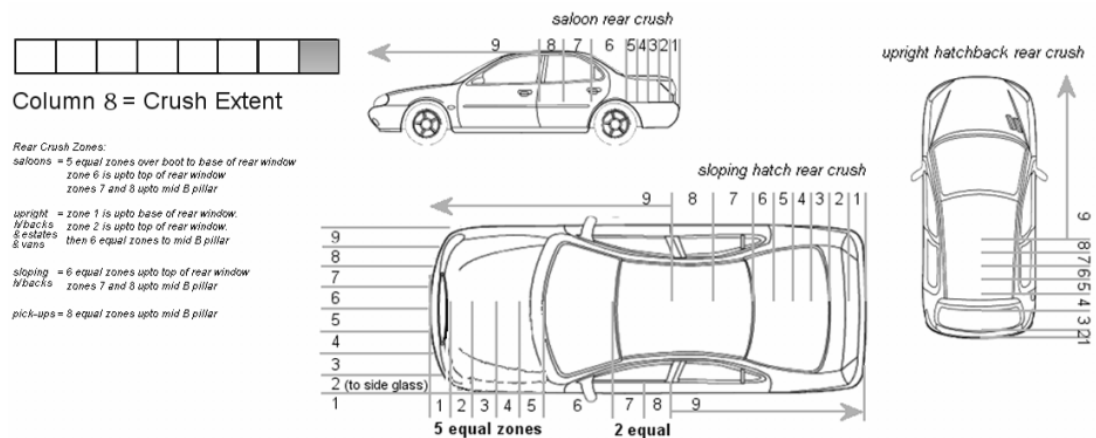


Fig. 56: CDC 8 – Crush Extent

The eighth digit describes the extent of the crush using a zonal system code of between 1 and 9.

Defines the extent of deformation within the deformation location direction (i.e. for a frontal direction, divide the whole length of the car into 10 equal parts; the value indicating which deformed segment is the most distant from the point of impact).

8. Reconstruction Parameters

8.1 Energy Equivalent Speed (EES)

The term Equivalent Energy Speed (EES) has been defined by Burg, Martin and Zeidler in the year 1980 and was suggested for a common use. EES is a speed measure which will be transformed into deformation energy during the collision.

For accident reconstruction and for accident research there are tools necessary for a realistic assumption of the accident circumstances. But in most of the cases there are not enough data for a reliable statement of the crash, especially the crash severity and the relationship between the crash severity and the occupant load is difficult and controversial problem.

The plastic deformation energy of the damaged car is expressed as a kinetic energy of the car with the virtual velocity value EES. For an authentic EES-estimation various crash-tests with different conditions are necessary, because the energy absorption depends on various parameters.

Two phases can be distinguished during the crash of a vehicle: there is a compression phase and a restitution phase. The compression phase lasts from the contact of the vehicle with an obstacle (another vehicle or anything else) to the point of maximum compression. During this phase, the energy is stocked until the maximum deformation. The restitution phase begins when deformation is maximum and ends when the vehicle separates from the obstacle. During this phase, the deformation energy is released.

International Standard definition for EES (ISO/DIS 12353-1:1996(E)):

„The equivalent speed at which a particular vehicle would need to contact any fixed rigid object in order to dissipate the deformation energy corresponding to the observed vehicle residual crush.“

EES calculation

Unlike delta-V, EES is a scalar quantity, having magnitude (e.g. 50 km/hr) but no direction. As the name implies, it is a measure of the energy dissipated by a crashed vehicle and may be thought of as an energy-based measure of impact severity.

EES values can be calculated for different types of vehicles using various approximation equations. If one EES is known, it is possible to determine the EES of the second, random vehicle. It is likewise possible to determine the deformation energies in the case of a collision with a stationary deformable obstacle.

No direction is assigned to this quantity and it is therefore a scalar. The deformation energy can be written as follows:

$$E_D = \frac{1}{2} \cdot m \cdot EES^2 \text{ [kph]} \quad 8-1$$

E_D : deformation energy
 m : mass of the vehicle [kg]
 EES : Energy Equivalent Speed [kph]

EES depends only on the energy dissipated E_D and the mass of the vehicle m . These two parameters are not sufficient to determine the change of velocity ΔV of a crashed vehicle.

If the EES of one vehicle that was involved in a vehicle to vehicle collision is known, then it is possible to determine the unknown EES based on the principle of action equals reaction by approximating the other crush.

$$\frac{EES_1}{EES_2} = \sqrt{\frac{m_2 \cdot s_{Def1}}{m_1 \cdot s_{Def2}}} \quad [\text{kph}] \quad 8-2$$

$$EES_2 = \sqrt{\frac{2 \cdot E_D}{m_2 \cdot \left(\frac{s_{Def1}}{s_{Def2}} + 1 \right)}} \quad [\text{kph}] \quad 8-3$$

m_1, m_2 mass of each vehicle
 s_{Def1}, s_{Def2} crush depth of each vehicle, outer surface to impact point in line with impact force
 E_D energy lost by both vehicles in the collision due to damage

If no immediately similar tests are available for comparison purposes, then the deformation energy can be calculated from the damage measured on the vehicle using either the speed-deformation curve generated from a number of impact results at various speeds or a force-displacement curve prepared from a single impact test. Other methods used to calculate EES are: energy grids, approximation equations or damaged based algorithms. EES can work with partial information from the crash (i.e. the damage profile from one vehicle only) as it is only a measure of the energy dissipated by that vehicle.

Estimating EES using an EES Database

PC-Crash supports an EES Database in the software from Dr. Melegh (Melegh@auto.bme.hu) which could be ordered from Dr. Melegh or from DSD (Dr. Steffan Datentechnik, Salzburgerstraße 34, A-4020 Linz; g.steffan@dsd.at). A new EES database will be included in the next PC-Crash version (PC-Crash 7.2) as well which has been developed by DSD and AZT (Allianz Zentrum für Technik GmbH, Kraftfahrzeugtechnik, Münchener Straße 89, D-85737 Ismaning; <http://www.allianz-azt.de/azt/index.html>).

The EES catalogue contains photos of damaged vehicles categorized into vehicle model and collision severity groups. This enables the user to quickly see if the EES of the calculated impact is reasonable, based on a visual comparison of the damage.

Which kinds of data are stored in that database? You can choose between make, EES and impact direction and the database will filter the information. The range of EES is from low speed 5 kph up to approximately 100 kph depends on car and impact direction. Additional information is overlap and deformation. The EES values are estimated by motor vehicle legal assessors and are data from real world accidents. For vehicles from AZT test parameters have been developed but these tests only perform low speed.

Allianz-Zentrum für Technik (AZT) started their work on the scientific analysis of accident repairs as early as 1971. The essential aims of this analysis can be set out as follows:

- The creation of objective assessment criteria with regard to ease of repair, and the repair characteristics of vehicles
- Optimisation of repair procedures in close cooperation with vehicle manufacturers

The test condition report can be ordered by: ernst.tomasch@tugraz.at , g.steffan@dsd.at or directly http://www.allianz-azt.de/azt/Kraftfahrzeugtechnik/Content/Seiten/Presse/Kontakt/kontakt_azt.html

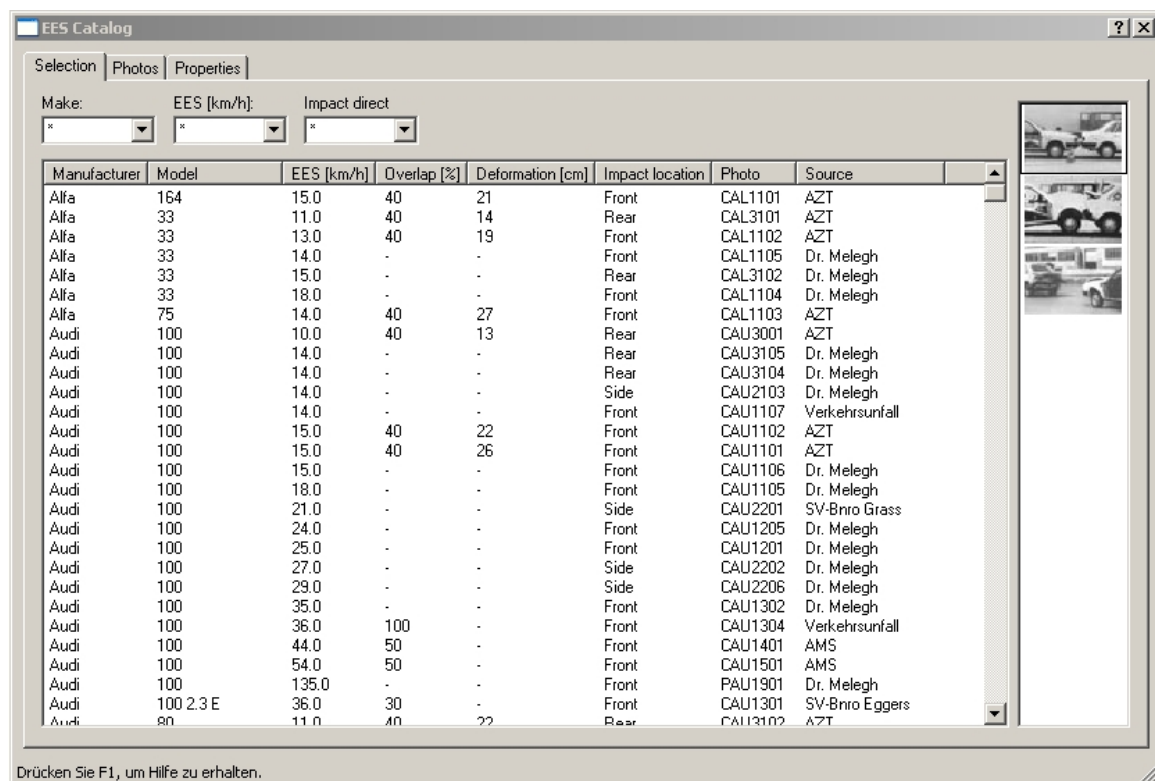


Fig. 57: EES Database pictures

8.2 DELTA-V - Δv

The Greek capital letter Δ , pronounced "delta", is used to denote "change of": the letter v denotes velocity. So Δv , or "delta-v" as it is written to avoid the use of foreign script, just means change of velocity. Vehicle crush deformation and energy equivalence relationships are technical accident reconstruction tools for estimating the change in velocity during an impact. Delta-v is a basis for evaluation damage severity and potential injury severity.

Definition of Delta-v: "change in velocity of a vehicle's occupant compartment during the collision phase of a motor vehicle crash (i.e. from the moment of initial contact between vehicles until the moment of their separation)".

Delta-v is a vector, in other words it is a quantity with magnitude and direction. It is the vector difference between an initial velocity and a final velocity.

International standard (ISO/DIS 12353-1:1996(E)) definition of *Delta-v*:

"Vector difference between impact velocity and separation velocity."

$$\Delta v = v_f - v_i \text{ [kph]} \tag{8-4}$$

where v_f is final velocity
 v_i is initial velocity

For eccentric bevelled impacts, the velocities and the linear momentum have to be divided into x and y direction.

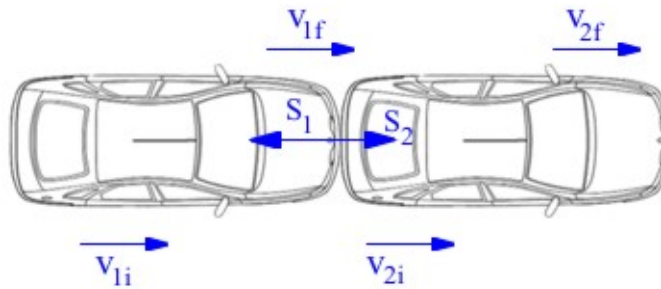


Fig. 58: Straight line centric impact

$$\begin{aligned} m_1 \cdot (v_{1f} - v_{1i}) &= -S_1 \\ m_2 \cdot (v_{2f} - v_{2i}) &= S_2 \end{aligned} \tag{8-5}$$

$$\Delta v_1 = v_{1f} - v_{1i} = -\frac{m_2 \cdot (1 + \epsilon)}{m_1 + m_2} \cdot (v_{1i} - v_{2i}) \tag{8-6}$$

$$\Delta v_2 = v_{2f} - v_{2i} = \frac{m_1 \cdot (1 + \epsilon)}{m_1 + m_2} \cdot (v_{1i} - v_{2i}) \quad 8-7$$

Special cases for straight line centric impacts:

Mass [kg]	Coefficient of restitution	Velocity [kph]	
$m_1=m_2$	$\epsilon=1$	$v_{1f} = v_{2i}$	$v_{2f} = v_{1i}$
	$\epsilon=0$	$v_{1f} = v_{2i}$	
$m_2 \rightarrow \infty$	$\epsilon=1$	$v_{1f} = -v_{1i}$	$v_{2f} = 0$
	$\epsilon=0$	$v_{1f} = v_{2f} = 0$	

Tab. 18: Special cases for straight line centric impacts

As you can see the influence on Delta-v for a straight line centric impact is following:

Assumption: no sliding collision!

- Weight of vehicles
- Coefficient of restitution
- Relative velocity $v_{1i}-v_{2i}$

ϵ will be described in chapter Coefficient of Restitution.

What is Delta-v? It is simply a change in the velocity vector. For our purposes, it is the change in the velocity vector at the centre of mass of the vehicle. This change in velocity can be as a result of a change in speed, a change in direction, or both. A vehicle travelling at 30 kph in a northerly direction that, after impact, is travelling at 30 kph in a southerly direction, has experienced a 60 kph Delta-v due to the change in direction. If a vehicle travelling 30 kph stops without changing direction, the Delta-v is 30 kph. If the Delta-v occurs over several seconds and is relatively small, it usually causes little or no injury. If the deceleration is high over in a small time, injury or death is usually the result. Remember, it is not the fall that kills, it is the sudden stop

The initial and final velocities are the instantaneous velocities of the centre of a mass of the crash-tested vehicle immediately before and after impact. An instantaneous velocity could be defined like the intuitive notion of travelling a certain speed in a certain direction at a certain time. Where the beginning of an impact is at the first time of contact and finished after the vehicle separates from the barrier. The focus is on the magnitude of Delta-v rather than its direction, but this is no rejection of the vector nature of Delta-v. A side impact is finished when the force on the vehicle from a side impact trolley is similar in magnitude to the frictional forces on the vehicle from the floor. In this sense the impact is over before a side impact trolley and crash-tested vehicle come to rest.

The direction of Delta-v is often not stated, especially when it may be implicitly understood. In the side test a trolley pushes the stationary vehicle laterally and the

Delta-v is directed along the trolley’s line of travel. In the frontal EuroNCAP test for example, the crash-tested vehicle retains only some slight movement at the end of impact with the immovable barrier and so Delta-v is primarily "negative", i.e. directed opposite to the vehicle's original line of travel or in case of an offset it could be side- and backwards.

By Newton’s Third Law, the force acting on one vehicle must be equal in magnitude, but opposite in direction to that acting on the other vehicle. Therefore, each vehicle is acted upon by the same impulse.

Example:

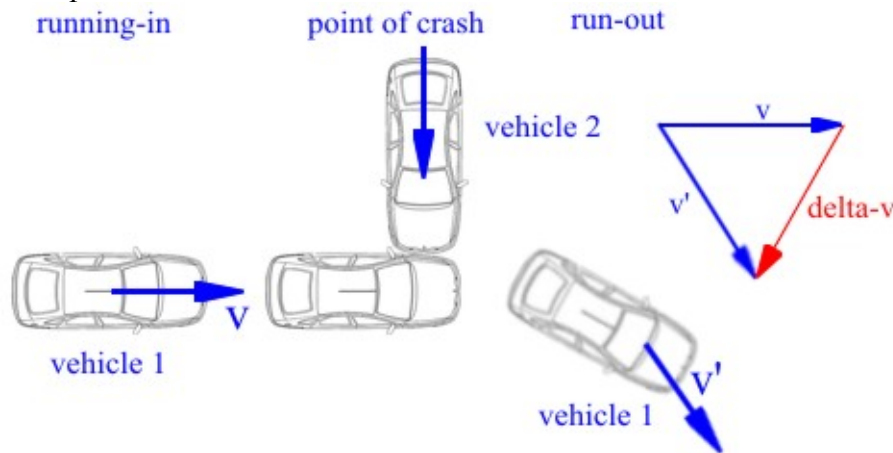


Fig. 59: Change of Velocity as Vector Quantity

A vehicle has a collision with 40 kph. After the collision the angle changes to $\alpha'=60^\circ$ and the run-out velocity $v'=20$ kph. What’s the value of Δv now? In the following table the calculation of Δv is described. Δv is not the difference between the running-in velocity and the run-out velocity, this would be 20 kph. Δv is a vector and the x- and y-components must be taken into account.

Collision running-in	Collision run-out		Collision changing
$v = 40$ kph	$v' = 20$ kph		$\Delta v = \sqrt{\Delta v_x^2 + \Delta v_y^2}$ $\Delta v = 35$ kph
$\alpha = 0^\circ$	$\alpha' = 60^\circ$		
↓	↓		↑
$v_x = 40$ kph	$v_x' = v' \cdot \cos(\alpha') = 10$ kph	→	$\Delta v_x = v_x' - v_x = -30$ kph
$v_y = 0$ kph	$v_y' = v' \cdot \sin(\alpha') = 17$ kph	→	$\Delta v_y = v_y' - v_y = 17$ kph

Tab. 19: Calculation of Δv

In this example the difference of the running-in and running-out velocity of 20 kph is not the Delta-v which could be expected. The calculated Delta-v are the 35 kph where the x and y components are taken into account as well. This calculation shows the relevancy of the nature of Delta-v and can't be neglected.

8.3 Closing Speed

In many cases, knowledge of the closing speed, or relative speed, of the vehicles at impact can determine directly the speed of one of the vehicles within reasonably narrow limits. The closing speed can be determined from measured damage or “crush” of the vehicles, vehicle weights and stiffness coefficients of the vehicles obtained from crash tests. Many collisions, e.g. intersection collisions, occur with the direction of travel of the two vehicles at impact forming some angle other than 0° or 180° .

For example, if the struck vehicle is known to be at rest at impact, the striking vehicle’s speed can be determined directly since its speed is the calculated closing speed. Also, if one vehicle is known to be moving slowly, e.g. just started from rest at a traffic light or stop sign, and is struck perpendicularly by a somewhat faster moving vehicle the difference between the closing speed and the faster vehicle’s speed will be small. Consider a vehicle known to have started from rest and to have moved into an intersection such that its upper limit of speed is 10mph. If it is struck by a vehicle going 40 mph at impact, the closing speed of 41.2 mph is only 3% higher than the striking vehicle’s speed at impact.

In general, determination of pre-impact speeds can be achieved from the Law of Conservation of Momentum. This necessitates knowing the post-impact momentum of each vehicle and their pre-impact directions of travel. Measurements to determine post-impact momentum are frequently flawed by lack of road-surface marks to precisely indicate immediate post-impact velocity directions. Steer input can result from vehicle damage (damaged wheels) or inhomogeneities along the surface travelled after impact, thus point-of-impact to point-of-rest can be very different from the initial post-impact velocity direction. Also, the post impact initial speed can be uncertain due to unknown post-impact degree of braking(if any), uncertain degree of roll resistance due to dam-aged wheels or uncertain angle between post-impact directions of travel and the roll directions of the vehicle’s wheels as well as various other sources of uncertainty. In these cases, closing speed at impact is an additional piece of information for solving for speeds and is a check for closing speed derived by other means.

Vehicles A and B approach each other with an angle between their lines of motion (directions of their velocity vectors). Vehicle A has a velocity of \vec{v}_{AE} and B has a velocity of \vec{v}_{BE} . The velocity of A relative to B (A’s velocity of approach as seen by an observer riding in B) is \vec{v}_{AB} . This is the vector difference $\vec{v}_{AE} - \vec{v}_{BE}$.

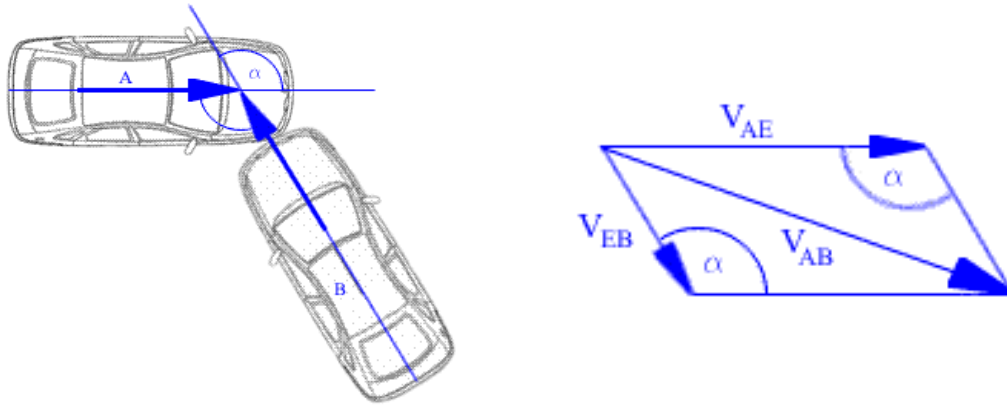


Fig. 60: Closing speed

Thus, by vector addition we get the closing speed i.e. $\vec{v}_{AB} = \vec{v}_{AE} + \vec{v}_{EB} = \vec{v}_{AE} - \vec{v}_{BE}$. This is shown in the diagram of vector addition by the parallelogram method. Also note an observer in A sees B approaching at velocity \vec{v}_{BA} which is just $-\vec{v}_{AB}$.

By the definition of a completely inelastic collision, the two colliding objects have the same final velocity (same final speed and same final direction). The initial momentum lines of action will be the same as the lines of action of the initial velocities, but will be of different magnitude.

8.4 Equivalent Test Speed (ETS), Equivalent Barrier Speed (EBS), Barrier Equivalent Velocity (BEV)

The most common method of testing vehicles is by impacting them against or with rigid barriers. Therefore, the reconstruction of vehicle-to-vehicle collisions is benefited by an understanding of the comparability of barrier impact and vehicle-to-vehicle collision. In particular, the relationship between Delta-v and barrier equivalent velocity, BEV, is sought in a form most readily useful to accident reconstruction. In general the vehicle Delta-v is not equal to BEV except in instances where the masses and stiffnesses of the impacting vehicles have a specific relationship. BEV can be used as an energy comparison and is not the speed change felt by an occupant in vehicle. The barrier equivalent velocity can be calculated for each vehicle. This is accomplished by setting the barrier equivalent kinetic energy for each respective vehicle equal to the damage energy on the vehicle. BEV can also be calculated directly from the damage profile. It involves both magnitude and direction and is therefore a vector. BEV does not assume that the vehicle comes to rest and can take into account a final velocity of more than 0 km/h.

Definition of EBS (Equivalent Barrier Speed): EBS/ETS/BEV is defined as the speed in the case vehicle at which equal energy would be absorbed in a frontal energy impact into a test barrier without bouncing back i.e. an estimation of the velocity change at impact that would be required of a crash test if it were to re-create the same amount of crush that occurred in the real crash with a vehicle of equal mass and stiffness.

8.5 Difference between EES and Delta-v

Accident reconstruction and injury mechanics in offset frontal collisions have to give special consideration to cases that involve massive glance off of the vehicles. For that case the difference between Delta-v and EES can be extremely high. In a collision without glance-off, such as a barrier impact with 100 % overlap, EES and Delta-v are of similar values. If glance-off occurs in an impact with only partial overlap, the EES can be considerably higher than the Delta-v, especially at high collision speeds. For an oncoming traffic accident whereby both vehicles will drive in the same direction they drove before the impact happened and glance-off occurs after the impact Delta-v will be lower than EES.

The following examples illustrations are intended to give an idea of the rather complicated relation between Delta-v and EES, as those values can differ more or less or in a special case even can be the same. To keep it simple the case of ideal impact is assumed, nay rebound is disregarded. From the physical viewpoint EES and Delta-v are different.

Reference: F. Zeidler: Die Bedeutung der Energy Equivalent Speed (EES) für die Unfallrekonstruktion und die Verletzungsmechanik; Daimler-Benz AG, Sindelfingen, Germany

Central impact against rigid obstacle: Delta-v equals EES	
	$V_1 = 50 \text{ kph}$ $EES = 50 \text{ kph}$ $\Delta V_1 = 50 \text{ kph}$
Impact of two similar vehicles at theoretical ideal impact configuration: Delta-v equals EES	
	$m_1 = m_2$ $v_1 = 80 \text{ kph}$ $v_2 = -20 \text{ kph}$ $EES_1 = 50 \text{ kph}$ $EES_2 = 50 \text{ kph}$ $\Delta V_1 = 50 \text{ kph}$ $\Delta V_2 = 50 \text{ kph}$
Example for the case of a vehicle/vehicle impact according to different stiffness properties	
	$M_1 = M_2$ $v_1 = 80 \text{ kph}$ $v_2 = 20 \text{ kph}$ $EES_1 = 25 \text{ kph}$ $EES_2 = 34 \text{ kph}$ $\Delta V_1 = 30 \text{ kph}$ $\Delta V_2 = 30 \text{ kph}$

Tab. 20: Examples for EES and Δv

8.6 Difference between BEV and Delta-v

Accident investigators have occasionally and mistakenly assumed that the magnitude of Delta-v during a vehicle collision is simply proportional to the post collision crush of the vehicle.

Reference: P. V. Hight, D. B. Lent-Koop: Barrier Equivalent Velocity, Delta-v and CRASH3 Stiffness in Automobile Collisions; Accident Research and Analysis, California; Southampton University, England; SAE Paper 850437

- Change of speed Delta-v during impact may not be the BEV speed.
- If the vehicle strikes a heavier vehicle but there is similar stiffness and similar magnitude of deformation then the Delta-v is greater than BEV.
- If the vehicle strikes a heavier vehicle with stiffness in proportion to weight and thus sustains less deformation than the vehicle then the Delta-v is the BEV.
- If the vehicle strikes a much stiffer vehicle but the damage to the stiffer vehicle is not available then as useful Delta-v auto range can be predicted. The Delta-v is less than BEV.
- Mathematically two similar vehicles closing at twice BEV should give the same BEV crush to each vehicle. In practice there is some intermeshing of the vehicles so crush distance is slightly greater with less rebound of the vehicles. The barrier impact is often more severe with a slightly greater speed change.
- When a vehicle strike another in excess of five times their weight, the exact weight ration is not important because closing speed and Delta-v approach BEV.

8.7 Coefficient of Restitution

As defined by Newton the impact can be divided into two phases: „compression“ and „restitution“ phase. For a full impact at the end of the compression phase the velocities of both vehicles at the impulse point are identical. Due to elasticity of the vehicle structure, the two vehicles will separate again. The coefficient of the restitution is defined as ratio between restitution and compression impulse.

The identification of coefficients of restitution in vehicle to vehicle collisions is impractical since each vehicle to vehicle combination has its unique restitutive response. Vehicle to barrier coefficients of restitution can be measured for specific vehicles. Coefficients of restitution between two vehicles for which the vehicle to barrier coefficients of restitution are known may be predicted.

Expressed in a more useful and more common form, the coefficient of restitution, ϵ , is the ratio of the post-impact separating velocity of the colliding bodies to their pre-impact closing velocity. The coefficient of restitution varies from zero for a perfectly plastic impact to unity for a perfectly elastic collision, and has been shown to depend upon the impact velocity and the shape and size of the colliding bodies. The coefficient of restitution lies in the range between 0.1 and 0.3 in real vehicle to vehicle collisions. Bumper-to-bumper collisions at low closing velocity are primarily elastic. The bumpers deform to some degree during impact and then rebound to nearly their pre-impact condition, coefficient of restitution values higher than 0.3. Generally,

the higher the residual deformations of the vehicles the lower the coefficient of restitution.

The impact could be divided into two phases which already has been described above:

Phase of compression: impact force increases until an equal velocity of both vehicles will be reached.

Mathematical description of conservation of linear momentum during the phase of compression:

$$S_C = \int_{t_1}^{t_2} F_C(t) \cdot dt \quad 8-8$$

Phase of restitution: impact force decreases and the velocity of the vehicles are different.

Mathematical description of conservation of linear momentum during the phase of restitution:

$$S_R = \int_{t_2}^{t_3} F_R(t) \cdot dt \quad 8-9$$

Time step t_1 to t_2 is for the compression phase and t_2 to t_3 for the restitution phase.

$$\varepsilon = \frac{S_R}{S_C} \quad \text{with} \quad 0 \leq \varepsilon \leq 1 \quad 8-10$$

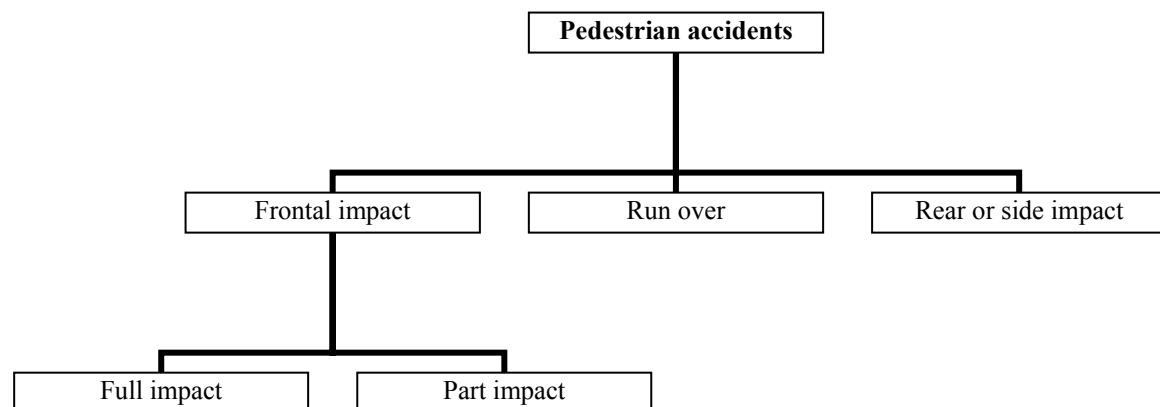
For vehicle frontal impacts against a rigid barrier ε depends on impact velocity only. In case of low velocities ε is almost elastic and for high velocities ε is almost plastic.

$$\varepsilon = \frac{v_{2f} - v_{1f}}{v_{1i} - v_{2i}} \quad 8-11$$

v represents the velocity of the vehicles and the indices 1 and 2 represents vehicle one and vehicle two whereby index i is for the initial velocity and index f for the final velocity. $v_{2f} - v_{1f}$ represents the relative separating velocity of the two bodies after impact, and $v_{1i} - v_{2i}$ their relative closing velocity before impact.

9. Pedestrian accidents

In many accident situations where pedestrians are involved, no good scene data is available, but the injuries of the pedestrians as well as the contact locations on the car are known. If there are skid marks, interferences in skid marks or marks from shoes or clothes of pedestrians the point of collision can be reconstructed. Especially shoes develop marks on the pavement. The start of abrasion marks of shoes is more or less equal with the point of contact with the vehicle and the point of collision.



For a full frontal impact the pedestrian will be hit with the front area of the vehicle and will be brought up closely to vehicle velocity. The impact direction is more or less the direction of vehicle movement. In case of a part frontal impact the pedestrian will be hit by the frontal area of the vehicle but won't be thrown forwards. The movement of the pedestrian is more alongside the vehicle. Most of run over accidents are fatalities. Rear impacts happen when a vehicle moves rearwards out of a parking lot.

When a car hits a pedestrian the movement of the pedestrian due to the impact can be divided into three phases:

- Contact phase
- Flight phase
- Sliding phase (ground contact phase)

Contact phase

The first phase is the contact phase, where one or more bodies of the pedestrian have contact with the vehicle and the pedestrian is accelerated. High contact forces can be seen during this phase.

Flight phase

Depending on the deceleration of the vehicle the pedestrian separates from the car after the contact phase and travels through the air without any contacts neither with the car nor with the ground.

Sliding phase

As a result of gravity the pedestrian has ground contact after the flight phase, depending on the pedestrian to ground friction the velocity of the pedestrian is reduced until the pedestrian reaches its final stop position.

The six different most common vehicle shapes are shown below:

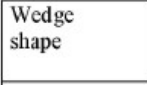
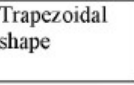

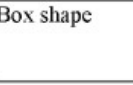



Wedge shape	Trapezoidal shape	Pontoon	Box shape	Bonnet height	Bonnet angle	Front angle
				≤ 0.7m	≤ 20°	
					≤ 20°	≤ 70°
					> 20°	≤ 70°
				Front vehicle edge R > 0.25m		
						>70°
				Upright contact plane		

Fig. 61 Geometrical front shape classifications (DIN 75204) and enhanced by DEKRA

The shape of the front hood of a car hitting a pedestrian has a major influence on the post impact movement of the pedestrian. The slope of the contact plane on the car influences the projection angle of the pedestrian and therefore the total trajectory of the pedestrian.

Estimate the throwing distances using throwing range approach of Stcherbatcheff/Kühnel/Rau for deceleration of 8m/s² in frontal impacts:

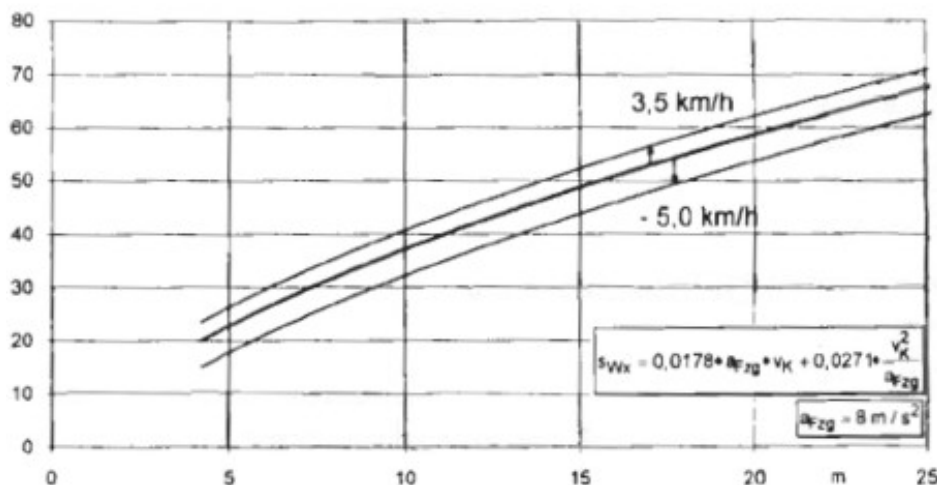


Fig. 62: Throwing range approach of Stcherbatcheff/Kühnel/Rau

The horizontal axis shows the throwing distances and the vertical axis the velocity of the vehicle. An assumption was made that the vehicle has a deceleration of 8 [m/s²].

10. References

Books and Papers:

- J. Lenard & B. Hurley, The assessment of vehicle impact severity in CCIS, Loughborough University, 1999
- M. S. Reveley D. R. Brown: A Comparison Study of Skid and Yaw Marks; S.E.A. Inc. Columbus, OH; SAE Paper 890635
- R. R. Hegmon: Tire-Pavement Interaction; Federal Highway Administration Office of Research, Development and Technology; SAE Paper 870241
- D. P. Martin, G. G. Schaefer: Tire-Road Friction in Winter Conditions for Accident Reconstruction; MDE Engineers Inc.; SAE Paper 960657
- F. Zeidler: Die Bedeutung der Energy Equivalent Speed (EES) für die Unfallrekonstruktion und die Verletzungsmechanik; Daimler-Benz AG, Sindelfingen, Germany
- C. Y. Warner, G. C. Smith, M. B. James, G. J. Gemane: Friction Applications in Accident Reconstruction; Collision Safety Engineering Inc., Orem, UT; SAE Paper 830612
- F. Zeidler, H.-H. Schreier, R. Stadelmann: Accident Research and Accident Reconstruction by the EES-Accident Reconstruction Method; Daimler-Benz AG, Sindelfingen, Germany; SAE Paper 850256
- E. L. Robinson: Derivation of Closing Speed as a Function of Dissipated Energy; Robinson & Associates, L.L.C.; SAE Paper 2000-01-1318
- Collision Deformation Classification – SAE J224 MAR80
- J. Lenard, R. Frampton, P. Thomas: The Influence of European Air Bags On Crash Injury Outcomes; Vehicle Safety Research Centre, Loughborough University, United Kingdom; NHTSA Paper Number 98-S5-O-01
- J. Lenard, B. Hurley, P. Thomas: The Accuracy of CRASH3 for calculating collision severity in modern European cars; Vehicle Safety Research Centre, Loughborough University, United Kingdom; NHTSA Paper Number 98-S6-O-08
- A. Morris, Brian Fildes: Preliminary Experience of Passenger Airbag Deployments in Australia; Accident Research Centre Monash University, Australia; NHTSA Paper Number 98-S5-W-17
- A. L. Turner: A Review of crash severity assessment programs applied to retrospective real-world accident studies; Transport Research Laboratory, United Kingdom; NHTSA Paper Number 98-06-O-09

- C. Riviere, T. Mara, Y. Page, L. Adelard, J.C. Gatina, J.Y. Lecoz: Estimating the Energy Equivalent Speed with an Artificial Neuronal Network,
- H. Steffan, B. C. Geigl, A. Moser, H. Hoschopf: Comparison of 10 to 100 km/h rigid barrier impacts; Graz University of Technology, Institute for Mechanics and Mechanisms, Austria, NHTSA Paper Number 98-S3-P-12
- H. Appel, G. Krabbel: Unfallforschung, Unfallmechanik und Unfallrekonstruktion; Verlag Information Ambs GmbH, Kippenheim; 1. Auflage 1994
- N. J. Carpenter, J. B. Welcher: Stiffness and Crush Energy Analysis for Vehicle Collisions and its Relationship to Barrier Equivalent Velocity (BEV); Biomechanical Research & Testing, LLC; SAE Paper 2001-01-0500
- J. A. Neptune, J. E. Flynn, P. A. Chavez, H. W. Underwood; Speed from Skids: A Modern Approach; J2 Engineering, Inc.; SAE Paper 950354
- M. S. Reveley, D. R. Brown, D. A. Guenther: A Comparison Study of Skid and Yaw Marks; S.E.A., Inc., The Ohio State Univ. Columbus, OH; SAE Paper 890635
- M. D. Pepe, J. S. Sobek, D. A. Zimmerman: Accuracy of Three-Dimensional Photogrammetry as Established by Controlled Field Tests; Wolf Technical Services Inc.; SAE Paper 930662
- W. E. Cliff, D. D. MacInnis, D. A. Switzer: An Evaluation of Rectified Bitmap 2D Photogrammetry with PC-Rect; MacInnis Engineering Associates; SAE Paper 970952
- P. V. Hight, D. B. Lent-Koop: Barrier Equivalent Velocity, Delta-V and CRASH3 Stiffness in Automobile Collisions; Accident Research and Analysis, California; Southampton University, England; SAE Paper 850437
- H. Burg, H. Rau: Handbuch der Verkehrsunfallrekonstruktion; Verlag Information Ambs GmbH, Kippenheim
- M. Lamby: Definition der kollisionsbedingten Geschwindigkeitsänderung Δv ; Am Stollhenn 21, 6500 Mainz, Germany; Verkehrsunfall und Fahrzeugtechnik September 1999, Heft 9
- M. Gröth: Spuren im Zusammenhang mit Verkehrsunfällen; 5428 Nastätten, Germany; Verkehrsunfall und Fahrzeugtechnik Dezember 1992, Heft 12
- H. Steffan: Vorlesungsskriptum Unfallmechanik im Verkehrswesen; 8010 Graz, Austria; Institut für Mechanik
- W. Hirschberg: Vorlesungsskriptum Kraftfahrzeugtechnik; 8010 Graz, Austria; Institut für Fahrzeugtechnik
- PC-Rect 3.0 User Manual, DSD Linz, Austria
- CCIS Report

Arai, Y., et al. (2001). Accidents and Near-Misses Analysis by Using Video Drive-Recorders in a Fleet Test. Paper 01-S4-O-225, ESV Conference, 2001.

ArcSim user Reference Manual (July 1997).

Brach, R.M. (1994). Uncertainty in Accident Reconstruction Calculations. SAE940722.

Cammica, M.X., et al. (2000). Driver Fatalities in Frontal Crashes of Airbag-Equipped Vehicles: A review of 1989-96 NASS cases.

Cliff, W.E., Montgomery, D.T. (1996). Validation of PC Crash – A Momentum-Base Accident Reconstruction Methods for Car-to-Car Accidents; as Confirmed by Crash Tests. SAE 960885

Day, T.D. (1999). An Overview of the EDSMAC4 Collision Simulation Model. SAE 1999-01-0102.

Day, T.D. (1999a). Difference between EDVDS and Phase 4. SAE 1999-01-0103.

European Accident Causation Survey, Volumes 3 & 5, France, 2002.

Fiala, E (1954). Lateral Forces on Rolling Pneumatic Tires, Zeitschrift V.D.I., 96, No. 29, 1954.

Fittato, D.A., Ruhl, R.A., Southcombe E.J., Burg, H., Burg, J. (2002). Overview of CARAT-4, a Multi body Simulation and Collision Modeling Program.

Friedman, D & Friedman, K. (1998). Roof Crush Versus Occupant Injury From 1988 to 1992 NASS.

Gabler, H.C., Hampton, C., Roston T.A. (2003). Estimating Crash Severity: Can Event Data Recorders Replace Crash Reconstruction? Paper No. 490, ESV Conference, 2003.

Geigl, B.C., et al. (2001). Reconstruction of Occupant Kinematics and Kinetics for Real World Accident. Linz, Austria.

Gillespie, T.D., Sayers, M.W. (1999). A Multi-body Approach with Graphical User Interface for Simulating Truck Dynamics. SAE Paper 1999-01-3705.

Harrison, H.R. & Nettleton, T. (1978). Principles of Engineering Mechanics, UK, 1978.

HVE User's Manual, Version I, Engineering Dynamics Corporation, Beaverton OR, February, 1996.

Lenard, J., et al. (2000). The Statistical Accuracy of Delta-V in Systematic Field Accident Studies. SAE 2000.

Leonard, M.M., et al. (2000). HVE EDSMAC4 Trailer Model Simulation Comparison with Crash Test Data. SAE 2000-01-0468.

Lewis, P.R. et al. (1996). A NASS-Based Investigation of Pelvic Injury within the Motor Vehicle Crash Environment. SAE 962419.

MADYMO Theory Manual, Version 6.0, TNO Automotive, Delft, The Netherlands, 2001.

MAIDS Reconstruction Guidelines. Reference: 2MAI/000719-0/TA2, 2000.

McHenry, B.G., McHenry, R.R. (2003). SMAC2003: The Automotive Iteration of SMAC. SAE 2003-01-0486.

Mooi, H.G. & Vries, Y.W.R. de (2002). Diepgaande analyse van 12 tramongevallen. Report 02.OR.BV.062.1.HGM, TNO Automotive, Delft, The Netherlands.

Morsink, P.L.J. (2001). Multi-body space-frame modelling for crash simulation: a methodology description. Report 00.OR.BV.062.2/PM, TNO Automotive, Delft, The Netherlands.

Moser, A., et al. (1999). The Pedestrian Model in PC-Crash – The Introduction of a Multi Body System and its Validation. SAE 1999-01-0445.

OECD, (2001). "Motorcycles: Common international methodology for in-depth accident investigations"

PC-Crash Manual, Version 6.0, DSD, Linz, Austria, 1999.

Ross, R. (1997). Review of existing in-depth studies. STAIRS-Work Package 1.i, 1997.

Schieschke, R., Hiemenz, R. The Relevance of Tire Dynamics in Vehicle Simulations.

Spit, H.H. (2000). Evaluation of PC-Crash: as a tool for professional traffic accident research and reconstruction. Report 00.OR.BV.2712.1/HHS, TNO Automotive, Delft, The Netherlands.

Steffan, H., et al. (1999). A New Approach to Occupant Simulation through the Coupling of PC-Crash and MADYMO. SAE 1999-01-0444.

Stucki, S.L., Fessahale, O., (1998). Comparison of Measured Velocity Change in Frontal Crash Tests to NASS Computed Velocity Change. SAE 980649.

Thomas, P. & Frampton, R. (2003). Crash testing for real -world safety-. What are the priorities for casualty reduction? ESV conference, paper No 351, U.K.

- Vries, Y.W.R. de, Margarits, D., Mooi, H.G. (2003). Moped and mofa accidents in The Netherlands from 1999-2001: Accident and injury causation. ESV Conference, Paper No. 348, Delft.
- Vries, Y.W.R. de & Mooi, H.G. (2001). The analysis of Dutch national data on heavy truck accidents: The necessary extension of traditional frequency counts with logistic regression analysis. ESV Conference, Paper No. 153, Delft
- Wismans, J.S.H.M. et al. (2002). 'Injury biomechanics', lecture notes from The Technical University Eindhoven, The Netherlands.
- Yerazunis, W.S., et al. (1999). An Inexpensive, All Solid-state Video and Data Recorder for Accident Reconstruction. SAE 1999-01-1299.
- Zweep, C.D. van der, et al. (2003). Numerical fleet studies 2002-2003. Report 03.OR.BV.067.1/CVDZ, TNO Automotive, Delft, The Netherlands.
- W. E. Cliff, D. D. MacInnis, D. A. Switzer: An Evaluation of Rectified Bitmap 2D Photogrammetry with PC-Rect; MacInnis Engineering Associates; SAE Paper 970952
- L. Hoffmeister: Vergleichende Untersuchung zur Genauigkeit verschiedener Verfahren zur Vermessung von Straßenverläufen für die Unfallrekonstruktion; Fachhochschule Köln, University of Applied Sciences Cologne
- D. A. Switzer T. M. Candrljic: Factors Affecting the Accuracy of Non-Metric Analytical 3-D Photogrammetry, Using PhotoModeler; SAMAC Engineering, Ltd.; SAE Paper 1999-01-0451
- R. D. Robinette, R. J. Fay, R. E. Paulson: Delta-V: Basic concepts, computational methods and misunderstandings; Fay Engineering Corp.; SAE Paper 940915
- V. W. Antonetti: Estimating the Coefficient of Restitution of Vehicle-to-Vehicle Bumper; Impacts Amatech Review; SAE Paper 980552
- R. Ross, J. Lenard, B. Hurley, P. Thomas, D. Otte, G. Vallet: Crash severity calculations- Theory and Practice; STAIRS - Work Package 1.iv, Version 5; 1998
- K. Engels: Die Bedeutung des Spurzeichenverhaltens von PKW mit ABV für die Unfallrekonstruktion; Der Verkehrsunfall Heft 2, Februar 1990
- J. Ahlgrimm, J. Grandel: Verkehrsunfallaufnahme bei Fahrzeugen mit Anti-Blockier-System (ABS); Der Verkehrsunfall Heft 5, Mai 1997
- M. Göth: Spuren in Zusammenhang mit Verkehrsunfällen, Der Verkehrsunfall Heft 12, Dezember 1992
- A. Moser, H. Hoschopf, H. Steffan, G. Kasanicky: Validation of the PC-Crash Pedestrian Model; DSD Linz and USI-šilina; SAE Paper 2000-01-0847

K. Kompaß, M. Witte: Die BMW Sitzbelegungserkennung, Der Verkehrsunfall Heft 2, Februar 1996

J. Dettinger: Beitrag zur Verfeinerung der Rekonstruktion von Fußgängerunfällen; Der Verkehrsunfall Heft 1, Januar 1997

J. Dettinger: Beitrag zur Verfeinerung der Rekonstruktion von Fußgängerunfällen; Der Verkehrsunfall Heft 12, Dezember 1996

W. Pfeffer: Die Speicherung von Kollisionsdaten im Airbag-Steuergerät; Der Verkehrsunfall Heft 7/8, Juli/August 2000

W. E. Cliff, A. Moser: Reconstruction of Twenty Staged Collisions with PC-Crash's Optimizer; MacInnis Engineering Associates (MEA), Dr. Steffan Datentechnik (DSD); SAE Paper 2001-01-0507

B. Richter, H. Appel, R. Hoefs, K. Langwieder: Entwicklung von PKW im Hinblick auf einen volkswirtschaftlichen optimalen Insassenschutz. Abschlussbericht zum Forschungsprojekt TV 8036 im Auftrag des Bundesminister für Forschung und Technologie (BMFT)

Danner, M./ Halm, J., Technische Analyse von Verkehrsunfällen, 1994

Internet sites

www.aiexperts.com

<http://www.accident-report.org/>

<http://www.edccorp.com>

<http://www.mchenrysoftware.com>

<http://www.vsre.co.uk>

<http://www.ukots.org>

www.etrto.org/ (24.03.2004)

<http://www.aiexperts.com/> (21.04.2004)

<http://www.phocad.de/> (27.04.2004)

<http://www.bentley.com> (27.04.2004)

<http://www.trimble.com> (27.06.2004)

<http://home.comcast.net/~neburoker1/galileo-positioning-system.htm> (27.06.2004)

http://europa.eu.int/comm/dgs/energy_transport/galileo/index_en.htm (27.06.2004)

<http://www.nhtsa.dot.gov/cars/rules/rulings/UpgradeTire/Econ/TireUpgradeII.html>
(11.02.2004)

<http://www.fisita2004.com/programme/programme/F2004U121> (15.12.2003)

<http://www.jpcity.de/Verkehrsunfallaufnahme.htm> (01.03.2004)

George M. Bonnett: Understanding Delta V from Damage; <http://www.rec-tec.com/DeltaV.html> 16.12.2003

11. Appendix

Appendix A

Friction coefficient for different road surfaces

Description of road surface	dry below 48 km/h	dry above 48 km/h	wet below 48 km/h	wet above 48 km/h
PORTLAND CEMENT				
New, sharp	0.80 – 1.20	0.70 – 1.00	0.50 – 0.80	0.40 – 0.75
travelled	0.60 – 0.80	0.60 – 0.75	0.45 – 0.70	0.45 – 0.65
Traffic polished	0.55 – 0.75	0.50 – 0.65	0.45 – 0.65	0.45 – 0.60
ASPHALT, TAR				
New, sharp	0.80 – 1.20	0.65 – 1.00	0.50 – 0.80	0.45 – 0.75
travelled	0.60 – 0.80	0.55 – 0.70	0.45 – 0.70	0.40 – 0.65
Traffic polished	0.55 – 0.75	0.45 – 0.65	0.45 – 0.65	0.40 – 0.60
Excess tar	0.50 – 0.60	0.35 – 0.60	0.30 – 0.60	0.25 – 0.55
GRAVEL				
Packed, oiled	0.55 – 0.85	0.50 – 0.80	0.40 – 0.80	0.40 – 0.60
Loose	0.40 – 0.70	0.40 – 0.70	0.45 – 0.75	0.45 – 0.75
CINDERS				
packed	0.50 – 0.70	0.50 – 0.70	0.65 – 0.75	0.65 – 0.75
ROCK				
crushed	0.55 – 0.75	0.55 – 0.75	0.55 – 0.75	0.55 – 0.75
ICE				
Smooth	0.10 – 0.25	0.07 – 0.20	0.05 – 0.10	0.05 – 0.10
Snow				
packed	0.30 – 0.55	0.35 – 0.55	0.30 – 0.60	0.30 – 0.60
loose	0.10 – 0.25	0.10 – 0.20	0.30 – 0.60	0.30 – 0.60

Friction coefficient for different road surfaces; SAE 830612

Friction of automobile and truck tire

Description of road surface	Automobile tire	Truck tire
Dry concrete	0.85	0.65
Dry asphalt	0.80	0.60
Wet concrete	0.70 – 0.80	0.50
Wet asphalt	0.45 – 0.80	0.30
Packed snow	0.15	0.15
Ice	0.05	0.11 (dry) 0.07 (wet)
Dry dirt	0.65	
Mud	0.40 – 0.50	
Gravel or sand	0.55	
Wet, oily, smooth concrete		0.25
Hard-packed snow w/ chains		0.60
Dry ice w/ chains		0.25

Friction of automobile and truck tire; SAE 830612

Velocity decrement values

Velocity decrement values	
Indicated speed km/h (kph)	Percent reduction of friction coefficient [%]
64 (40)	3
80 (50)	7
97 (60)	9
113 (70)	11
129 (80)	14
145 (90)	18

Velocity decrement values; SAE 830612

Tire friction μ as a function of vehicle speed

$$\mu = \mu_0 - v \cdot V$$

	Dry peak	Dry sliding	Wet peak	Wet sliding
μ_0	0.95	0.85	0.75	0.70
v	0.0027	0.004	0.0053	0.0080

Tire friction μ as a function of vehicle speed

Tire/Surface Classification

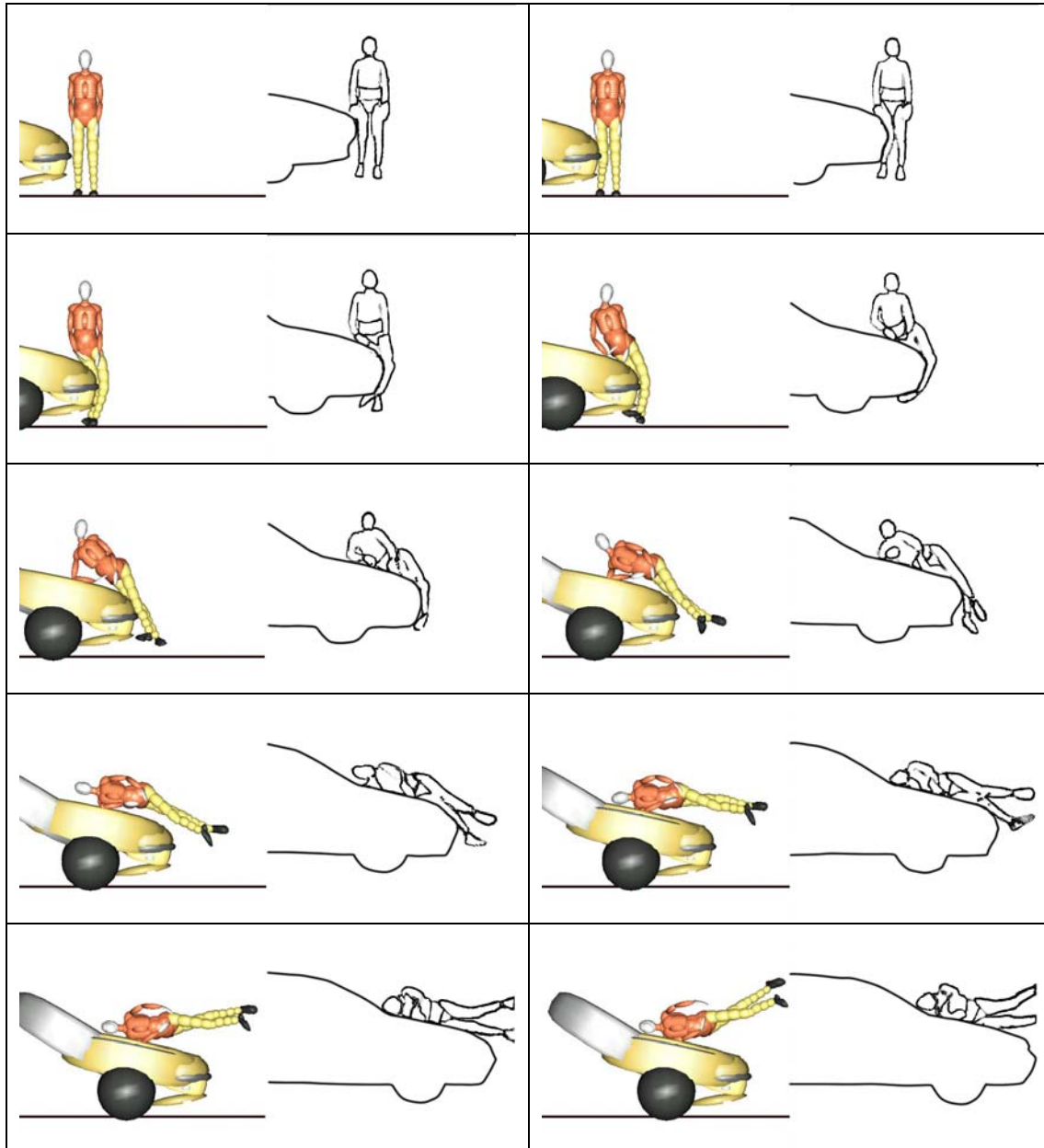
Tire/Surface Classification	Description (test temperature from –42 to –4°C)	Range of μ values**
Ice	A solid sheet of frozen water thick enough that it is not broken through by studs or chains. Looks like glass. When at the melting point will have a layer of water on it	0.054 – 0.19
Ice with studded snow tires	Ice as above with studded tires on the rear wheels with limited data for all wheels	0.092 – 0.16
Ice with steel tire chains	Ice as above with steel reinforced tire chains	0.12 – 0.18
Ice w/ low tire pressure	Ice as above with tire pressure of 83 to 221kPa	0.13 – 0.15
Thick black ice	A continuous layer of ice over asphalt or concrete which is difficult for the average driver to see. It is thick enough that it is not broken up by the sliding of locked tires.	0.12 – 0.26
Thin black ice	Icy layer generally covering the pavement and difficult for the average driver to see. It is thin enough that it is partly broken up when locked tires slide on it.	0.17 – 0.49
Snow and ice	A continuous layer of snow compacted to form an icy surface.	0.12 – 0.39
Snow and ice glazed at traffic light	Compact snow and ice at a traffic light where prior vehicles have sat with the warmth of the engines and moisture in the warm exhaust forming glare ice over the surface.	0.09 – 0.22
Snow ice with sand	Compact snow and ice with a spread of sand, almost gravel, particles 3 to 6 mm in diameter.	0.15 – 0.45
Snow and ice with sand in ruts	Compact snow and ice with worn ruts and rivulets with a spread 3 to 6 mm diameter sand which has migrated into the ruts. No exposed paving.	0.20 – 0.29
Snow and ice with an overlay of fresh snow	Compact snow and ice onto which has fallen a fresh layer of snow or frozen fog 3 to 100mm which has not been tracked.	0.18 – 0.45
Snow and ice with an overlay of old snow	Compact snow and ice onto which has accumulated a layer of rough, old crusty snow 100 to 200mm thick which has not been tracked	0.43 – 0.45
Snow and ice with 20% exposed ruts	Compact snow and ice which has been worn at the tire tracks to expose 20% of the asphalt paving in the ruts.	0.20
Tracked snow	Snow which fell onto bare pavement and compacted by vehicles, but not sufficient to be called snow and ice	0.24 – 0.37
Untracked snow	Fresh snow fallen onto bare pavement and not compacted by prior vehicles.	0.15 – 0.42
Deep untracked snow	Snow so deep that the vehicle is not supported on its tires	0.92 – 0.95
Heavy frost	Almost ice conditions. Heavy white coating and very visible to the driver	0.37 – 0.48
Frost	General white coating covering entire lane. Visible to the driver and completely recognizable as frost.	0.48 – 0.58
Partial frost	Light or partial coating of frost on the road surface. Visible to the driver as intermittent frosting appearance.	0.61 – 0.64
Bare	Completely bare dry asphalt road surface. Data taken to observe the effects of low temperature on the friction coefficient of tires on this commonly tested surface.	0.59 – 0.72

Tire/Surface Classification; SAE 960657

Appendix B

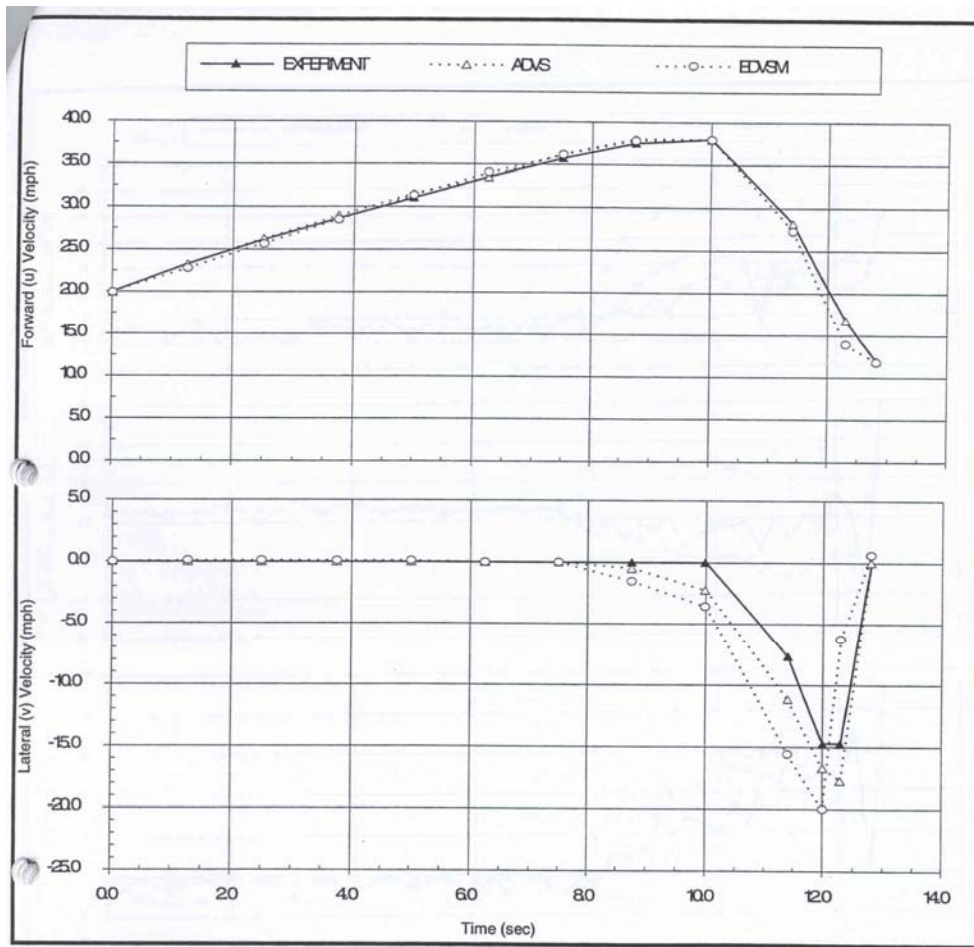
Reconstruction validation results

Pedestrian MADYMO model

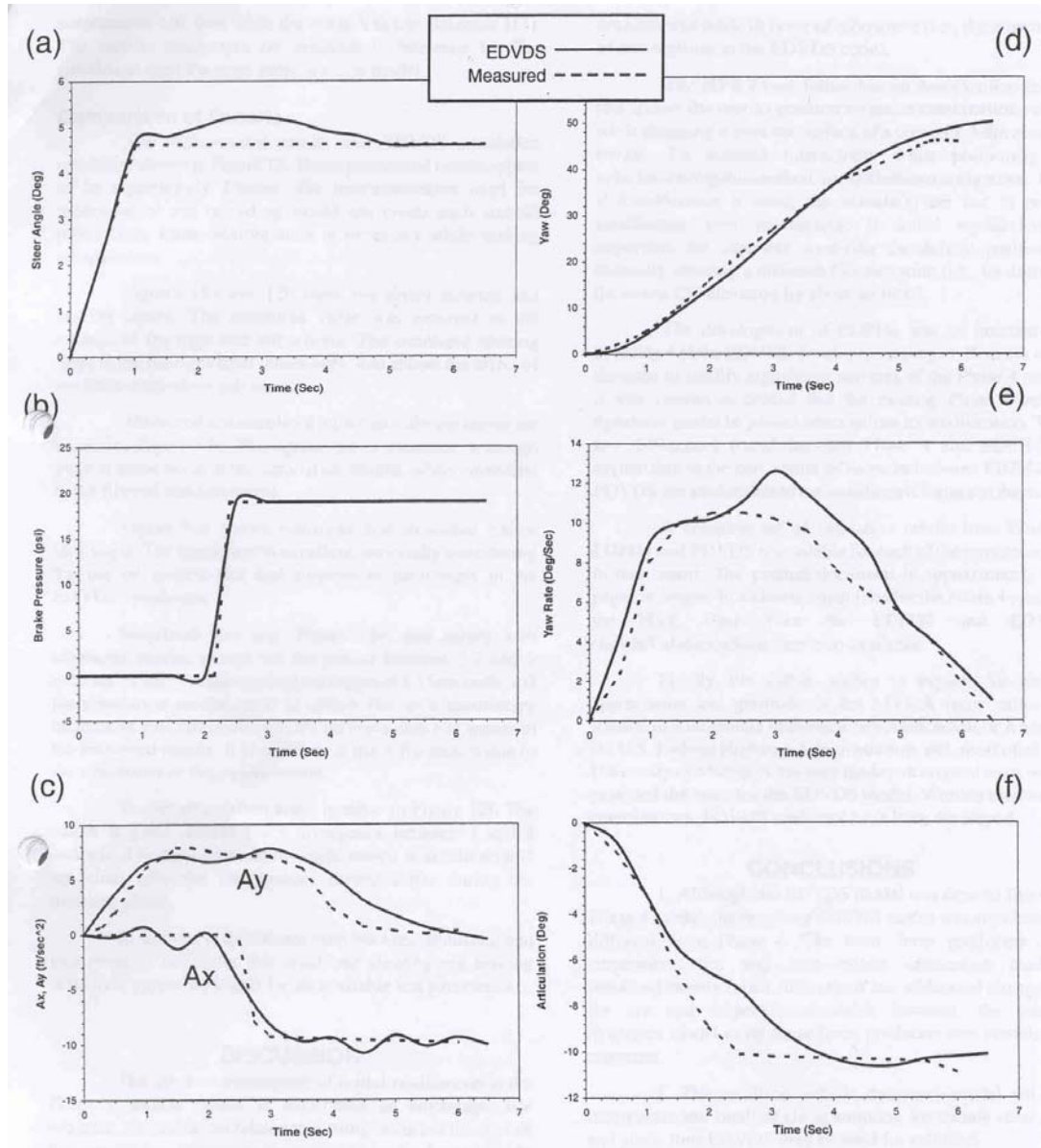


Comparison between the test (cadavers) and the simulations for kinematics of the pedestrian substitutes from 0 to 225 ms with time step $\Delta t = 25$ ms.

EDVSM



Comparison of EDVSM and test results for Forward and Lateral velocities

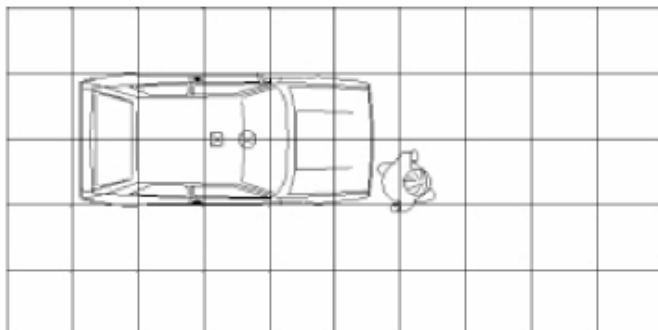


Comparison of Steering and Braking result

PC-Crash: Pedestrian model

Test configurations:

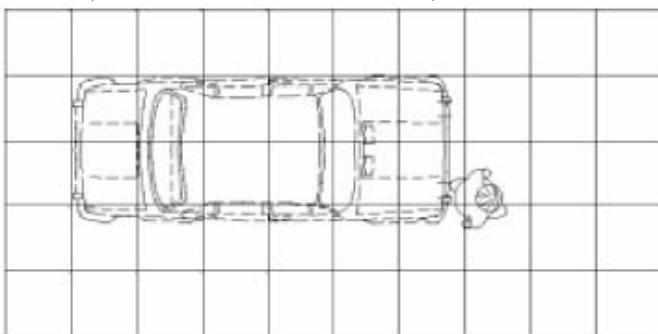
Test 1 (55 km/h VW Polo)



Impact configuration – test 1 (55 km/h VW Polo)

Vehicle	Volkswagen Polo
Mass	730 kg
Impact Speed	54,2 km/h
Dummy Mass	85 kg
Longitudinal Displacement	10,95 m
Lateral Displacement	03,50 m

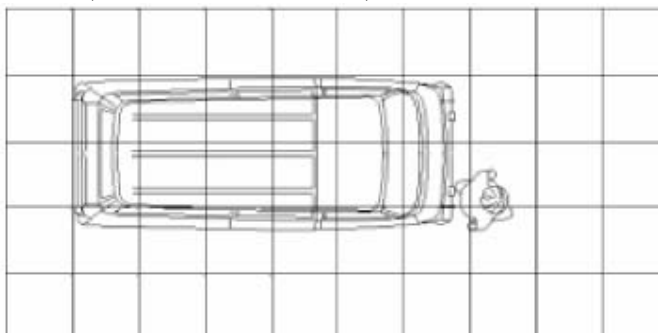
Test 2 (50 km/h Polski Fiat 125P)



Impact configuration - Test 2 (50 km/h Polski Fiat 125P)

Vehicle	Fiat 125p
Mass	1030 kg
Impact Speed	51,4 km/h
Dummy Mass	85 kg
Longitudinal Displacement	17,50 m
Lateral Displacement	03,20 m

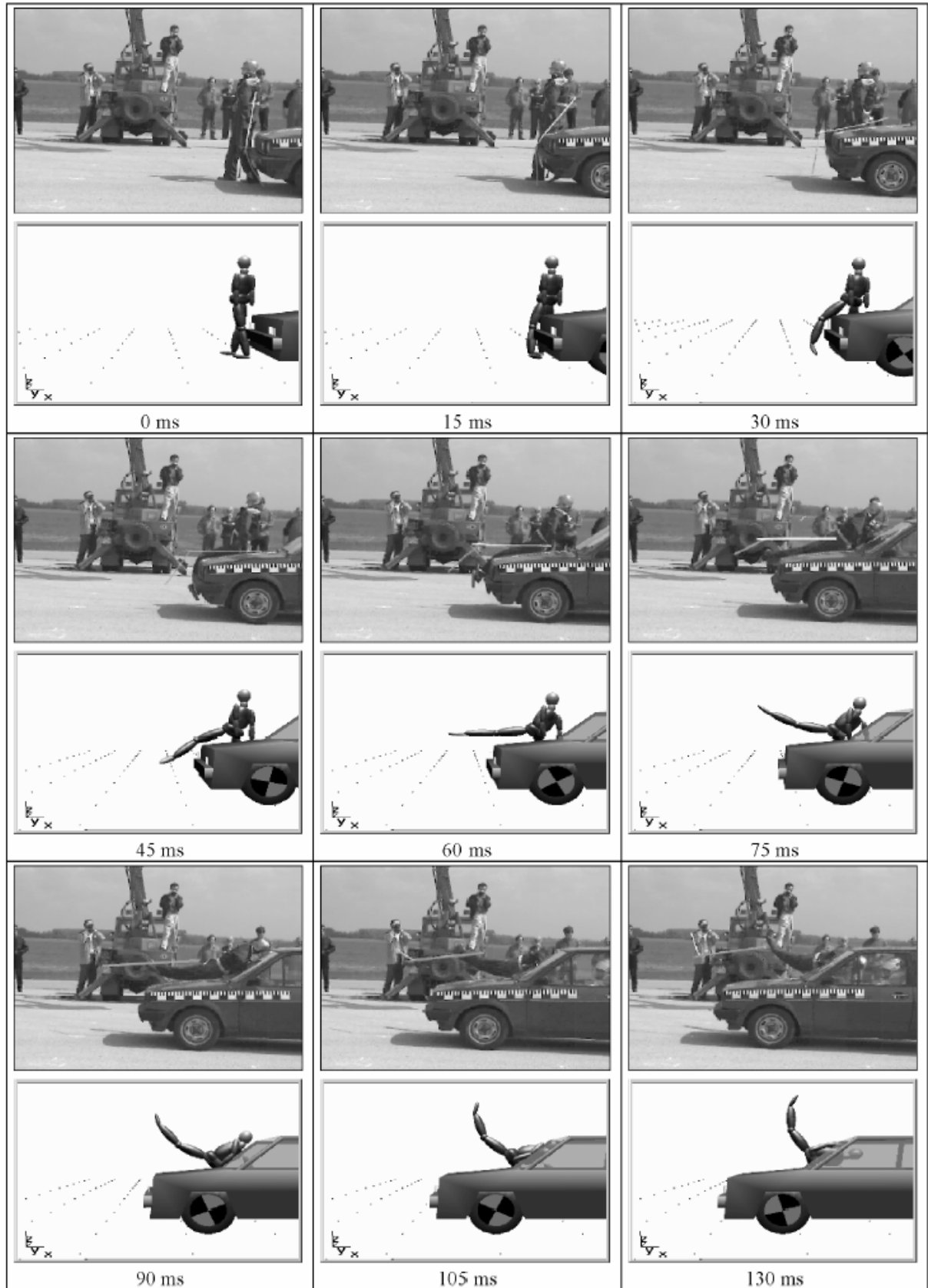
Test 3 (40 km/h Skoda 1203)

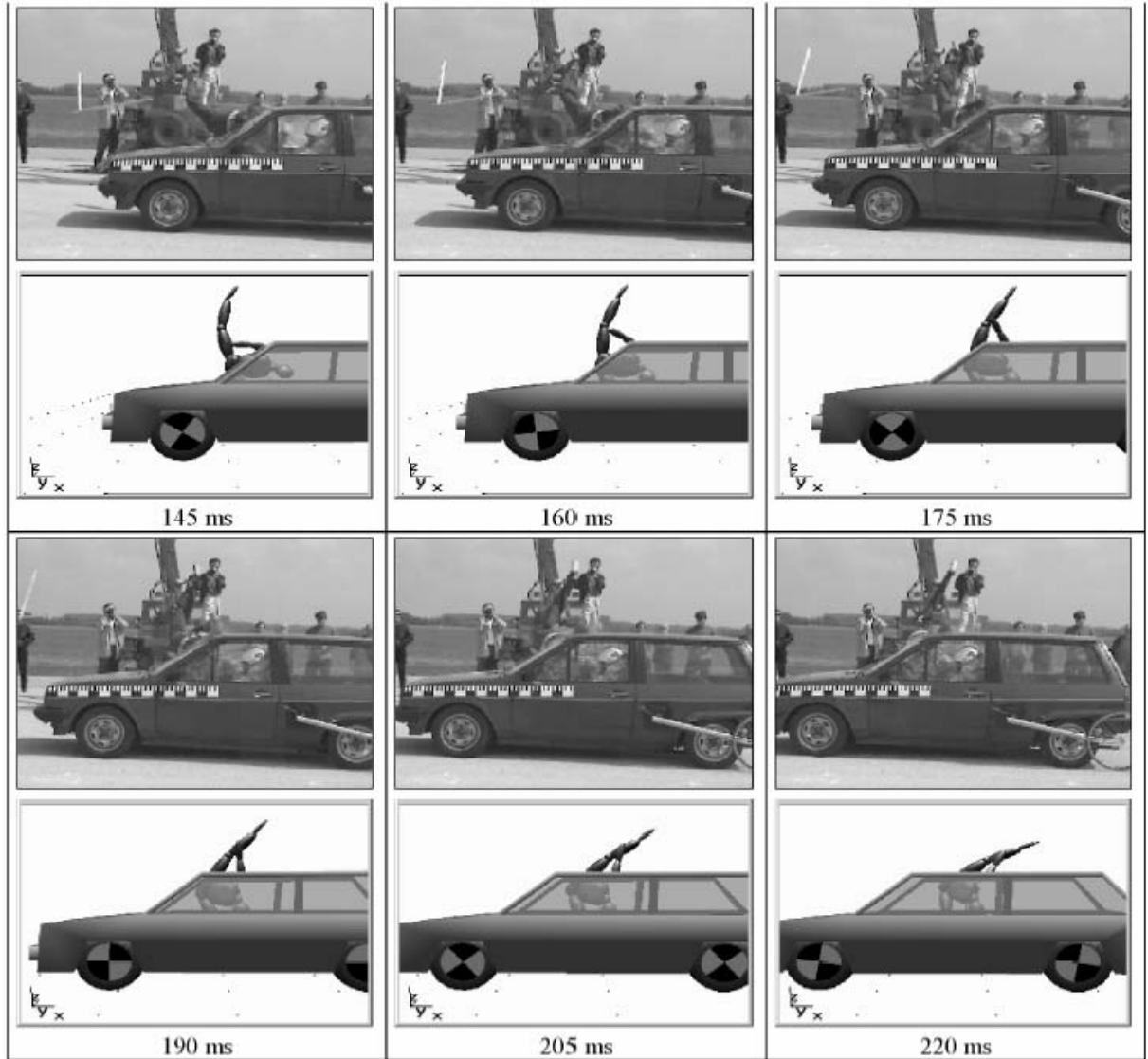


Impact configuration - Test 3 (40 km/h Skoda 1203)

Vehicle	Škoda 1203
Mass	1250 kg
Impact Speed	41,4 km/h
Dummy Mass	85 kg
Longitudinal Displacement	14,80 m
Lateral Displacement	03,00 m

Test 1 (55 km/h VW Polo)





Appendix C

Deformation Classification

Reference Sheet for CDC

Collision Deformation Classification (CDC)

Column 1&2 = Direction of Force

Column 3 = General Location

If rollover then code to area of greatest crush

Column 4&5 = Horizontal Location

If Front or Rear impact code along width.

R0 = 1/4 from right side, *excluding* longitudinal
 L0 = 1/4 from left side, *excluding* longitudinal
 R1 = 1/2 from right side
 L1 = 1/2 from left side
 C0 = Centre (engine width)
 Z1 = 1/4 from right side
 Y1 = 1/2 from left side
 Z0 = 1/2 from right side
 Y0 = 1/2 from left side
 D0 = Distributed across entire width

Side Impacts
 If Side impact gr. if Box 3 is coded T or U then code along length.
 F0 = Front compartment
 P0 = All of Passenger compartment
 P1 = Passenger Compartment - Front seat
 P2 = Passenger Compartment - Rear seat
 B0 = Rear compartment
 Y0 = Front and passenger compartment
 Y1 = Front compartment and front seat
 Z0 = Rear and passenger compartment
 Z1 = Rear compartment and rear seat
 D0 = Distributed across entire side

Column 6 = Vertical Location

A = all
 G = belt line & above
 H = above longitudinal to top of vehicle
 M = above longitudinal to belt line
 E = everything below belt line
 L = longitudinal and below (including undercarriage)
 W = wheels & tyres only

If box 3 is coded T or U then code across width

Column 7 = Damage Pattern

A = Gross Underrun (2 step)
 O = Rollover
 N = Narrow <41cm not including a corner
 E = Narrow <41 including a corner
 W = Wide >41cm
 S = Side or end Swipe (10cm or less)

Column 8 = Crush Extent

saloon rear crush

upright hatchback rear crush

sloping hatch rear crush

Rear Crush Zones:
 saloons = 9 equal zones over boot to base of rear window
 zone 6 is upto top of rear window
 zones 7 and 8 upto mid B pillar
 upright = zone 1 is upto base of rear window
 hatches = zone 2 is upto top of rear window;
 8 = side 8 = vans then 6 equal zones to mid B pillar
 sloping = 6 equal zones upto top of rear window
 hatches = zones 7 and 8 upto mid B pillar
 pick-ups = 8 equal zones upto mid B pillar

5 equal zones 2 equal

Reference Sheet for CDC

Appendix D

Passenger Compartment Classification (PDC)

A coding system for the passenger’s compartment will be described in this section. The code consists of eight digits or letters like the CDC code consists of. The STAIRS protocol separates the car interior into eight sections with the height level A, B, C. For the PDC Code the areas are split into more sections using the CDC Coding system as well. STAIRS developed an intrusion matrix for the passenger’s compartment but there was no coding system made. This three dimensional intrusion matrix will be the basis for the PDC.

Currently the PDC is developed as an own code but there shouldn’t be a problem to add this to the CDC code in the case of using most of the CDC parameter already.



PDC 1&2 - Direction of Force (DoF)



The first two digits are made up for the direction of force. Similar to the collision deformation classification (CDC) and it is only necessary to adopt the direction in the passenger’s compartment classification.

PDC 3 – Direction of Intrusion



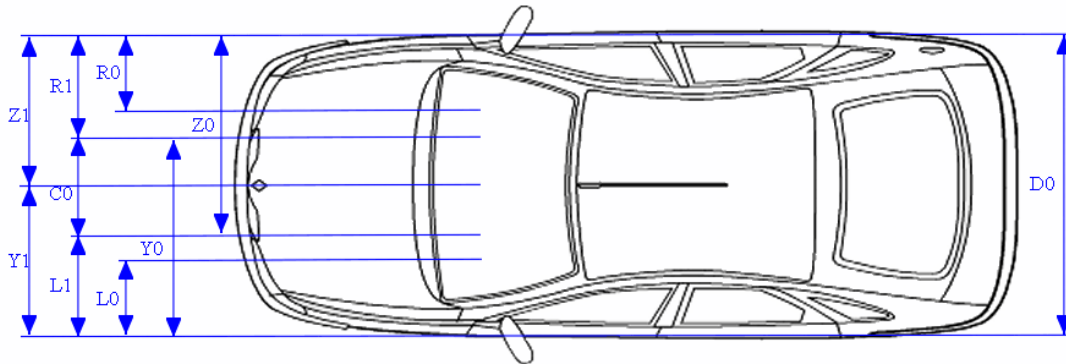
Intrusion Code	Intrusion description
B	For intrusion from rear end (back)
F	For intrusion from the front
L	For intrusion from left side
R	For intrusion from right side
T	For intrusion from the top (roof)
X	Non-classifiable

Direction of Intrusion

PDC 4&5 – Horizontal Location transversal



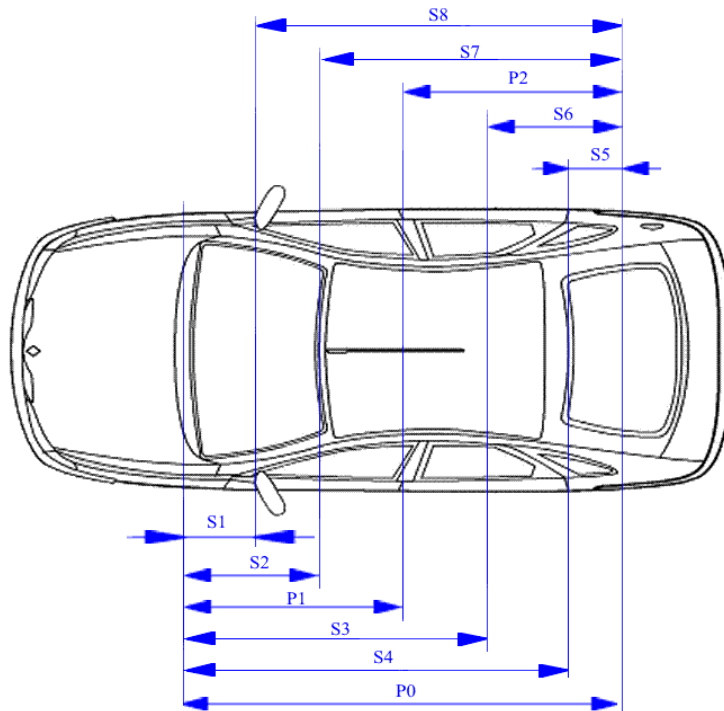
Based on the STAIRS protocol it is only possible to code the intrusion to the left or the right side of the vehicle and there are three coding possibilities to the height (*A - Windscreen, B - Dashboard, C - Footwell*).



PDC 4&5 – Horizontal Location transversal

According to the coordinate system this location would be measured in the transversal of the car.

PDC 6&7 – Lateral location



PDC 6&7 – Horizontal location lateral

The 6th and 7th columns are made of a letter and a number. According to the STAIRS protocol and SAE J224 MAR 80 paper the vehicle is split in eleven sections. P₀, P₁, P₂ are taken over from the existing CDC coding system.

Lateral Code	Lateral location description
P ₀	All of passengers compartment
P ₁	Passenger compartment – front seat; Footwell to B-pillar
P ₂	Passenger compartment – rear seat; Cell line to B-pillar
S ₁	Footwell to A-pillar
S ₂	Footwell to top of windscreen
S ₃	Footwell to mid of rear door
S ₄	Footwell to C-pillar
S ₅	Cell line to C-pillar
S ₆	Cell line to mid of rear door
S ₇	Cell line to top of windscreen
S ₈	Cell line to A-pillar

Lateral location description

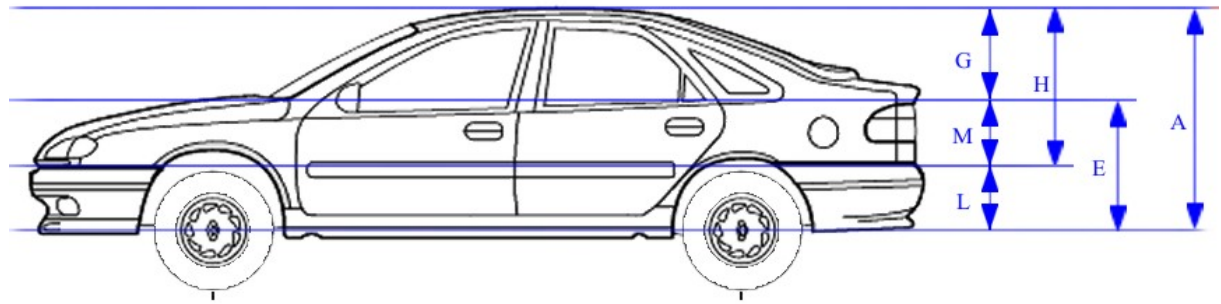
PDC 8 – Vertical Location



Finally the vertical location of the crush will be coded with letters. The letters A, B, C were introduced and developed for the intrusion matrix in the STAIRS protocol. With those three letters it is possible to describe the vertical deformation location. The vertical location will be coded with “A”, “E”, “G”, “H”, “L”, “M”. Characters “A”, “E” and “H” are combinations from “L”, “M” and “G”.

$$H = G + M$$

$$E = L + M$$

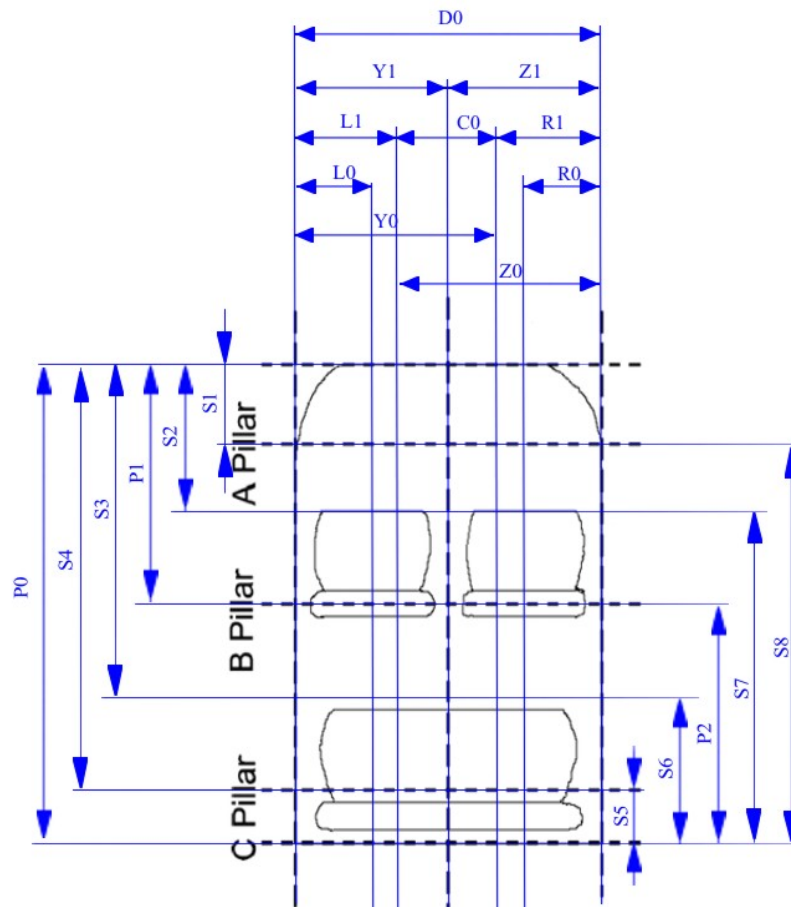


PDC 8 – Vertical Location

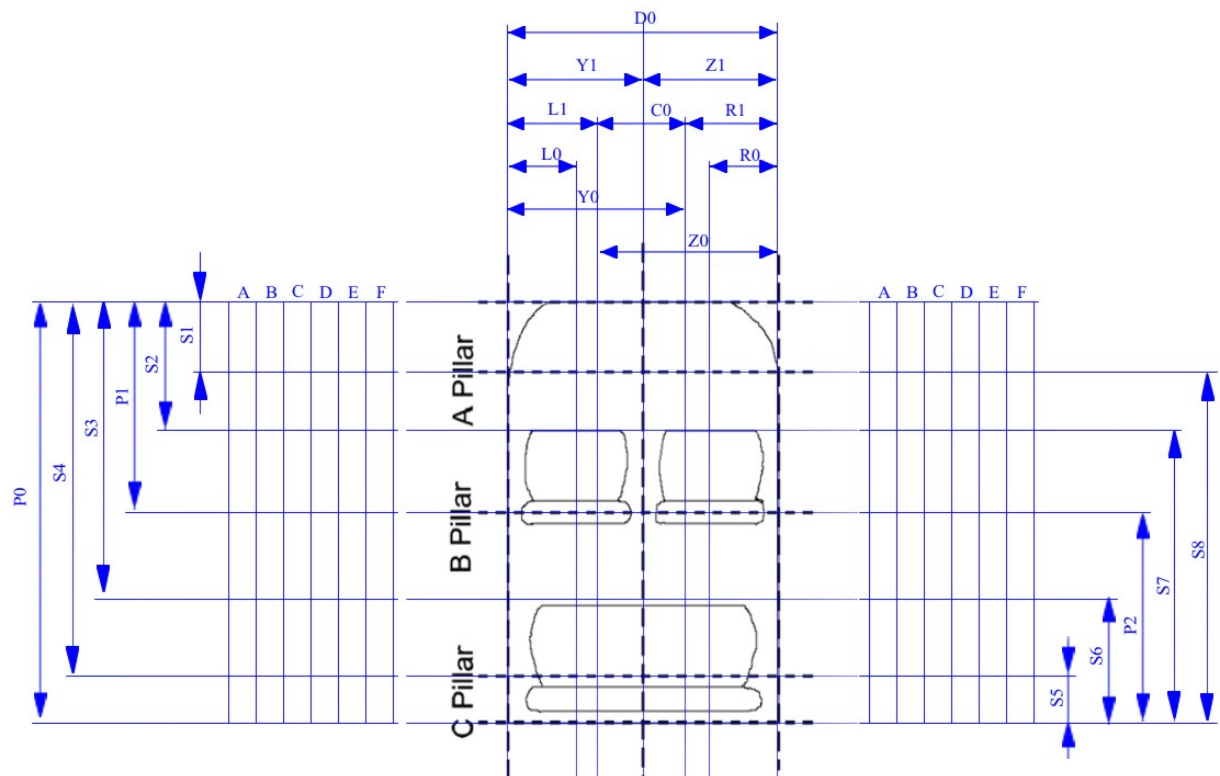
Vertical location of the direct contact damage
G = Glass Level & Above
M = Middle Section Only
L = Lower Section Only
W = Wheel/s only
E = Middle & Lower Level
H = Middle & Glass Level
A = All Three Levels

Vertical location of the direct contact damage

Passengers compartment intrusion matrix

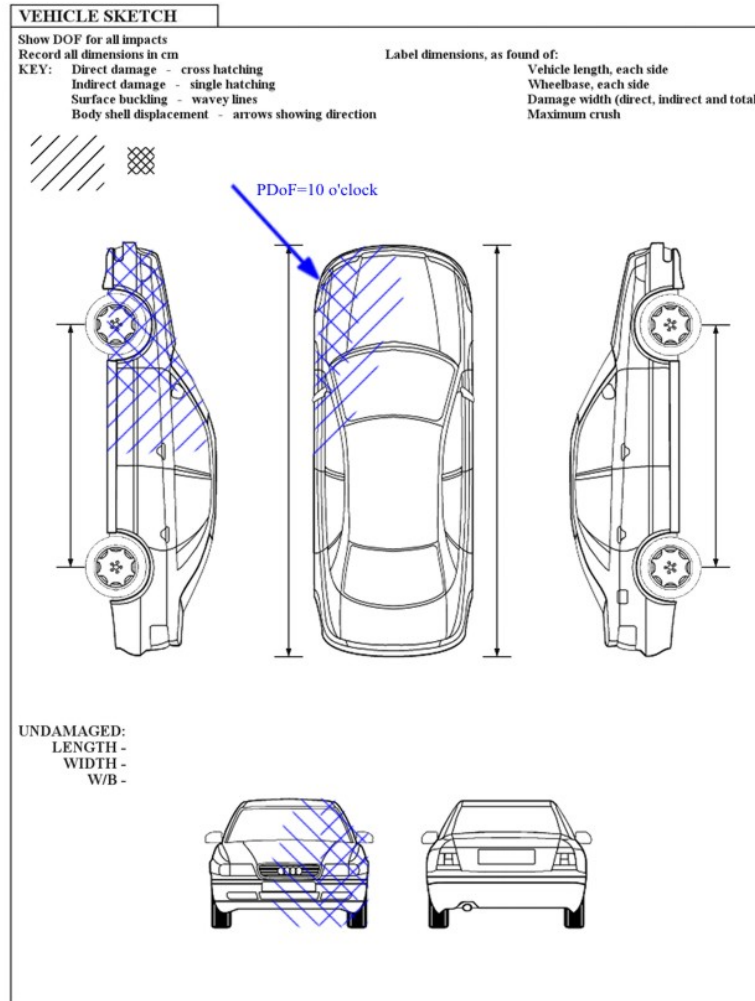


Passenger compartment intrusion matrix measurement

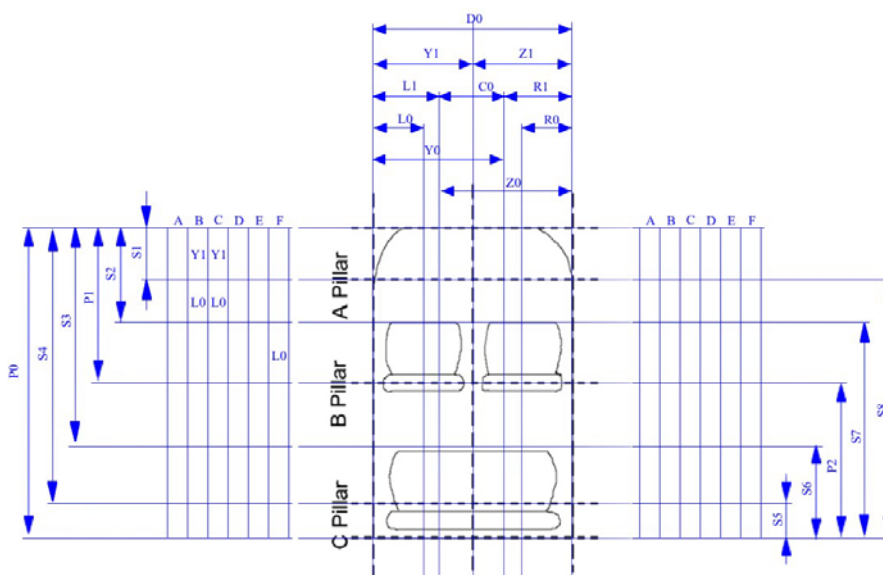


Passenger compartment intrusion matrix

PDC Example



PDC - Example



PDC - Example matrix

Appendix E

Tyre load and speed

Most tyres are marked with a Service Description comprising a Load Index (number) and a Speed Symbol (letter) e.g. 78S. Tyres fitted as original equipment are suitable for the maximum axle weight and speed capability of the car.

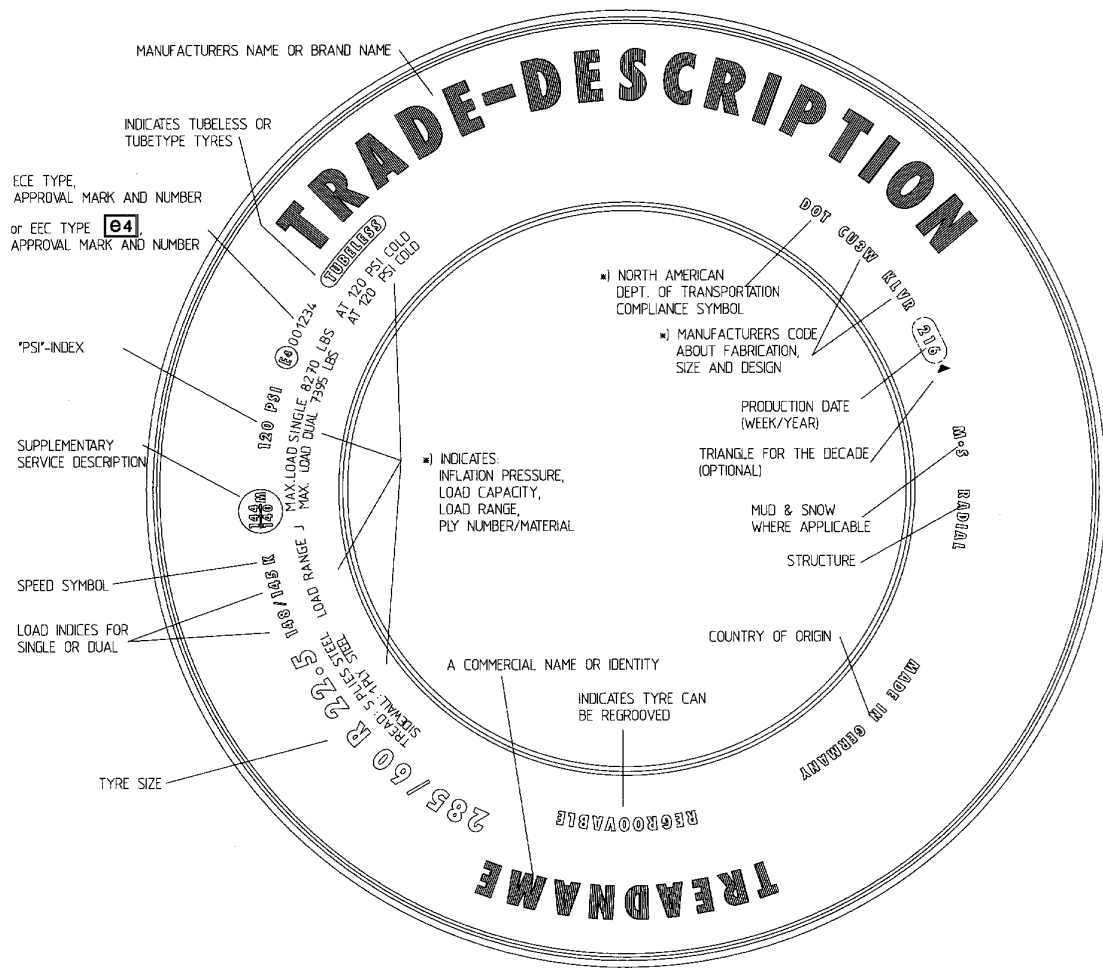
Replacement tyres must have a Load Index and a Speed Symbol at least equal to those of the original tyres. In the absence of a Service Description, consult a tyre specialist to ensure an appropriate replacement.

Exceptions are 'M+S' Winter tyres, in which case the speed capability of replacement tyres can be lower than that of the original tyres, but the driving speed must be restricted to the lower speed rating.

Overloading or exceeding the maximum speed of a tyre causes excessive heat build-up which can lead to tyre break-up.

Speed Rating	Speed (kph)
L	120
M	130
N	140
P	150
Q	160
R	170
S	180
T	190
U	200
H	210
V	240
W	270
Y	300
ZR	over 240

Tab. 21: Speed Rating of tyres



*) optional, only mandatory in countries where the MVSS-Standards are required

Tyre description

Appendix F (Satellite)

Galileo http://europa.eu.int/comm/dgs/energy_transport/galileo/index_en.htm

The Galileo positioning system (never abbreviated GPS) is a planned satellite navigation system, intended as a European alternative to the United States Global Positioning System (which is abbreviated GPS). The system is intended to be primarily for civil use and will be available at its full precision to all users.

As stressed in the European Commission White Paper on European transport policy for 2010, the European Union needs an independent satellite navigation system. Galileo is Europe's contribution to a global navigation satellite infrastructure (GNSS). GALILEO has been designed and developed as a non-military application, while nonetheless incorporating all the necessary protective security features. Unlike GPS, which was essentially designed for military use, GALILEO therefore provides, for some of the services offered, a very high level of continuity required by modern business, in particular with regard to contractual responsibility.

GALILEO is based on a constellation of 30 satellites and ground stations providing information concerning the positioning of users in many sectors such as transport (vehicle location, route searching, speed control, guidance systems, etc.), social services (e.g. aid for the disabled or elderly), the justice system and customs services (location of suspects, border controls), public works (geographical information systems), search and rescue systems, or leisure (direction-finding at sea or in the mountains, etc.).

Global Positioning System – GPS <http://www.trimble.com>

The Global Positioning System (GPS) is a worldwide radio-navigation system formed from a constellation of 24 satellites (Name: NAVSTAR; Manufacturer: Rockwell International; Orbital Period: 12 hours) and their ground stations (also known as the "Control Segment"; these stations monitor the GPS satellites, checking both their operational health and their exact position in space. The master ground station transmits corrections for the satellite's ephemeris constants and clock offsets back to the satellites themselves. The satellites can then incorporate these updates in the signals they send to GPS receivers; there are five monitor stations: Hawaii, Ascension Island, Diego Garcia, Kwajalein, and Colorado Springs.).

GPS uses these "man-made stars" as reference points to calculate positions accurate to a matter of meters.

How does GPS work?

- The basis of GPS is "triangulation" from satellites.
- To "triangulate," a GPS receiver measures distance using the travel time of radio signals.
- To measure travel time, GPS needs very accurate timing which it achieves with some tricks.
- Along with distance, you need to know exactly where the satellites are in space. High orbits and careful monitoring are the secret.
- Finally you must correct for any delays the signal experiences as it travels through the atmosphere.

Index

- 2D photogrammetry 17
- 3D photogrammetry 17
- Abrasion marks 32
- Accident collision type classification 90
- accident scene 11, 13, 21, 43, 50, 62
- Accident type 92
- Accuracies 18
- Acute angle 13
- AiDamage 77, 78
- angular momentum 10, 11, 69
- Aerial photography 23
- Backward Simulation 11
- Barrier Equivalent Velocity 111, 113
- BEV 5, 111, 113
- Biological traces 32
- Böhm* 11
- Border mark* 47
- Bowed vehicles 56
- Brake initial velocity 49
- C₁ to C₆ 17, 51, 52, 53, 54, 55, 56, 57, 58
- CARAT 64, 65, 66, 80, 119
- Casting marks 31
- CDC 79, 86, 87, 88, 99, 100, 101, 102, 103, 146, 147, 149
- centre of gravity 9, 10, 45, 71, 75, 90
- Chord measuring procedure* 15
- clock face 87, 88
- Closing Speed 110
- coefficient of restitution 10, 11
- Coefficient of restitution 10, 108
- Coefficient of Restitution 108, 113
- CoG 90
- Collision Deformation Code 86, 87
- compression* 104, 113, 114
- Conservation of energy* 9
- Conservation of Momentum 110
- CRASH3 51, 75, 76, 77, 78, 84, 113
- Crush Extent 103
- crush location 60
- D/C 51, 52
- damage field 52, 57, 60
- Damage marks 29
- Damage measurement 52
- Damage Pattern 102
- Damage width 51
- deformation energy 9, 104, 105
- delta-V 104
- Delta-v 107, 108, 109, 111, 112, 113
- Delta-V 5, 52, 60, 65, 66, 75, 76, 77, 78, 80, 87, 105
- direct contact 51, 57, 86, 100, 101, 102, 150
- Direction of Force 87, 88, 147
- DoF 86, 87, 88, 89, 91, 99, 147
- Drift traces* 46
- D-ring 33, 34, 50
- EBS 111
- EDSMAC 78, 79
- EDVDS 82, 83, 85, 119
- EDVSM 80, 81, 82, 83, 85, 141
- EES 9, 63, 71, 104, 105, 106, 112
- Energy Equivalent Speed 9, 104, 105, 112
- Equivalent Barrier Speed 111
- Equivalent Test Speed 111
- ETS 52, 60, 111
- Filling* 47
- First Law of Motion* 8
- Forward Simulation 12
- Front impacts 54
- Frontal impacts 91
- Galilei 8
- General Location 99
- Hertz 8
- Horizontal Location 100, 147, 148
- Hörz* 11
- Huygens 8
- HVE* 80, 82
- HVOSM 80, 81, 82
- Kudlich-Slibar* 10
- Law of Action-Reaction 10
- linear momentum 9, 10, 114
- Linear momentum 69
- MADYMO 66, 67, 68, 70, 84, 85, 140
- MAIDS 64
- Marquard* 10
- Material marks 29, 30
- Measure curves 15
- measurements 13, 17, 20, 22, 51, 52, 54, 63, 71, 77, 78, 80, 81
- Measuring procedures 13
- mid-point offset 60
- milling trace 45
- narrow penetrating profile 59
- Newton 8, 9, 10, 89, 109, 113
- NHTSA* 75, 78
- Obtused angle 13
- Offset 60
- on-scene* 62
- PC Video Rect* 21
- PC-Crash 69, 70, 71, 72, 74, 85, 105, 120
- PC-Rect 20, 21
- PDOF 65, 89
- PHASE 82
- PHASE4 82, 83
- PHIDIAS 21, 22
- Photogrammetry 17, 18, 118
- PhotoModeler 22, 23
- principal direction of force 87, 89, 90
- Principal Direction of Force 65, 87
- rear impacts 52, 54, 55, 77, 91, 97, 98
- Rear impacts 54, 55
- relative speed 110
- restitution* 104, 113, 114
- retrospective* 62
- Right angle coordinate measurement of curves* 17
- Right angle coordinate procedure 14

RISCAC 65, 66, 80
Rolling friction 41
Saint Venant 8
Second Law of Motion 8
Setting a datum 55, 56
side impacts 52, 56, 57, 60, 73, 89, 90, 95, 97
Side impacts 54, 56
Skid mark breaks 46
Skid marks 43, 44, 48, 49
Sliding collisions 12
Sliding friction 41
Sliding marks 45
SMAC 65, 66, 78, 79, 80
SMASH 75
Spacing 57, 58, 59
Spacing mark 48
Speed Rating 153
Static friction 41
Stiffness 75, 77, 113
Swivel 33, 34
Third Law of Motion 8
TNO 66, 68, 71
tongue 33, 34, 50
Trace development 47
trace interruptions 46
Trace reinforcement 46
transverse sliding traces 46
Triangle measuring procedure 13, 14
Triangulation 16
Tyre load 153
Tyres 153
Vertical Location 101, 149, 150
Wavelike skid mark formation 46
Wavy trace 46
Webbing marks 35, 36
Wiping marks 31
Yaw 44
yaw marks 43, 44
 ϵ 10, 72, 108, 113, 114